



# The Role of Flagella and Bacterial Motility in Virulence of *Salmonella*

Von der Fakultät für Lebenswissenschaften
der Technischen Universität Carolo-Wilhelmina zu Braunschweig
zur Erlangung des Grades
einer Doktorin der Naturwissenschaften
(Dr. rer. nat.)
genehmigte
D i s s e r t a t i o n

von **Julia Andrea Horstmann, geb. Deditius**
aus Castrop-Rauxel

| | |
|---|---|
| 1. Referentin: | Professorin Dr. Petra Dersch |
| 2. Referent: | Professor Dr. Michael Steinert |
| eingereicht am: | 27.03.2017 |
| mündliche Prüfung (Disputation) am: | 15.06.2017 |

Druckjahr 2017

# Vorveröffentlichungen

Teilergebnisse aus dieser Arbeit wurden mit Genehmigung der Fakultät der Lebenswissenschaften, vertreten durch die Mentorin der Arbeit, in folgenden Beiträgen vorab veröffentlicht:

## Publikationen

**Deditius J. A.**, Felgner S.*, Spöring I.*, Kühne C., Frahm M., Rohde M., Weiß S. und Erhardt M. (2015): Characterization of Novel Factors Involved in Swimming and Swarming Motility in *Salmonella enterica* Serovar Typhimurium. *PLoS ONE* 10(8): e0135351.
*Gleichermaßen beigetragen

**Horstmann J. A.**, Zschieschang E.*, Truschel T.*, de Diego J., Lunelli M., Rohde M., May T., Strowig T., Stradal T., Kolbe M. und Erhardt M. (2017): Flagellin Phase-dependent Swimming on Epithelial Cell Surfaces Contributes to Productive *Salmonella* Gut Colonization. *Cellular Microbiology*, doi: 10.1111/cmi.12739.
*Gleichermaßen beigetragen

## Tagungsbeiträge

**Deditius J. A.** und Erhardt M. (2013): Effect of the *Salmonella* virulence master regulator HilD on flagellar gene expression and motility (Poster). EMBO/EMBL Symposium: New Approaches and Concepts in Microbiology, Heidelberg.

**Deditius J. A.** und Erhardt M. (2014): Effect of the *Salmonella* virulence regulator HilD on motility (Poster). North Regio Day on Infection, NoRDI V, Braunschweig.

**Deditius J. A.** und Erhardt M. (2015): Effect of the *Salmonella* virulence regulator HilD on motility (Poster). Annual Conference of the Association for General and Applied Microbiology (VAAM), Marburg.

**Horstmann J. A.** und Erhardt M. (2016): The role of flagellar phase variation in virulence of *Salmonella* (Poster). Gordon Research Conference Sensory Transduction in Microorganisms, Signaling Diversity in Microbial Systems. Ventura, CA, USA.

## Acknowledgements

An dieser Stelle möchte ich meinen besonderen Dank an folgende Personen richten, ohne deren Mithilfe diese Arbeit nicht möglich gewesen wäre:

Mein Dank geht zunächst an Dr. Marc Erhardt für die Bereitstellung des interessanten und spannenden Projekts, sowie die Betreuung dieser Arbeit. Auch möchte ich mich für die konstante Förderung und das Vertrauen in meine Arbeit bedanken.

Ebenfalls danke ich meiner Mentorin Prof. Dr. Petra Dersch für hilfreiche Ideen und Diskussionen innerhalb der Thesis Komitees und Meetings.

Prof. Dr. Michael Steinert danke ich für die freundliche Übernahme des Korreferats und Begutachtung dieser Arbeit. Bei Prof. Dr. André Fleißner bedanke ich mich für die Übernahme des Prüfungsvorsitzes.

Der „HZI International Graduate School for Infection Research“ danke ich für die ideelle Förderung meines Promotionsvorhabens durch Ermöglichung von Weiterbildungen und der finanziellen Unterstützung für den Besuch internationaler Konferenzen.

Dem Boehringer Ingelheim Fonds danke ich für die Finanzierung meines Forschungsaufenthaltes an der University of Edinburgh.

Dr. Till Strowig und Prof. Dr. Theresia Stradal danke ich für die Teilnahme an meinem Thesis Komitee und den hilfreichen Tipps zu fachfremden Fragestellungen. Bei Prof. Dr. Manfred Rohde bedanke ich mich für die vielen elektronenmikroskopischen Aufnahmen.

Ein sehr großer Dank geht an alle jetzigen und ehemaligen Mitglieder der Nachwuchsgruppe „Infektionsbiologie von Salmonellen“, insbesondere Caroline Kühne, Imke Spöring, Florian „Flan“ Fabiani und Dr. Sebastian Felgner für die vielen Diskussionen, guten Ideen und die Durchsicht dieser Arbeit. Vielen Dank für die freundschaftliche Atmosphäre und all den amüsanten Episoden. Nadine Körner und all meinen ehemaligen Studenten danke ich für den praktischen Beitrag zu dieser Arbeit.

Der gesamten MIBI Gruppe danke ich für das tolle Arbeitsklima und die freundliche Zusammenarbeit. Vielen Dank für die Hilfe zu fachlichen Problemen und die Einweisung in neue Geräte. Auch danke ich den Gruppen MIKI und ZBIO für die Unterstützung zu Mausversuchen und zellbiologischen Methoden.

Ein besonderer Dank gilt meiner Familie und Freunden für die bedingungslose Unterstützung und für das Verständnis, das mir in allen Lebenslagen entgegen gebracht wurde.

Mein größter Dank geht an meinen wundervollen Ehemann André, ohne den diese Arbeit nicht möglich gewesen wäre. Vielen Dank für deine Liebe und deinen Rückhalt vor allem in frustrierenden Zeiten.

*„Besser als tausend Worte ohne Sinn ist ein einziges vernünftiges Wort, das dem, der es hört, Ruhe schenken kann.“ - Buddha*

**Am Ende wird alles gut.**

# Contents

# List of Figures

# List of Tables

# List of Abbreviations

| | |
|---|---|
| $Amp^R$ | Ampicillin resistance |
| AnTc | Anhydrotetracycline |
| APS | Ammonium persulfate |
| Ara/ara | Arabinose |
| BMM | Bone marrow-derived macrophages |
| BSA | Bovine serum albumine |
| c-di-GMP | Cyclic di-guanylic acid |
| CFU | Colony forming unit |
| CI | Competitive index |
| $Cmn^R$ | Chloramphenicol resistance |
| CUP | Chaperone-usher pathway |
| DAPI | 4',6-diamidino-2-phenylindole |
| $ddH_2O$ | double distilled water |
| DMEM | Dulbecco's modified eagle medium |
| DMSO | Dimethylsulfoxide |
| DNA | Desoxyribonucleic acid |
| dNTP | Desoxyribonucleiosid-triphosphate |
| ECM | Extracellular matrix |
| EDTA | Ethylenediaminetetraacetic acid |
| FCF | FRT-chloramphenicol-FRT cassette |
| FCS | Fetal calve serum |
| FESEM | Field emission scanning electron microscopy |
| FGI | Flagellin glycosylation island |
| FKF | FRT-kanamycin-FRT cassette |
| FMI | Flagellin methylation island |
| FRT | Flp recombination target |
| fT3SS | Flagellar-specific type-III secretion system |
| GFP | Green fluorescent protein |
| HBB | Hook-basal body |
| HTH | Helix-turn-helix |
| IL-1$\beta$ | Interleukin 1$\beta$ |
| IPTG | Isopropyl-$\beta$-D-thiogalactopyranoside |
| $Kan^R$ | Kanamycin resistance |
| Lpf | Long polar fimbriae |
| LPS | Lipopolysaccharide |
| MLN | Mesentheric lymph nodes |

| | |
|---|---|
| MOI | Multiplicity of infection |
| mRNA | Messenger RNA |
| n | Number of biological replicates |
| NEAA | Non-essential amino acids |
| NLR | Nod-like receptor |
| NSS | Near surface swimming |
| OD | Optical density |
| PAMP | Pathogen associated molecular pattern |
| PCA | Principle component analysis |
| PCR | Polymerase chain reaction |
| pfu | Plaque forming unit |
| PI | Propidium iodide |
| PMF | Proton motive force |
| PRR | Pattern recognition receptor |
| SCV | *Salmonella* containing vacuole |
| SDS | Sodiumdodecylsulfate |
| Spi | *Salmonella* pathogenicity island |
| tafi | Thin aggregative fimbriae |
| TCA | Trichloroacetic acid |
| TEM | Transmission electron microscopy |
| TEMED | Tetramethylethylenediamine |
| $Tet^S$ | Tetracycline sensitivity |
| TLR | Toll-like receptor |
| vT3SS | Virulence-associated type-III secretion system |
| WT | Wildtype |

# List of Symbols and Units

| | |
|---|---|
| $\alpha$ | anti (used for antibodies) |
| $\beta$ | beta |
| bp | Basepairs |
| °C | Degree Celsius |
| $\Delta$ | Delta (used for gene deletions) |
| F | Farad |
| kb | Kilobasepairs |
| kDa | Kilo Dalton |
| M | Molar mass |
| $\Omega$ | Ohm |
| $\Psi$ | Psi |
| TPM | Transcripts per million |
| V | Volt |
| W | Watt |
| xg | Multiple of acceleration of gravity |

# List of Amino Acids

| | | |
|---|---|---|
| Alanine | Ala | A |
| Arginine | Arg | R |
| Asparagine | Asn | N |
| Aspartic acid | Asp | D |
| Cysteine | Cys | C |
| Glutamic acid | Glu | E |
| Glutamine | Gln | Q |
| Glycine | Gly | G |
| Histidine | His | H |
| Isoleucine | Ile | I |
| Leucine | Leu | L |
| Lysine | Lys | K |
| Methionine | Met | M |
| Phenylalanine | Phe | F |
| Proline | Pro | P |
| Serine | Ser | S |
| Threonine | Thr | T |
| Tryptophan | Trp | W |
| Tyrosine | Tyr | Y |
| Valine | Val | V |

# Summary

**The Role of Flagella and Bacterial Motility in Virulence of *Salmonella***

Flagella are sophisticated nanomachines and important virulence factors of many pathogenic bacteria. Besides the ability to swim through liquid environments, the flagellum also contributes to successful infection of the host cell by enhancing cell adhesion and invasion. The flagellum consists out of three main parts: (i) the basal body, (ii) a flexible hook, and (iii) a long helical filament. Due to its purposes in distinct infection phases, flagellar gene expression, assembly, and functionality has to be regulated tightly in response to environmental cues. In this thesis, new motility regulators have been identified and mechanisms of flagella modification have been characterised according to their contribution to motility and pathogenesis of *Salmonella*.

In the first chapter, five genes (*rflP*, *yjcC*, STM1267, STM3363, and *rfaG*) have been shown to influence swimming and/or swarming motility via alterations of flagellar gene expression or assembly.

In the second chapter, a recently described transcriptional activator of flagellar gene expression, HilD, was characterised regarding its contribution to bacterial motility. HilD overexpression resulted in non-motile bacteria independently of flagellar assembly. It is likely that metabolic changes through collapse of the proton-motive force led to the described motility defect. Further, HilD was shown to activate expression of numerous fimbrial structures, such as Pef, Saf, or curli fimbriae.

In the third chapter, alternate expression of the two antigenically distinct flagellins, FliC and FljB, was investigated regarding its importance for *Salmonella* physiology. FliC flagellin variants facilitated target-site selection and Spi-1 injectisome-dependent invasion during swimming on epithelial host cell surfaces. FljB-expressing bacteria were outcompeted by FliC-expressing bacteria during eukaryotic cell invasion and colonisation in the gastroenteritis mouse model.

The fourth chapter focused on the posttranslational modification of the filament by the methylase FliB. FliB methylated lysine residues of the surface-exposed D2 and D3 domains of both flagellins, FliC and FljB. Moreover, flagellin methylation affected epithelial cell adhesion and invasion in a mannose-dependent manner. Consequently, strains deficient in flagellin methylation were outcompeted during dissemination in the gastroenteritis mouse model.

Altogether, regulation of flagellar gene expression, stability, or flagella function through posttranslational modifications is a crucial prerequisite to ensure efficient adaptation to changing environments and successful infection of the host. These new insights in mechanisms of *Salmonella* pathogenesis promote the understanding of bacterial infections and contribute to the development of new therapeutical strategies.

# Zusammenfassung

**Die Rolle des Flagellums und bakterieller Motilität in der Virulenz von *Salmonella***

Flagellen sind komplexe Nanomaschinen und wichtige Virulenzfaktoren für viele pathogene Bakterien. Neben gerichteter Fortbewegung in flüssigen Medien trägt das Flagellum durch erhöhte Adhäsion und Invasion von eukaryotischen Zellen maßgeblich zur effektiven Infektion der Wirtszelle bei. Das Flagellum besteht aus drei Hauptkomponenten: (i) dem Basalkörper, (ii) einem flexiblen Haken und (iii) einem langen helikalen Filament. Durch unterschiedliche Aufgaben während des Infektionszyklus ist eine strenge Regulierung der Genexpression, Assemblierung und Funktionalität des Flagellums als Antwort auf veränderte Umweltbedingungen von großer Bedeutung. In dieser Arbeit wurden neue Motilitätsregulatoren und deren Mechanismen der Flagellenmodifikation in Hinsicht auf Motilität und Pathogenität von *Salmonella* identifiziert und näher charakterisiert.
Im ersten Kapitel wurden fünf Gene (*rflP*, *yjcC*, STM1267, STM3363 und *rfaG*) ermittelt, die das Schwimm- und Schwärmverhalten durch Änderung der flagellaren Genexpression oder des Flagellenaufbaus beeinträchtigt haben.
Im zweiten Kapitel wurde ein zuvor beschriebener Transkriptionsaktivator der flagellaren Genexpression, HilD, bezüglich dessen Auswirkung auf Motilität charakterisiert. HilD-Induktion führte zu einem Verlust an Motilität unabhängig von der flagellaren Assemblierung. Die Ergebnisse weisen auf einen Mechanismus durch einen veränderten Metabolismus und einer Kollabierung der protonenmotorischen Kraft hin. Weiterhin resultierte die Überexpression von HilD in einer erhöhten Expression verschiedener Fimbrien (Pef, Saf oder Curli Fimbrien).
Im dritten Kapitel wurde die Expression unterschiedlicher Flagelline, FliC und FljB, bezüglich der biologischen Relevanz in *Salmonella* analysiert. FliC-flagellierte Bakterien ermöglichten die Auswahl geeigneter Infektionsstellen und somit auch die Spi-1-abhängige Invasion während des Schwimmens nahe der Wirtszelloberfläche. Desweiteren hatten FliC-exprimierende Bakterien einen Vorteil während der Kolonisierung im Gastroenteritis-Mausmodell.
Das vierte Kapitel fokusierte sich auf die posttranslationale Modifikation des Filaments durch die Methylase FliB. FliB methylierte Lysinreste der exponierten D2 und D3 Domänen sowohl von FliC als auch von FljB. Die Methylierung des Flagellins trug außerdem zur Mannose-abhängigen Adhäsion und Invasion von Epithelzellen bei. Bakterien ohne methyliertes Flagellin waren demnach stark hinsichtlich der Kolonisierung im Gastroenteritis Mausmodell benachteiligt.
Zusammengefasst ist die Regulierung der flagellaren Genexpression, Stabilität und Funktionalität eine wichtige Voraussetzung, um eine effiziente Anpassung an wechselnde Umweltbedingungen zu gewährleisten und demnach eine erfolgreiche Infektion zu ermöglichen. Diese neuen Erkenntnisse und Mechanismen der Pathogenität von Salmonellen treiben das Verständnis bakterieller Infektionen voran und tragen zur Entwicklung neuer therapeutischer Strategien bei.

# 1 Introduction

*Salmonella* is one of the most common causes of foodborne diseases worldwide. Every year, millions of Salmonellosis cases occur worldwide in humans with more than one hundred thousand deaths [World Health Organization, 2016]. In Germany, 13,823 cases of human Salmonellosis with 16 deaths were reported in 2015 [Robert-Koch Institut, 2015]. Thus, infections caused by *Salmonella* are not only an economic, but also a great health problem. While symptoms of Salmonellosis are relatively mild and self-limiting, immunocompromised patients, infants or elderly are affected by severe dehydration, which can be life threatening. As bacterial resistances are increasing globally, an antimicrobial therapy is only recommended in serious cases like systemic infections and sepsis [World Health Organization, 2016]. Therefore, careful investigation of *Salmonella* pathogenesis enables establishment of new treatments against *Salmonella* infections.

## 1.1 The genus *Salmonella*

*Salmonellae* are Gram-negative, rod-shaped bacteria, which have a length of 2 µm to 5 µm and are motile (Fig. 1.1). They were first described by the American veterinary pathologist Daniel Elmer Salmon, whose assistant isolated the species *Salmonella choleraesuis* in 1885 [Schultz, 2010]. The genus *Salmonella* belongs to the family of *Enterobacteriaceae* and is closely related to the *Escherichia*, *Shigella*, or *Yersinia* genera. Two species are described for *Salmonella*: *S. bongori* and *S. enterica*. *S. bongori* is restricted to cold-blooded animals, whereas *S. enterica* is mostly found in warm-blooded hosts [Grimont and Weill, 2007, Lan et al., 2009, Fierer and Guiney, 2001]. *S. enterica* is divided into six subspecies that include over 2,500 serovars. These serovars can be further classified based on their surface structures (O-antigens) and flagella (H-antigens) according to the Kauffmann-White-scheme. However, serovars of

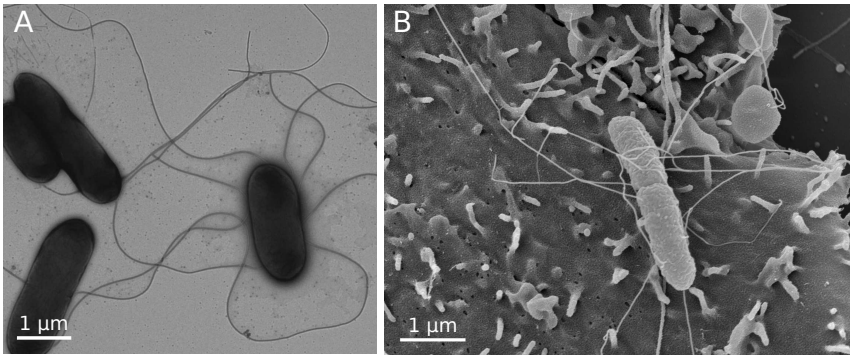


**Figure 1.1: Electron micrographs of *Salmonella enterica* serovar Typhimurium.**
(A) Transmission electron microscopy (TEM) of flagellated WT bacteria. (B) Field emission scanning electron microscopy (FESEM) of *Salmonella* on murine epithelial cells (MODE-K). Microscopy pictures were taken by Prof. Dr. Manfred Rohde, HZI.

*S. enterica* subspecies are mainly designated in respect to their diseases, origins, or habitats [Murray et al., 1999, Coburn et al., 2007]. In general, all serovars can be divided into two main groups: typhoidal and nontyphoidal *Salmonellae*. Typhoidal *Salmonellae* include the serovars Typhi and Paratyphi A and B, which are highly adapted to humans and cause systemic infections like typhoid fever. Nontyphoidal *Salmonellae* usually cause self-limiting gastrointestinal disease and have a broad range of hosts including humans, poultry, swine, or cattle. Differences among *S.* Typhi and *S.* Typhimurium during infections account to gene variations (∼10 %) like the Vi antigen that is only present in *S.* Typhi [de Jong et al., 2012]. However, 80 % of all reported Salmonellosis cases are caused by the nontyphoidal serovars *S.* Enteritidis (20 %) and *S.* Typhimurium (60 %) [World Health Organization, 2016]. Thus, *S.* Typhimurium represents an appropriate model strain to study *Salmonella*-related disease.

## 1.2 *Salmonella* pathogenesis

Under natural conditions, the zoonotic pathogen *Salmonella* is transmitted by ingestion of contaminated water or food or by the fecal-oral route (Fig. 1.2). To establish a successful infection within the host, a titer of at least $10^6$ bacteria is required [de Jong et al., 2012, Finlay, 1994]. Once *Salmonella* reaches the stomach, the bacteria have to overcome the acidic pH conditions by e.g. activating the acid tolerance response [Foster and Hall, 1991]. Within the small intestine, *Salmonella* crosses the intestinal mucus layer and adheres to intestinal epithelial host cells. *Salmonella* preferably adheres and enters specialised M cells within the intestinal epithelium. However, invasion of nonphagocytic enterocytes can also occur at their apical pole [Jones et al., 1994, Takeuchi, 1967]. During the invasion process, host cell signalling pathways are activated resulting in actin cytoskeleton rearrangements [Finlay et al., 1991, Francis et al., 1992]. These rearrangements induce the formation of so-called ruffles, which lead to engulfment of *Salmonella* in large vesicles. In this subepithelial location, the bacteria can survive and replicate through modification of the endocytic vacuole into *Salmonella*-containing vacuoles (SCVs) [Francis et al., 1993, Finlay and Falkow, 1988, Garcia-del Portillo and Finlay, 1994]. In parallel, the engulfment of bacteria induces the first line of immune responses, including the recruitment of phagocytes and the production of proinflammatory cytokines (e.g. TNF-$\alpha$) [Hobbie et al., 1997]. Innate cells, such as macrophages, migrate towards infected epithelial cells. There, they actively phagocytose particles that are recognized as “non-self”, such as *Salmonella* [Jones et al., 1994]. After phagocytosis, *Salmonella* triggers a similar response as seen in epithelial cells to enable bacterial replication. By migration of those infected phagocytes, *Salmonella* is able to disseminate systemically and replicate within deeper organs like liver and spleen [Foster and Hall, 1990].

## 1.3 Virulence factors

*Salmonella* harbours a battery of virulence factors that are highly conserved. Most of these virulence factors are encoded on *Salmonella* pathogenicity islands (Spi) or on the virulence plasmid (pSLT) [Misselwitz et al., 2012, Crawford et al., 2010]. In *Salmonella*, there are five pathogenicity islands that have been shown to be involved in virulence and during host-pathogen interactions (Spi-1 to Spi-5). The most relevant virulence factors, such as flagella, adhesins, and injectisomes, will be described in the following.

### 1.3.1 Bacterial flagella

One important virulence strategy is bacterial motility. Motile bacteria are able to direct their own movement towards important nutrients or away from harmful substances [Wiedemann et al., 2014]. Two types of motility exist in *S.* Typhimurium: (i) swimming motility through liquid environments and (ii) swarming motility on surfaces. Both strategies depend on surface appendages, called flagella. Flagella are long, thin, helical propellers that protrude from the cell body and rotate to confer motility [Zhou et al., 1999a]. Structurally,

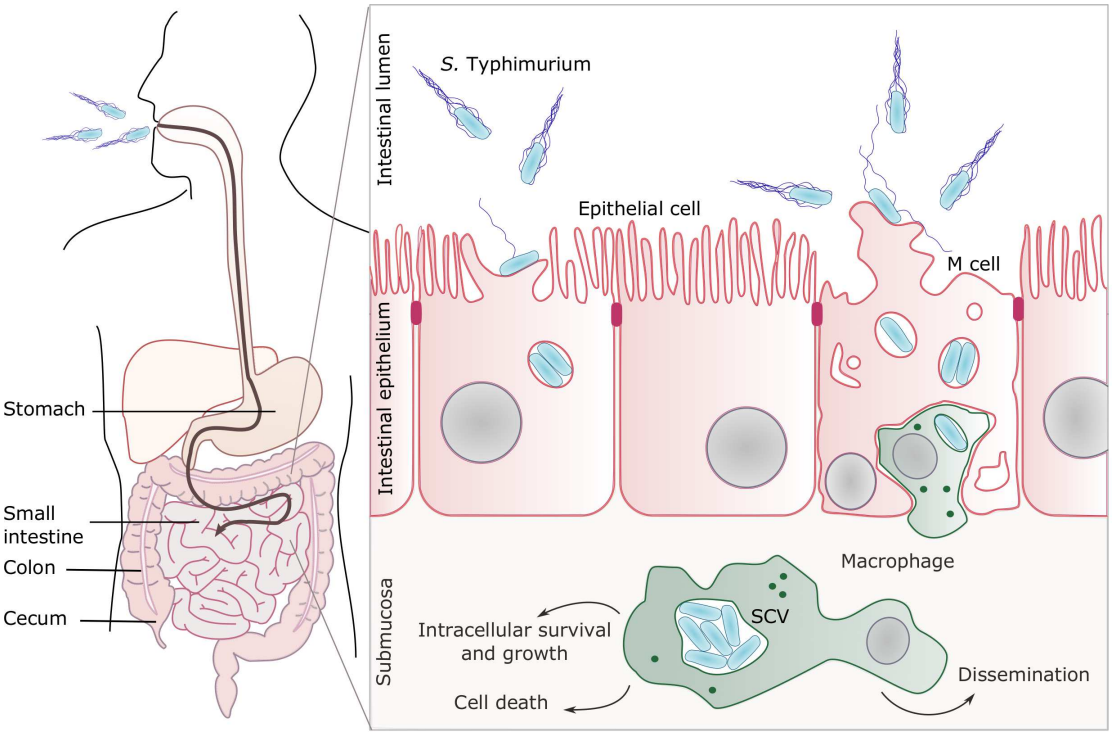


**Figure 1.2: Route of infection by *Salmonella* Typhimurium.**
*Salmonella* is taken up by consumption of contaminated food or water. They colonise the small intestine and induce a rearrangement of the host's actin cytoskeleton, leading to active engulfment in a process called invasion. Within *Salmonella*-containing vacuoles (SCVs) *Salmonella* is able to survive and replicate, allowing successful dissemination into deeper tissue like liver or spleen.

the flagellum is a complex nanomachine made of thousands of copies of approximately 30 different proteins and extends up to 20 µm beyond the cell surface [Jones et al., 1994]. It consists of three main parts: the basal body, the hook, and the filament (Fig. 1.3). The basal body is composed of an engine (MotAB) and components that anchor the flagellum in the bacterial membrane. These include rotor and stator protein complexes that are necessary for motor-force generation and flagellar rotation [Francis et al., 1993, Sansonetti, 2002]. A rod extends the rotor from the inner membrane to the outer membrane. The flexible hook is made up of about 120 copies of the protein FlgE and has an average length of 55 nm [Hirano et al., 1994, Erhardt et al., 2011, Erhardt et al., 2010]. It functions as a universal joint that connects the basal body with the third structure, the filament. This filament forms the helical propeller and consists of approximately 20,000 subunits of flagellin (FliC or FljB).
The flagellum is synthesised in a hierarchical process. As most of flagellar components are assembled external to the inner membrane, the majority of proteins have to be exported through a flagellar-specific type III secretion system at the base of the basal body (fT3SS; FlhAB, FliHIJ,

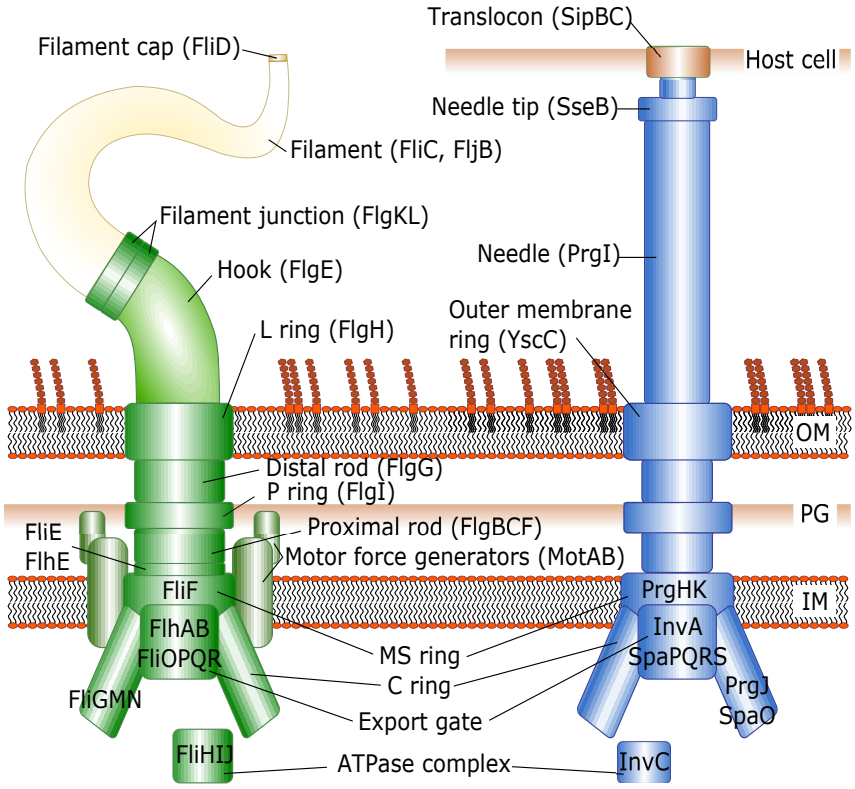


**Figure 1.3: Schematic comparison of the flagellum and the Spi-1 injectisome.** (Left) The flagellum consists of a basal body, which includes a flagellar-associated type III secretion system (fT3SS), a flexible hook, and the filament. (Right) The injectisome is built up of a basal body with a virulence-associated type III secretion system (vT3SS), which is structurally related to the fT3SS, a needle complex, and a translocon complex at the tip of the structure. OM = outer membrane; PG = peptidoglycan; IM = inner membrane.

and FliOPQR). This fT3SS forms independently of the MS- (FliF) and C-rings (FliGMN) and is located at the base of the basal body within the cytoplasmic membrane. Next, the rod (FliE, FlhE, and FlgBCFG), P-ring (FlgI) and L-ring (FlgH) self-assemble to form a channel for protein secretion of extracellular components, such as the hook-protein FlgE and, at later stages, flagellin. The export of flagellar subunits occurs in an unfolded or partially folded state. The unfolding of proteins is presumably mediated by three cytoplasmic proteins, FliHIJ, that form an ATPase complex [Akeda and Galán, 2005]. However, protein secretion itself only depends on proton motive force (PMF), which consists of the membrane potential $\Delta\Psi$ and the proton gradient $\Delta$pH [Paul et al., 2008, Minamino and Namba, 2008].

The flagellum is able to rotate either clockwise or counterclockwise. Counterclockwise rotation enables the formation of a large flagellar bundle, which results in a forward-driven movement, also called the run-phase. Once the rotational direction for one or more flagella changes to clockwise rotation, the bundle falls apart and the bacterium reorientates in the so-called tumble-phase. To coordinate this biased random walk towards a concentration gradient, *Salmonella* has evolved several chemoreceptor systems. The two-component system CheA-CheY senses environmental stimuli, which leads to autophosphorylation of the sensor kinase CheA [Briegel et al., 2012]. The phosphoryl group is then transferred to the response regulator CheY. Increased levels of phosphorylated CheY result in binding to FliM in the C-ring and thereby trigger a switch in rotational direction of the flagellar rotor from counterclockwise to clockwise rotation. Consequently, a decrease in phosphorylated CheY reverts to the default counterclockwise rotation and thus prolonged running phases towards favourable sites [Eisenbach and Caplan, 1998, Boyd and Simon, 1982, Lertsethtakarn et al., 2011, Wadhams and Armitage, 2004]. Chemotaxis plays an important role during infection, since mucins or glycoproteins, the main components of mucus, display effective chemoattractants [Stecher et al., 2004]. By using this directed movement towards host cells, interactions between *Salmonella* and the host are possible and facilitate cell adhesion and invasion [Jones et al., 1981].

Beside involvement of flagella in bacterial motility and chemotaxis, flagella are also involved in many other processes that lead to successful colonisation of the host. Physical forces between flagella and the host cell surface allow *Salmonella* to scan the host's surface topology and to find the optimal infection site. This process is called near surface swimming [Misselwitz et al., 2012]. Moreover, the flagellar filament is of great importance for intestinal cell adhesion , which enables triggering of membrane ruffling and initiate invasion [Chaban et al., 2015].

Flagella are associated with the recognition and modulation of the host immune system (Fig. 1.4). Pattern recognition receptors (PRRs) are able to sense highly conserved bacterial structures, known as pathogen associated molecular patterns (PAMPs) like flagellin. Extracellular flagellin is recognized by the Toll-like receptor TLR5 [Smith et al., 2003]. These receptors are located on the surface of endocytic compartments and lead to the activation of the innate immune

system by releasing cytokines and activating immune cells [Akira et al., 2006]. Intracellular flagellin is sensed by the Nod-like receptors (NLR) Ipaf or Naip5 resulting in the activation of caspase-1 and interleukin 1$\beta$ [Miao et al., 2007, Miao et al., 2006]. As *Salmonella* wants to avoid recognition by the immune system, it downregulates flagellar gene expression during intracellular survival [Eriksson et al., 2003]. In addition, they exhibit several other mechanisms for evasion. These mechanisms include expression of alternating flagellin proteins in a process called flagellar phase variation [Bonifield and Hughes, 2003] or post-translational modification of flagellin to mask recognition sites [Arora et al., 2005].

### 1.3.2 Adhesion factors

Once the bacteria have reached the preferred site of infection, attachment between bacterial and eukaryotic cells is essential [Zierler and Galán, 1995]. Close contact is mediated by various adhesive structures on the bacterial cell surface. These adhesins are divided into two major classes, fimbrial and non-fimbrial adhesins, and differ according to their assembly pathway [Soto and Hultgren, 1999]. Most of the *Salmonella* adhesins belong to the group of fimbrial adhesins. In *Salmonella* Typhimurium, 13 fimbrial operons are described (*fim*, *pef*, *std*, *lpf*, *bcf*, *stb*, *stc*, *sth*, *sti*, *stj*, *stf*, *csg*, and *saf*) [McClelland et al., 2001]. Only the two operons *fim* and *csg* are expressed under standard laboratory conditions [Humphries et al., 2003]. However, all structures are expressed *in vivo* [Humphries et al., 2005]. Fimbriae are surface appendages

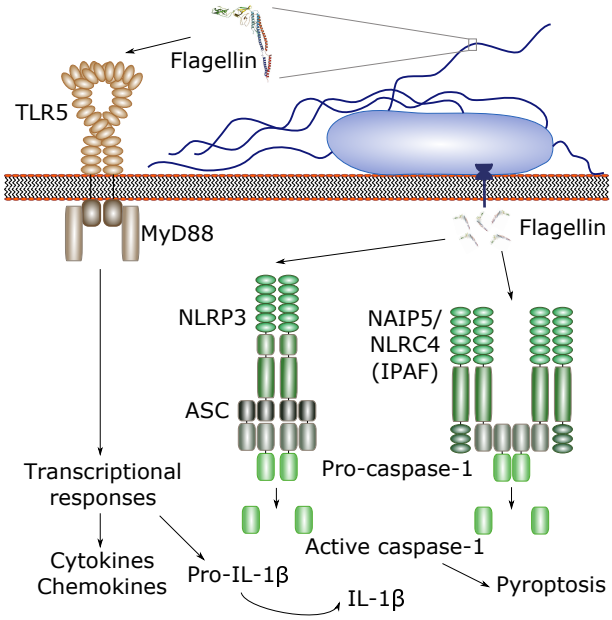


**Figure 1.4: Flagellin recognition by the host innate immune system.** Extracellular flagellin is recognised by the Toll-like receptor TLR5, resulting in the induction of cytokine release and activation of immune cells. Intracellular flagellin is recognised by Nod-like receptors, such as Ipaf or Naip5, leading to activation of caspase-1 and interleukin 1$\beta$ (IL-1$\beta$).

and assembled either by the chaperone-usher pathway (CUP) or by the extracellular nucleation pathway. Within the CUP, fimbrial subunits are translocated through the cytoplasmic membrane into the periplasm via N-terminal secretion signals in a Sec-dependent manner. Subsequently, specific chaperones direct subunits to the usher, which is integrated into the outer membrane and coordinates the assembly of the fimbrial structures. The interaction with the host cell surface is enabled once the fimbrial tip binds to host cell receptors. These receptors are membrane proteins, sugar residues, or lipid structures.

The most studied fimbrial operon that encodes for fimbriae of the CUP is the *fim* operon. This operon encodes type I fimbriae and consists of six genes *fimAICDHF* that bear the information for structural subunits and the three regulator-encoding genes *fimZYW* [McClelland et al., 2001]. Type I fimbriae bind to oligomannoside chains of the extracellular matrix protein laminin on eukaryotic cells via the structural tip component FimH [Kukkonen et al., 1993, Bäumler et al., 1997]. Other fimbrial structures, such as Pef fimbriae, are encoded on the virulence plasmid pSLT of *S.* Typhimurium [Friedrich et al., 1993] and bind to the Lewis X ($Le^x$) blood group antigen (Gal$\beta$1-4(Fuc$\alpha$1-3)GlcNAc). This antigen is expressed by crypt epithelial cells, suggesting binding during later stages of infection [Chessa et al., 2008a]. The *std*, *lpf*, *bcf*, *stb*, *stc*, and *sth* fimbrial operons are required during long-term persistence in mice [Weening et al., 2005]. Moreover, Std fimbriae bind to terminal $\alpha$(1-2)fucose receptors and thereby mediate adhesion to colonic epithelial cells and successful intestinal colonisation [Chessa et al., 2008b, Chessa et al., 2009]. Long polar fimbriae (Lpf) adhere to cells of the Peyer's patches that are associated to the lymphatic tissue [Bäumler et al., 1996].

Thin aggregative fimbriae (tafi) have a different morphology than the fimbriae described above. These fimbriae are also termed curli fimbriae and assembled by the nucleation-precipitation pathway. Curli fimbriae are encoded by two operons, *csgDEFG* and *csgBA* [Römling et al., 1998, Barnhart and Chapman, 2006, Collinson et al., 1991]. They are involved in adhesion and invasion of *Salmonella* into host cells by binding to the extracellular matrix protein fibronectin [Collinson et al., 1993, Dibb-Fuller et al., 1999]. Furthermore, they are connected to auto-aggregation of *Salmonella*, biofilm formation and adhesion to other surfaces. CsgD is the master regulator of curli fimbriae transcription. First, CsgB and CsgA are secreted through the general secretion pathway into the periplasm. Then, the outer membrane lipoprotein CsgG mediates secretion across the outer membrane. Afterwards, the nucleator CsgB polymerises extracellular CsgA to form curli fibers [Barnhart and Chapman, 2006].

The heterogenous group of non-fimbrial adhesins includes mono- and oligomeric adhesive structures that are either secreted through a type I secretion system or auto-transported. An example for such adhesins is the large protein SiiE. It is encoded on Spi-4, which comprises six genes *siiABCDEF* in one operon. SiiC, SiiD, and SiiF form a type I secretion system that secretes SiiE. This giant adhesin consists of 53 repetitive Ig domains and enables contact-

dependent adhesion to epithelial cells during the initial step of infection [Morgan et al., 2004, Gerlach et al., 2007b].

### 1.3.3 Injectisomes

For successful invasion and intracellular replication, *Salmonella* utilises syringe-like virulence factors, also known as injectisomes. The virulence-associated T3SS (vT3SS) is able to secrete structural components of the injectisome as well as effector proteins into host cells [Blocker et al., 2003, Abby and Rocha, 2012]. Several proteins within the vT3SS and fT3SS are homologous regarding sequence and function, suggesting that the vT3SS is structurally related to the fT3SS (Fig. 1.3). Also, this indicates that the vT3SS may have been evolved from the bacterial flagellum through gene deletions and insertions [Abby and Rocha, 2012]. However, some structures differ between the injectisome and flagellum. This includes the flagellar P- and L-rings, which are exchanged by a single secretin-like ring in the injectisome, the C-ring, and the extracellular structures. In comparison to the flagellar hook and filament, the injectisome harbours a needle and a pore-forming translocon complex [Diepold and Wagner, 2014].
*Salmonella* expresses two distinct injectisomes encoded on Spi-1 and Spi-2. The structural components of the Spi-1-encoded injectisome are encoded on the *prg/org* and *inv/spa* operons, whereas the *sic/sip* operons encode for effector proteins and the translocon (SipBCD). This pore-forming structure inserts in the host cell membrane, enables close association and thereby delivery of effector proteins into the host cytosol. Additionally, several chaperones are encoded on Spi-1. These chaperones prevent premature interactions, protein degradation, and mediate recognition by the vT3SS. Once effector proteins are secreted into the host cell, they trigger Spi-1-dependent invasion of *Salmonella* into epithelial cells by rearrangements of the actin cytoskeleton and subsequent engulfment of the bacteria. Important effector proteins are SopE, SopE2, and SopB. The guanidine exchange factors (GEF) SopE and the homologous SopE2 stimulate the GDP/GTP nucleotide exchange and thereby activate the small Rho GTPases Cdc42 and Rac-1 [Hardt et al., 1998, Stender et al., 2000, Bakshi et al., 2000]. This results in actin cytoskeletal rearrangements and the activation of NF-$\kappa$B, which leads to reprogramming of host gene expression and induction of the proinflammatory cytokines IL-8 and TNF-$\alpha$ [Hobbie et al., 1997, Patel and Galán, 2006]. SopE, however, is not present in all *Salmonella* isolates [Mirold et al., 1999]. SopB is encoded on Spi-5 and is involved in dearrangement of the phosphatidylinositol signalling pathway. This leads to increased chloride secretion and diarrhea [Norris et al., 1998]. Moreover, SopB activates the GTPase RhoG, which mediates cell actin cytoskeletal modifications [Patel and Galán, 2006]. Another Spi-1 effector is SipA that binds actin to stabilise actin filaments [Kaniga et al., 1995, Zhou et al., 1999b].
Once the bacteria are taken up by the host, *Salmonella* utilises the Spi-2 injectisome to survive and replicate inside SCVs [Ochman et al., 1996, Hensel et al., 1995, Méresse et al., 2001]. Within Spi-2 the *ssa* genes encode the vT3SS, which secretes effector proteins that are encoded

by *sse* genes. The corresponding chaperones are encoded by *ssc* genes. Additionally, regulators for Spi-2 are encoded by *ssr* genes [Kuhle and Hensel, 2004]. Via secretion of Spi-2-related effector proteins, the host cell cytoskeleton is modified and results in a loss of vesicular transport of antimicrobial host factors and maintenance of the SCV [Rajashekar et al., 2008, Kuhle and Hensel, 2004, Uchiya et al., 1999]. Thus, the expression of Spi-2-encoded genes is essential to survive *in vivo* and to establish systemic infections [Knodler et al., 2002].

## 1.4 Regulation of virulence factors

Since every virulence system functions at distinct phases during infection, tight control of gene regulation is required to maintain their function [Hautefort et al., 2008]. Beside environmental signals that lead to altered expression of virulence traits, there is a large number of regulators described for each system (Fig. 1.5). Regulation of genes located on Spi-1 is complex and needed for invasion once the bacteria have reached the preferred site of infection *in vivo*. However, *in vitro* transcription of Spi-1 can be mimicked by low oxygen and high osmolarity [Lee et al., 1992,

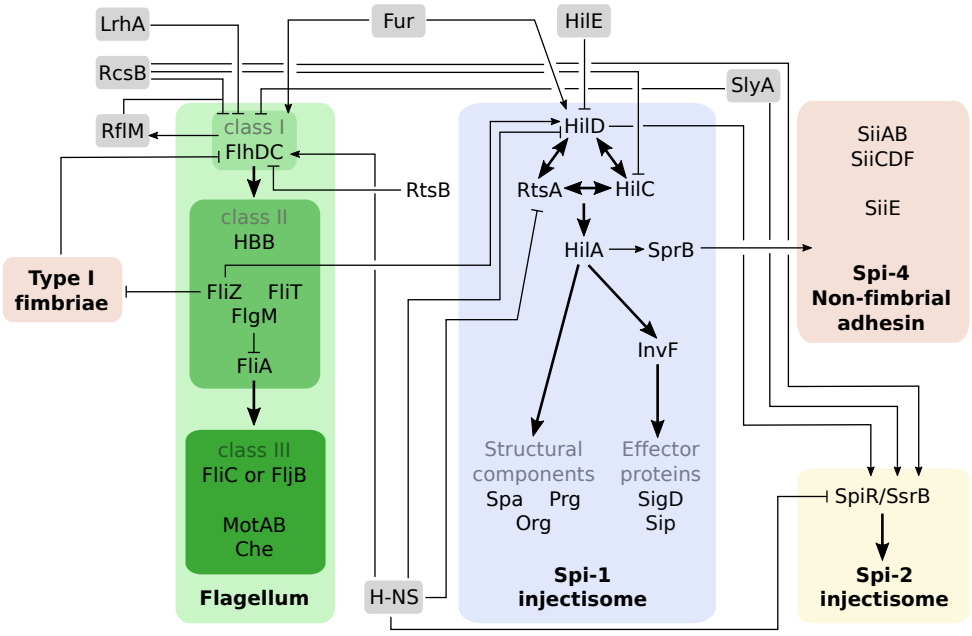


**Figure 1.5: Gene expression networks of the most relevant virulence systems in *Salmonella*.** On top of the flagellar biosynthetic cascade is the heteromultimeric complex $FlhD_4C_2$, which activates expression of hook-basal body and regulatory proteins. Upon completion of the hook, FliA induces transcription from class 3 promoters, including gene products that form the filament and the motor complex. In contrast, a feed-forward loop of HilD, HilC, and RtsA regulates the master regulator of the Spi-1 injectisome, HilA. HilA activates expression of structural needle components and Spi-1 effector proteins, but also of the Spi-4 encoded non-fimbrial adhesin SiiE. Spi-2 expression is positively regulated by HilD. All shown virulence systems share regulatory pathways to maximise the efficiency of *Salmonella* virulence at distinct infection phases.

Bajaj et al., 1996]. Three AraC-like regulators are on top of the Spi-1 transcriptional cascade: HilC, RtsA, and HilD. HilC and HilD are both encoded on Spi-1 [Schechter et al., 1999], whereas *rtsA* is located outside the Spi-1 locus [Ellermeier and Slauch, 2003]. Each regulator activates its own transcription and the expression of the other regulators [Ellermeier et al., 2005]. Together, this feed-forward loop activates transcription of *hilA*, which encodes the master regulator of Spi-1 [Boddicker et al., 2003, Ellermeier and Slauch, 2007]. HilA belongs to the OmpR/ToxR family of transcriptional activators and is encoded on Spi-1 [Bajaj et al., 1995]. It plays an important role during host cell invasion, since a *hilA* knockout mutant exhibits a similar phenotype than an entire Spi-1 deletion strain [Ellermeier et al., 2005]. HilA directly binds the promoter region of the *prg/org* and *inv/spa* operons. Thereby it enables the expression of proteins that form a functional Spi-1 injectisome [Bajaj et al., 1996, Bajaj et al., 1995]. Moreover, HilA positively regulates expression of InvF, which is a member of the AraC family and the main activator of *sic/sip* operon transcription and leads to expression of effector proteins [Kaniga et al., 1994, Darwin and Miller, 1999]. Recently, it was shown that HilA is also able to directly activate expression of several effector proteins [Thijs et al., 2007]. Another regulator involved in this pathway is HilE that is encoded outside of Spi-1. HilE interacts posttranscriptionally with HilD and results in repression of *hilA* transcription [Baxter et al., 2003].

Genes located on Spi-2 are induced after entering epithelial cells or macrophages and then expressed continuously during the course of infection. Thus, conditions mimicking the intracellular environment such as low osmolarity, low calcium concentration or acidification activate Spi-2 expression [Garmendia et al., 2003]. Regulation of Spi-2 is mediated by the two-component regulatory system SsrA-SsrB, which is also encoded on Spi-2. SsrA is located within the membrane and functions as sensor kinase. SsrB acts as a transcriptional regulator [Ochman et al., 1996, Cirillo et al., 1998]. In addition to its Spi-2 regulatory function, SsrB also activates the expression of Spi-2 effector proteins encoded outside Spi-2, such as SifA and SifB [Garmendia et al., 2003]. Transcription of *ssrB* and *ssrA* is not linked due to the presence of two promoters in front of each gene. This indicates that SsrB is autoregulated and induces *ssrA* transcription [Feng et al., 2003].

Type I fimbriae are upregulated during stationary growth phase and the regulators are FimW, FimY, and FimZ. FimZ represents a response regulator that is able to bind DNA and cooperatively acts with the transcriptional activator FimZ to induce fimbrial gene expression [Yeh et al., 1995, Tinker and Clegg, 2000]. In contrast, the regulator FimW represses type I fimbriae [Tinker et al., 2001].

Flagella are expressed during colonisation of the intestine and downregulated intracellularly to evade recognition of flagellin by the immune system. Many environmental stimuli are involved in this process [Chilcott and Hughes, 2000] and the regulon of flagellar biosynthesis comprises more than 60 genes, 17 operons [Chilcott and Hughes, 2000], and is organised in a transcriptional hierarchy of three promoter classes [Chevance and Hughes, 2008,

Anderson et al., 2010]. The flagellar master operon *flhDC* is on top of this hierarchy and transcribed from a class I promoter [Yanagihara et al., 1999]. This operon encodes FlhD and FlhC that form the heteromultimeric complex $FlhD_4C_2$ [Chilcott and Hughes, 2000]. $FlhD_4C_2$ directs $\sigma^{70}$-RNA polymerase to transcribe genes that are controlled by class II promoters [Liu and Matsumura, 1994, Wang et al., 2006]. These genes code for proteins that are required to form the flagellar hook-basal body (HBB) complex and additional regulators such as the flagella-specific alternative sigma factor $\sigma^{28}$ and its corresponding anti-sigma factor FlgM [Iriarte et al., 1995, Liu and Matsumura, 1995, Ding et al., 2009]. Prior to HBB completion, early substrates, such as structural components of the HBB complex, are secreted by the fT3SS. Upon completing the HBB, the secretion apparatus undergoes a conformational switch in substrate specificity, which enables secretion of late substrates. The anti-sigma factor FlgM belongs to these late substrates and secretion of FlgM releases $\sigma^{28}$, leading to $\sigma^{28}$-dependent transcription from class III promoters [Ohnishi et al., 1992, Chadsey et al., 1998, Karlinsey et al., 2000, Hughes et al., 1993, Kutsukake, 1994]. Proteins transcribed from class III promoters include the structural components of the filament, also known as flagellin, chemotaxis-associated proteins and motor force generators.

Furthermore, the biosynthesis of flagella is tightly regulated at various levels, such as *flhDC* transcription, translation, and $FlhD_4C_2$ stability. In this context, transcription of *flhDC* occurs from multiple transcriptional start sites, whose transcriptional activities depend on the respective regulators and bacterial growth phase [Kröger et al., 2012, Kröger et al., 2013, Mouslim and Hughes, 2014]. $FlhD_4C_2$ activates its own repressor, RflM, in a regulatory feedback loop [Singer et al., 2013, Kühne et al., 2016]. Additionally, the class II gene product FliT inhibits the promoter binding activity of $FlhD_4C_2$ and increases proteolysis of FlhC through ClpXP upon HBB completion and late secretion of its chaperone FliD [Yamamoto and Kutsukake, 2006, Sato et al., 2014, Aldridge et al., 2010]. FliZ, another class II gene product, positively regulates flagellar class II and class III transcription by indirectly increasing $FlhD_4C_2$ activity [Kutsukake et al., 1999]. It represses transcription of the EAL-domain protein RflP, which binds to FlhD and targets $FlhD_4C_2$ to ClpXP-dependent proteolysis [Wada et al., 2011b, Wozniak et al., 2009, Takaya et al., 2012].

Interestingly, all described pathogenicity elements share regulatory pathways to maximise the efficiency of *Salmonella* virulence. This cross-talk enables a fast transcriptional transition from the invasion phase to the intracellular survival and replication. The flagellar class II gene product FliZ is known to repress fimbrial genes and to activate posttranscriptionally Spi-1 gene expression via HilD [Saini et al., 2010, Kutsukake et al., 1999, Lucas et al., 2000]. RtsA induces expression of Spi-1, whereas flagella biosynthesis is inhibited by RtsB [Ellermeier and Slauch, 2003]. Recently, we demonstrated that HilD directly binds to the P5 promoter of *flhDC* and thereby enhances flagellar gene expression [Singer et al., 2014]. The Spi-1 master regulator HilA also activates transcription of Spi-4 by induction of the positive regulator SprB. This

results in the expression of *sii* genes and SiiE-mediated adhesion [Gerlach et al., 2007a, Main-Hester et al., 2008]. In contrast, the expression of Spi-2 genes such as *ssaH* and *sseL* are repressed by HilA. However, HilD is described to activate Spi-2 transcription through direct binding to the *ssrAB* promoter [Bustamante et al., 2008]. Another regulator of Spi-2 gene expression is SlyA [Boyen et al., 2008]. SlyA binds to the *ssrA* promoter and induces transcription of Spi-2 [Feng et al., 2004, Okada et al., 2007]. The fimbriae-related regulators PefI and SrgD are associated with negative regulation of *flhDC* transcription [Wozniak et al., 2009]. FimZ as activator of type I fimbriae additionally represses *flhDC* and Spi-1 gene expression [Saini and Rao, 2010].

In *Salmonella*, there are numerous two-component regulatory systems that sense environmental conditions and, in response to such signals, regulate the expression of various virulence systems. For instance, the sensor kinase PhoQ detects low extracellular cation concentrations or low pH within the SCV and activates the regulator PhoP [García Véscovi et al., 1996]. PhoP then represses the transcription of *prg* genes and *hilA* to deactivate Spi-1 expression [Bajaj et al., 1996, Pegues et al., 1995, Behlau and Miller, 1993] and flagellar gene transcription [Adams et al., 2001]. Importantly, PhoP activates expression of *pag* genes that are essential for bacterial survival in macrophages [Miller et al., 1989, Belden and Miller, 1994], induces *ssrB* transcription and posttranscriptionally controls SsrA [Bijlsma and Groisman, 2005]. The two-component system BarA/SirA is involved in carbohydrate metabolism, motility, biofilm formation, and invasion [Teplitski et al., 2003, Altier et al., 2000b, Johnston et al., 1996, Teplitski et al., 2006, Romeo et al., 1993]. SirA induces the expression of *csrB* and *csrC*, which are small RNA molecules that inhibit the RNA binding protein CsrA [Fortune et al., 2006, Altier et al., 2000a]. CsrA binds *hilD* mRNA and prevents its translation. Thus, SirA positively regulates HilD expression. Furthermore, type I fimbriae are induced by direct binding of SirA to *fimA* [Teplitski et al., 2006] and flagellar gene expression is repressed by SirA [Goodier and Ahmer, 2001]. The Rcs phosphorelay system consists of the response regulator RcsB, the hybrid histidine kinase RcsC, and an intermediate phosphotransmitter RcsD. This system represses Spi-1 gene expression and *flhDC* transcription [Wang et al., 2007, García-Calderón et al., 2007, García-Calderón et al., 2005, Cano et al., 2002].

Nucleoid-associated proteins (NAP) also act as regulatory proteins by DNA binding and associated alteration of the DNA topology. The NAP H-NS is known as an important repressor of virulence systems acquired by horizontal gene transfer such as Spi-1 [Olekhnovich and Kadner, 2007, Olekhnovich and Kadner, 2006] and Spi-2 [Walthers et al., 2007, O'Byrne and Dorman, 1994]. H-NS also functions as an indirect activator of *flhD* transcription [Ko and Park, 2000]. Moreover, the iron-regulatory protein Fur represses several genes via direct interaction with its target DNA [Kadner, 2005]. This iron-dependent protein inhibits expression of *hns* [Troxell et al., 2011], which in turn induces HilD expression.

## 1.5 Objectives

Flagella biosynthesis, assembly and functionality are regulated by numerous described regulators that act on transcriptional or posttranscriptional levels [Erhardt and Dersch, 2015]. However, fine-tuning of flagella regulation within the infection process of *S.* Typhimurium is highly complex and still not completely understood. This thesis should address the following levels of flagellar regulation and their roles in pathogenicity of *S.* Typhimurium:

a) **Characterisation of Novel Factors Involved in Swimming and Swarming Motility in *Salmonella* Typhimurium.**
In a recent screen of a library with more than thousand single gene deletions in the *Salmonella* chromosome, Bogomolnaya et al. described 130 mutations that affected swimming and/or swarming motility [Santiviago et al., 2009, Bogomolnaya et al., 2014]. These mutations were mainly linked to virulence or the flagellar system. In this chapter, 24 presumed motility mutants and their mechanisms of altered motility are characterised in detail by analysing flagellar gene expression and biosynthesis.

b) **HilD Adjusts Motility of *Salmonella* Typhimurium in a Spi-1-dependent Manner.**
Previously, we showed that the Spi-1 master regulator HilD activates flagellar gene transcription through direct binding to the *flhDC* P5 transcriptional start site [Singer et al., 2014]. However, the contribution of HilD overexpression to bacterial motility has not been addressed thus far. Therefore, the motility phenotype upon HilD induction is analysed in order to better understand the cross-talk between the Spi-1 and flagellar virulence systems.

c) **Flagellin Phase-dependent Swimming on Cell Surfaces Contributes to Host Cell Invasion in *Salmonella* Typhimurium.**
The functionality of flagella is not only regulated on a transcriptional level via activators or inhibitors, but also by alternate expression of structural components. Many *Salmonella* serovars express one of two antigenically distinct flagellins, FliC or FljB, in a process called flagellar phase variation. The genetic regulation of this phase variation was extensively studied (reviewed in [McQuiston et al., 2008]). It was suggested that flagellar phase variation plays an important role during later stages of infection to evade the host's immune system [Ikeda et al., 2001, Koskiniemi et al., 2013]. However, many *Salmonella* serovars lost the *fljB* locus, such as the host restricted serovars *Salmonella* Typhi or Paratyphi A. In this chapter, the physiological importance of flagellar phase variation during early stages of infection is assessed using motility assays and *in vitro* and *in vivo* infection models.

d) **Flagellin Methylation is Crucial for Mannose-dependent Cell Adhesion of *Salmonella* Typhimurium.**
In *Salmonella*, the flagellum is also regulated on a posttranslational level. The methylase FliB modifies lysine residues of flagellin, resulting in the formation of $\epsilon$-N-methyl-lysine [Ambler and Rees, 1959, Tronick and Martinez, 1971, Stocker et al., 1961]. However, the methylated residues of the flagellin proteins and the biological relevance of flagellin methylation remained unknown. In previous studies, it was reported that deletion of *fliB* did not affect swimming and swarming motility, indicating instead a role in virulence of *Salmonella* [Frye et al., 2006]. Here, the methylated lysine residues of FliC and FljB are monitored for effects on bacterial motility, flagellin secretion, and filament assembly. Moreover, the effect of a *fliB* mutation on epithelial cell adhesion and invasion is examined and further characterised.

A detailed analysis of flagellar regulation on multiple levels and its contribution to *Salmonella* pathogenesis is of great importance to enhance our understanding of the host pathogen interaction and may therefore drive the development of new therapeutics against *Salmonella* infections.

# 2 Characterisation of Novel Factors Involved in Swimming and Swarming Motility in *Salmonella* Typhimurium

Flagellar gene regulation occurs on multiple levels: *flhDC* transcription, translation, and $FlhD_4C_2$ stability. Many regulators were described and extensively studied in the past decades. However, due to the high complexity of biosynthetic pathways and cross-regulation, new regulators are found at a regular basis leading to extension of the known regulatory network of virulence factors.
Santiviago et al. constructed a pool of deletion mutants in *Salmonella* Typhimurium covering 1023 genes [Santiviago et al., 2009]. Besides screening of alterations in fitness during competitive infection in mice [Santiviago et al., 2009], this library was tested for effects on swimming and/or swarming motility [Bogomolnaya et al., 2014]. Bogomolnaya et al. found 130 genes that influenced bacterial motility, but were not previously described as modulators. These genes were primarily linked to *Salmonella* virulence, the flagellar system, or were thought to have a regulatory function. In this chapter, the motility phenotypes for 24 gene deletion mutants and the underlying regulatory mechanisms are analysed.

## 2.1 Verification of motility phenotypes

To investigate putative motility modulating genes that are linked to virulence systems and their regulation, 24 single gene deletions were constructed [Datsenko and Wanner, 2000] (see Chapter 7.2.4). None of the tested mutations had an effect on bacterial growth, however, a Δ*rfaG* deletion strain showed strong aggregation, which might explain a reduction in the optical density at 600 nm (Fig. 2.1). To verify novel factors that are involved in regulation of motility in *Salmonella*, swimming and swarming motility was investigated using semi-solid agar plates (Fig. 2.2A+B). A Δ*fliF* strain served as negative control due to the loss of the MS-ring, which is essential for flagellar assembly. Of 12 mutations that putatively decrease motility, only four mutants showed a reduction in swimming and/or swarming motility (Δ*flgE*, Δ*fliH*, Δ*rfaG*, and Δ*yjcC*) (Fig. 2.2A). A Δ*rfaG* mutation resulted in a 70 % decrease in swimming and a complete loss of swarming motility. The Δ*yjcC* strain only exhibited a defect in swimming (20 % reduction), but not swarming motility, whereas Δ*flgE* and Δ*fliH* mutants were fully impaired in swimming and swarming (Fig. 2.2A). Both, the flagellar hook protein FlgE and the fT3SS ATPase complex protein FliH are essential structural and functional components of the flagellum, which explains the contribution of FlgE and FliH to flagellar motility [Minamino et al., 2003]. Of 12 mutations that were described to increase motility, only three gene deletions were confirmed to be involved (*rflP*, STM1267, and STM3363) (Fig. 2.2B). RflP is known to inhibit flagellar gene expression from class II promoters by posttranslational targeting of the $FlhD_4C_2$ complex to ClpXP-dependent degradation [Wada et al., 2011a, Takaya et al., 2012]. However, swarming motility was decreased up to 50 % (Fig. 2.2B). Deletions of the STM1267 and STM3363 genes did not affect swimming, but increased swarming motility by approximately 30 %. Notably, mutations in STM0266, STM0289, STM0295, *fimZ*, STM0847, STM0971, STM1131, STM1268, STM1575, STM1630, STM1896, *fliB*, *fljA*, *sptP*, *sipA*, STM3696, and *rygD* did not modulate

swimming or swarming motility (Fig. 2.2A+B). Side effects through various incubation times of motility plates or *Salmonella enterica* strain backgrounds were excluded by analysing swimming motility of three exemplary gene deletion strains (ΔSTM1896, ΔSTM1630, and ΔSTM3696) over time and four *Salmonella enterica* WT strains (Fig. 2.3).

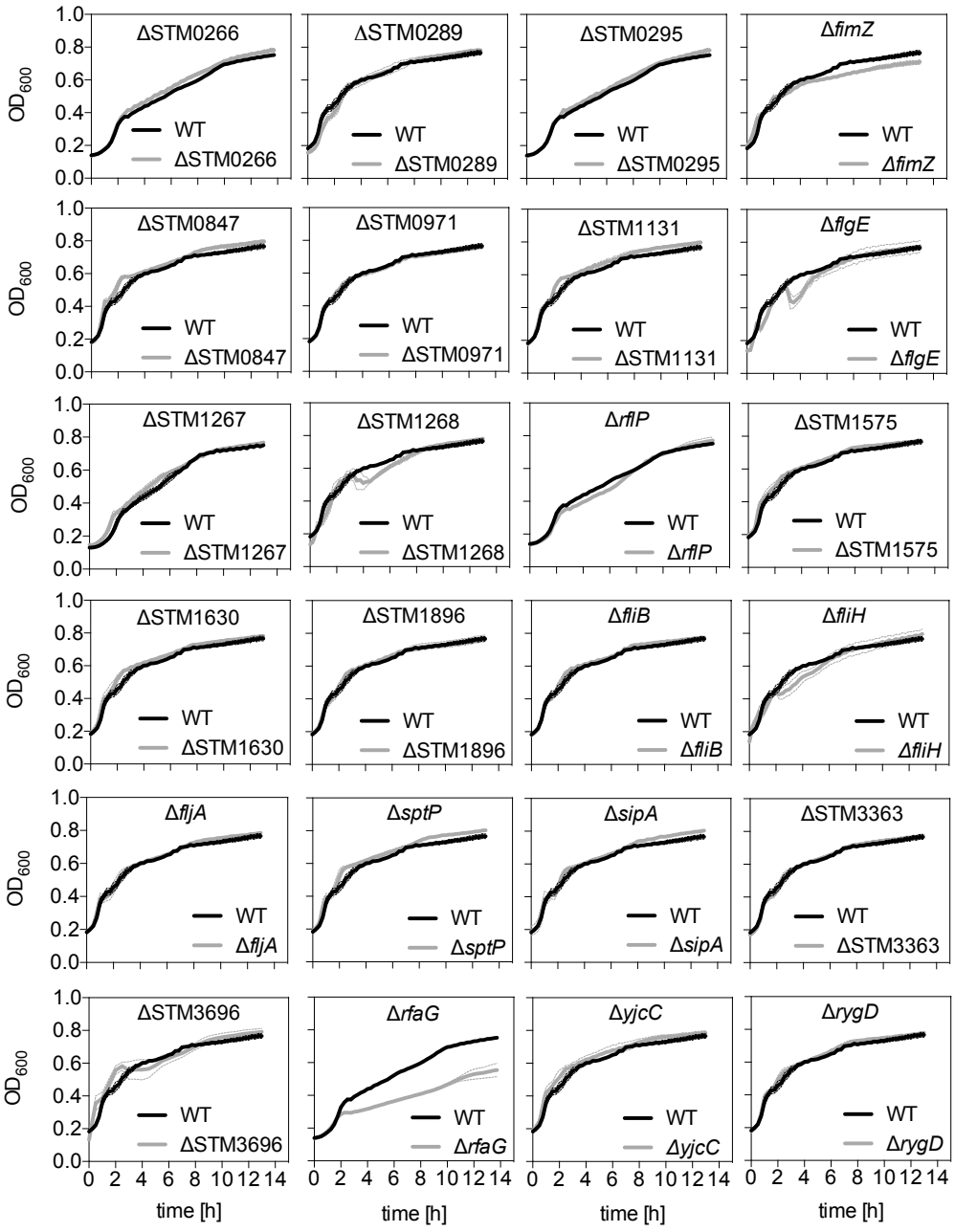


**Figure 2.1: Growth of single gene deletion mutants.** Bacterial growth was measured by absorption at 600 nm every 15 min for 13 h. Three biological replicates of each mutant are shown. Dotted lines represent the standard error of the mean. Adapted from [Deditius et al., 2015].

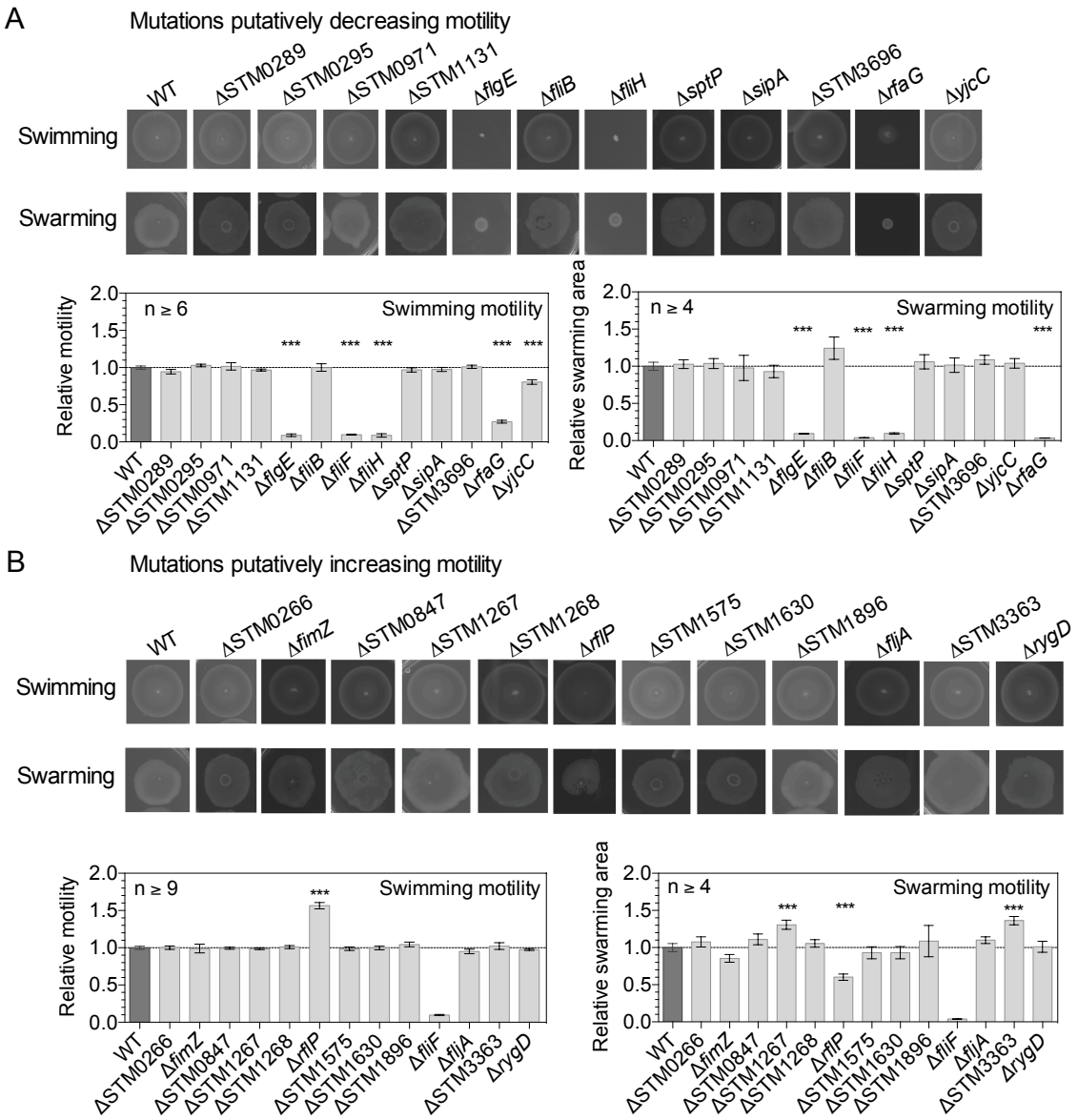


**Figure 2.2: Motility phenotypes of deletion mutants putatively altering motility.** Motility phenotypes of mutants were monitored on soft-agar plates after incubation at 37 °C. (A) Mutations that putatively decrease motility. (B) Mutations that putatively increase motility. Top: Representative motility plates for each mutant tested. The diameter of the motility swarm and the swarming area were measured and normalised to the WT. Bottom: Quantified relative motility. Biological replicates were analysed by the Student's *t*-test. Asterisks indicate a significantly different motility phenotype (*** = P<0.001) and error bars represent the standard error of the mean. Adapted from [Deditius et al., 2015]. Imke Spöring and Caroline Kühne contributed to swimming and swarming motility analyses.

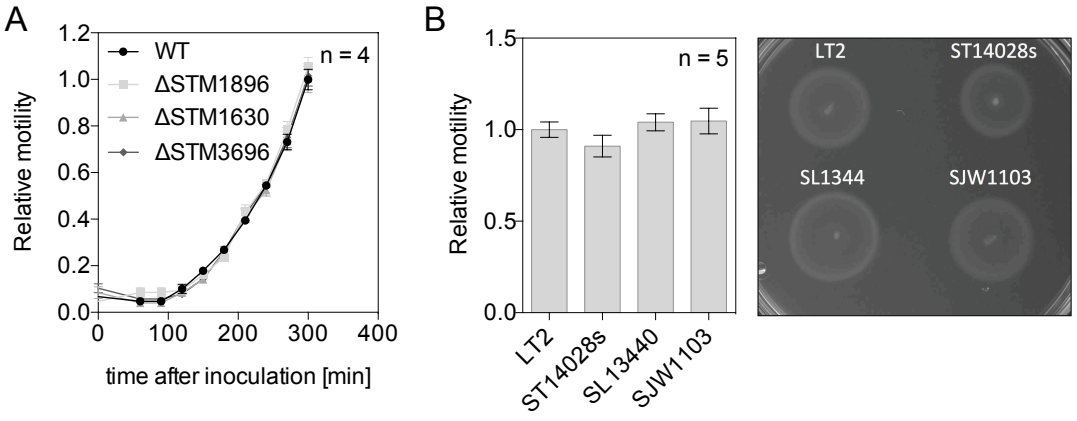


**Figure 2.3: Swimming motility dependent on incubation time and *Salmonella* strains.** (A) Swimming motility of single gene deletion mutants (ΔSTM1896::FRT, ΔSTM1630::FRT, ΔSTM3696::FRT) was monitored over time to exclude incubation time dependent swimming behaviours. (B) The *Salmonella enterica* serovar Typhimurium strains ATCC14028s, SL1344, LT2, and SJW1103 were examined on swimming motility agar. The diameter of the motility swarm was measured and normalised to LT2. Error bars represent the standard error of the mean. Adapted from [Deditius et al., 2015].

## 2.2 Analysis of the underlying mechanisms behind altered motility phenotypes

For characterisation of mutants that showed altered motility behaviours, transcriptional and structural analyses were performed. A deletion in *rflP* increased swimming motility as expected. However, a decrease in swarming motility was not described before. In *E. coli*, RflP represses Pap fimbriae and thereby adhesion of bacteria [Spurbeck et al., 2013]. Consequently, it was speculated that RflP might also be involved in expression of fimbriae in *Salmonella* Typhimurium resulting in increased adhesion of the Δ*rflP* mutant on the swarm agar. Expression of type I fimbriae was analysed by $\beta$-galactosidase activity assay using *lac* operon fusions to *fimH* and *fimW* (Fig. 2.4A). FimH is the fimbrial tip responsible for adhesion of the bacterium [Kisiela et al., 2011], whereas FimW represses type I fimbrial gene expression. A mutant that overexpresses FimZ was used as positive control. FimZ is an activator of type I fimbriae and overexpression showed higher transcription levels of *fimH* and *fimW* (Fig. 2.4A). These expression levels were neither influenced by a Δ*rflP* mutation, nor by RflP overexpression (Fig. 2.4A). Therefore, RflP is not involved in expression of type I fimbriae. Since *Salmonella* Typhimurium exhibits 13 fimbrial operons [McClelland et al., 2001], we investigated transcription levels of *csgAB*, *fimZ*, *pefA*, *siiC*, *siiE*, and *stdA* genes by quantitative real-time PCR (Fig. 2.4B). In agreement with the $\beta$-galactosidase activity assay, type I fimbriae were not upregulated in a Δ*rflP* mutant (Fig. 2.4B). Transcript levels of *pefA*, *stdA*, and *siiCE* genes were not significantly altered either. Deletion of *rflP* increased *csgA* and *csgB* transcription 3- and 100-fold, respectively (Fig. 2.4B), indicating a role of RflP in curli fimbriae repression.

YjcC (STM4264) is a putative phosphodiesterase with an EAL-motif. Deletion of *yjcC* decreased swimming motility and had no effect on swarming motility (Fig. 2.2A). $\beta$-galactosidase activity was assessed by Imke Spöring (Infection Biology of *Salmonella*, Helmholtz Centre for Infection Research) in strains that harboured *lac*-fusions to flagellar class I (*flhC*), class II (*fliL*), and class III (*fliC*) promoters. Transcription of *flhC*, *fliL* or *fliC* was not altered, suggesting that YjcC does not regulate motility by modifying flagellar gene expression (Data not shown).

Deletions of the STM1267 and STM3363 genes, that were not investigated before, were characterised regarding their flagellation, since both mutants exhibited increased swarming motility. To ensure staining of the filament, flagellin expression was locked in one of the two flagellin phases that are described for *Salmonella* Typhimurium (see Chapter 4). FliC flagellin was stained using a primary $\alpha$-FliC antibody and flagellation levels were analysed by counting the flagella per cell body. Under the applied experimental conditions, the control strain assembled 2-3 flagella per cell (mean = 2.3±1.4), which was comparable to a ΔSTM3363 deletion mutant (mean = 2.2±1.6) (Fig. 2.5A+C). The ΔSTM1267 mutant assembled more flagella per cell (mean = 3.1±1.5), suggesting that STM1267 is involved in repression of flagellar gene expression or assembly (Fig. 2.5C).

Gene deletion of *rfaG* decreased swimming and swarming motility. RfaG is a glucosyltransferase and is involved in lipopolysaccharide (LPS) biogenesis. TEM analysis of the control and mutant strains showed that a Δ*rfaG* mutant was predominantly deflagellated (Fig. 2.6A). The remaining

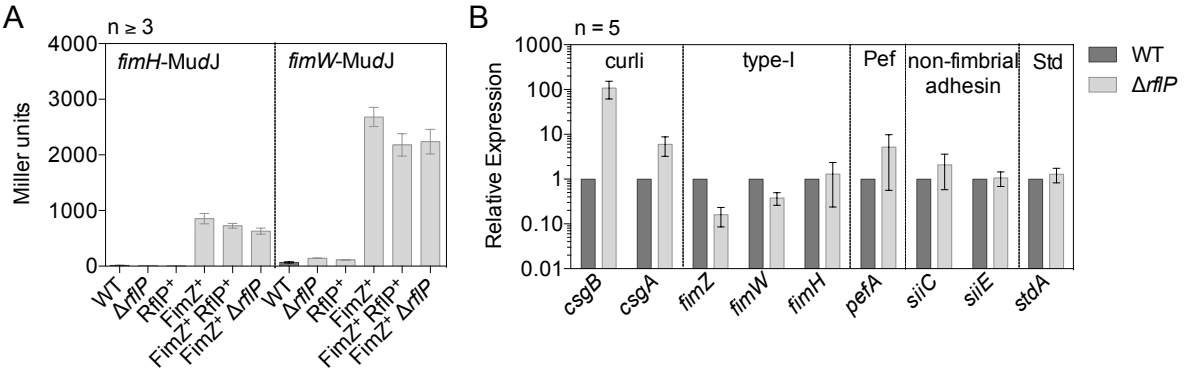


**Figure 2.4: RflP represses curli fimbriae gene expression.** (A) Type I fimbrial gene expression of a Δ*rflP*, RflP overexpression (RflP$^+$), or FimZ overproduced mutant (FimZ$^+$) was analysed by $\beta$-galactosidase assay. Transcription of *fimH* that encodes a fimbrial structure component and *fimW* that codes for a repressor of fimbria was examined. At least three independent biological replicates were analysed. Asterisks indicate gene expression levels that are significantly different to WT levels (*** = P<0.001) according to the Student's *t*-test. (B) Relative *csgA*, *csgB*, *fimZ*, *fimW*, *fimH*, *pefA*, *siiC*, *siiE*, and *stdA* gene expression of a Δ*rflP* mutant compared to the WT was analysed using qRT-PCR. Experiments were performed with 5 biological replicates. Error bars represent the standard error of the means. Adapted from [Deditius et al., 2015].

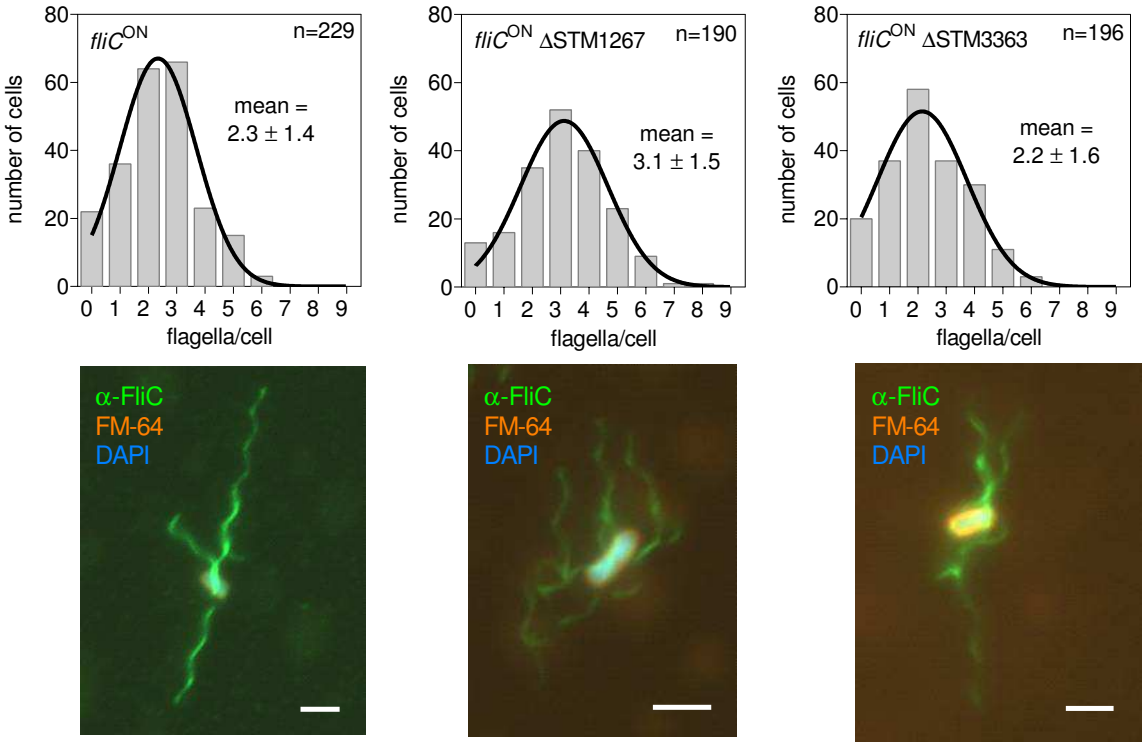


**Figure 2.5: STM1267 is involved in flagellar filament formation.** Top: Histogram of counted flagella per cell body of the WT, a ΔSTM1267, and ΔSTM3363 mutant. The average filament numbers per cell based on a Gaussian non-linear regression analysis and the standard deviation are indicated in the figure. Bottom: Flagellar filament formation was analysed by flagellin immunostaining using $\alpha$-FliC primary and $\alpha$-rabbit conjugated Alexa488 secondary antibodies (green) in a strain background locked for *fliC* expression. The membrane was stained with FM-64 (red) and DNA with DAPI (blue). Scale bar = 2 µm. Adapted from [Deditius et al., 2015].

30 % swimming motility of the Δ*rfaG* mutant correlates with the observation of few bacteria comprising a small number of flagella (Fig. 2.6A). Next, it was investigated if RfaG is involved in flagellar gene expression. Transcription was analysed by $\beta$-galactosidase assays with *lac*-fusions to flagellar class I (*flhC*), class II (*fliL*), and class III (*fliC*) promoters in a Δ*rfaG* deletion mutant. Gene expression of *flhC* was not affected in comparison to the control strain (Fig. 2.6B). However, Transcription from class II and class III promoters was significantly reduced (Fig. 2.6B), suggesting a posttranscriptional mechanism by which RfaG regulates flagellar gene expression. This hypothesis was tested using a 3xFLAG tagged FlhC [Wada et al., 2011a] and analysing protein levels. FlhC protein levels were strongly decreased upon deletion of *rfaG* (Fig. 2.6C). Accordingly, RfaG is involved in flagellar gene expression from class II promoters by posttranscriptionally modifiying $FlhD_4C_2$ stability or mRNA translation of class II gene products by an unknown pathway.

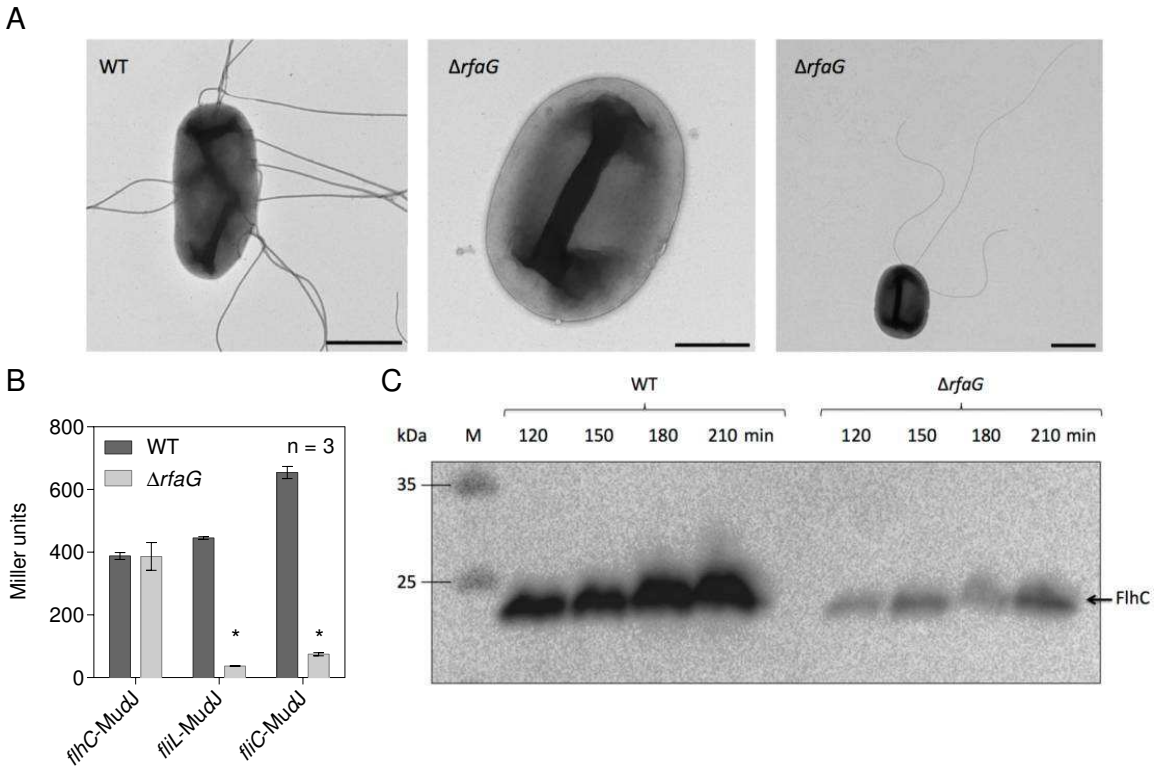


**Figure 2.6: Flagella numbers and flagellar class II and class III gene expression are decreased in a Δ*rfaG* mutant.** (A) Transmission electron microscopy (TEM) of WT and Δ*rfaG* strains. With the exception of few individual cells, the Δ*rfaG* mutant is non-flagellated. Scale bars: Left and right panel = 1 µm; Middle panel = 0.5 µm. Electron microscopy was conducted by Prof. Dr. Manfred Rohde (HZI). (B) Impact of a Δ*rfaG* mutation on flagellar gene transcription from class I (*flhC*-Mu*dJ*), class II (*fliL*-Mu*dJ*), and class III (*fliC*-Mu*dJ*) promoters. Dr. Sebastian Felgner (HZI) performed 2 of 3 replicates of the β-galactosidase assay. Error bars represent the standard error of the mean. (C) FlhC-3xFLAG protein levels in the WT and Δ*rfaG* strain. Bacteria were grown in LB medium and samples were analysed 120, 150, 180, and 210 min after inoculation. Protein levels were monitored by SDS-PAGE and immunoblotting using monoclonal α-FLAG antibodies. Adapted from [Deditius et al., 2015].

## 2.3 Discussion

Flagellar biosynthesis is tightly regulated to enable flagellar assembly in an ordered fashion. Regulation of the flagellar system occurs on multiple levels, such as transcription and translation of *flhDC* or $FlhD_4C_2$ stability. In a recent screen for novel motility regulators, 130 mutations were found to be involved in affecting swimming and/or swarming motility [Bogomolnaya et al., 2014]. In this chapter, 24 selected mutations were characterised regarding their contribution to motility regulation and the molecular mechanisms behind them. Seven of the 24 tested mutants were affected in swimming and swarming motility assays by showing decreased or increased motility behaviours. The high number of mutations that do not have an effect on motility might be due

to a combination of several issues. To exclude off-site effects of the constructed gene deletions in Bogomolnaya et al., mutations were re-transduced into a clean background in this thesis. Polar effects of the antibiotic resistance cassette were excluded by removal of the cassette via Flp-mediated recombination (see Chapter 7.2.5). Different media, inoculation methods, and quantification time points also account for varying results. Especially swarming motility is highly sensitive to humidity and wetness. Bogomolnaya et al. performed a high-throughput screening of mutants that might have complicated quantification.

In contrast to Bogomolnaya et al., mutations in *flgE* and *fliH* diminished both swimming and swarming motility, due to deletion of essential components of the flagellar structure and type III secretion system.

RflP represses motility by posttranslationally targeting FlhD for degradation [Wada et al., 2011a]. In agreement with this finding, a Δ*rflP* mutation increased swimming motility. However, swarming motility was decreased up to 50 % compared to WT swarming. Recently, it was described that RflP represses Pap fimbriae in *Escherichia coli* [Spurbeck et al., 2013]. Here, it was shown that a Δ*rflP* mutation increased mRNA levels of *csgA* and *csgB*. Increased expression of these major and minor subunits of curli fimbriae might result in a stickier phenotype on swarm agar and thereby reduce swarming motility. Also in *Myxococcus xanthus* and *Pseudomonas aeruginosa*, it was reported that type IV pili are involved in twitching and gliding motility [Wall and Kaiser, 1999]. Contrary, in a study by Anwar et al., deletion of *rflP* decreased expression of the master regulator CsgD [Anwar et al., 2014]. The Δ*rflP* mutant exhibited a reduced rdar (red, dry, and rough) morphotype on congo red plates [Anwar et al., 2014], indicating reduced expression of curli fimbriae. These contradictory observations might have been due to different media and growth conditions and need further investigation.

YjcC is a putative phosphodiesterase with an EAL-domain (Glu-Ala-Leu). This domain degrades cyclic di(3'→5')-guanylic acid (c-di-GMP) [Simm et al., 2007]. In *Salmonella* Typhimurium and *Escherichia coli*, c-di-GMP was implicated to function as a modulator of virulence, biofilm formation, and motility [Boehm et al., 2010, Fang and Gomelsky, 2010]. The c-di-GMP binding protein YcgR tightens its interaction with flagellar motor proteins to slow down flagellar rotation in the presence of c-di-GMP [Boehm et al., 2010, Paul et al., 2010]. These findings are consistent with the observed decrease in swimming motility of the *yjcC* deletion mutant without altering flagellar gene expression. Further, another EAL-containing protein YhjH (STM3611) regulates swarming motility [Simm et al., 2004]. It was reported that deletion of *yjcC* resulted in higher c-di-GMP levels and an increase in curli fimbriae and cellulose biosynthesis [Simm et al., 2007].

The genes STM1267 and STM3363 are not yet characterised. They encode hypothetical proteins and are conserved among *Salmonella* species. In this thesis, deletions of both genes increased swarming motility, but not swimming motility. A deletion of STM3363 did not influence filament assembly. STM3363 possesses a conserved Barstar-like domain that is described in *Bacillus*

*subtilis* and is involved in a toxin-antitoxin system [Hartley and Smeaton, 1973]. However, the mechanism by which this protein modulates motility still remains elusive. STM1267 exhibits a conserved domain of the YmgB superfamily, which is characterised in *Escherichia coli*. YmgB, also called AriR, decreases cellular motility and inhibits biofilm formation [Lee et al., 2007]. Here, a ΔSTM1267 mutation was shown to increase the number of flagella per cell body, which is consistent with the observed motility phenotype.

RfaG is involved in LPS biosynthesis by connecting the inner core with the outer part. In this thesis, both swimming and swarming motility was reduced. Consistently, flagellar assembly and flagellar expression from class II and class III promoters were decreased. Notably, transcription from the *flhDC* class I promoter was not altered, suggesting a posttranscriptional mechanism of motility modulation. Reduced FlhC protein levels confirmed this hypothesis, indicating that $FlhD_4C_2$ stability or translation of *flhDC* mRNA was affected. Previously, alterations in LPS biosynthesis were shown to contribute to motility in a variety of gram-negative bacteria [Gygi et al., 1995, Mireles et al., 2001, Toguchi et al., 2000, Wang et al., 2004a]. In *Escherichia coli*, genes that account for LPS biosynthesis affected swarming, but not swimming motility [Inoue et al., 2007]. Moreover, deletions of the inner core impaired swimming motility [Raetz and Whitfield, 2002]. LPS affects the surface tension between the agar and cell surface and confers hydrophilicity to the cell surface (reviewed in [Harshey, 2003]). Therefore, the mechanism by which LPS alterations influence flagellar motility needs further investigation.

Altogether, many additional genes were found to modulate bacterial motility in *Salmonella* Typhimurium, including a variety of unknown and poorly characterised genes. Besides the need for further investigation in the underlying mechanisms, these results contribute to a better understanding of motility regulation in *Salmonella* Typhimurium.

# 3 HilD Adjusts Motility in a Spi-1-dependent Manner and Induces Expression of Fimbrial Operons in *Salmonella* Typhimurium

During infection, *Salmonella* has to adapt rapidly to multiple different niches. Therefore, Spi-1 and flagellar gene expression have to be coordinated precisely in response to environmental signals. Both biosynthetic pathways share common regulators, such as HilD as described recently by Singer et al. [Singer et al., 2014]. HilD was shown to activate flagellar gene expression by direct interaction with the P5 transcriptional start site of the flagellar master operon *flhDC*. The respective effect of HilD expression on flagellar motility was initially investigated in the research group "Infection Biology of *Salmonella*" at the Helmholtz Centre for Infection Research [Deditius, 2013]. In this chapter, the impact of HilD on bacterial motility and the *Salmonella* transcriptome after long-term induction is further characterised.

## 3.1 Characterisation of the HilD-dependent motility phenotype

It was recently shown that HilD activates transcription of the flagellar master operon *flhDC*, but contrarily, overexpression of HilD diminishes swimming motility in semi-solid agar plates [Singer et al., 2014, Deditius, 2013]. This swimming motility defect was dependent on DNA binding of HilD since a helix-turn-helix mutant exhibited WT motility [Deditius, 2013]. A more detailed analysis of this phenotype using a strain with arabinose inducible chromosomal *hilD* ($\Delta araBAD$::*hilD*) revealed also an effect on swarming motility (Fig. 3.1A). Immunostaining of the filaments was conducted earlier [Deditius, 2013] and HilD did not affect flagellar assembly qualitatively. In this thesis, the numbers of flagella per cell body were quantified and did not show any differences (mean = 3±1.7 flagella/cell body, Fig. 3.1B), which supported the qualitative analysis performed before. Due to activation of *flhDC* transcription by HilD, swimming motility was assessed upon uncoupling of *flhDC* expression [Deditius, 2013]. Swimming motility was not restored after constitutive expression of *flhDC* and HilD overexpression, indicating that the observed phenotype is independent of HilD-mediated *flhDC* activation [Deditius, 2013]. Further, mutant strains with a randomised or deleted HilD binding site within the *flhDC* promoter region were analysed for their motility behaviour upon HilD induction. All tested HilD expressing strains were still non-motile (Fig. 3.2), which confirms the previous results with constitutive expression of *flhDC*.

## 3.2 The HilD-dependent motility defect is dependent on Spi-1

Since HilD is a key regulator for Spi-1 gene expression, the contribution of Spi-1 to the observed motility defect was characterised. The motility defect was shown to be linked to Spi-1 expression, since a deletion of Spi-1 restored swimming motility upon HilD induction [Deditius, 2013]. As presented in Fig. 3.3, HilD overexpression not only induced SicA effector protein expression after 2.5 h incubation, but also activated Spi-1 transcription homogenously. This facilitated analysis of the Spi-1-dependent mechanism behind the loss of motility. Tracking of single bacteria confirmed that a $\Delta$*spi-1* mutant displayed WT motility behaviour after HilD induction

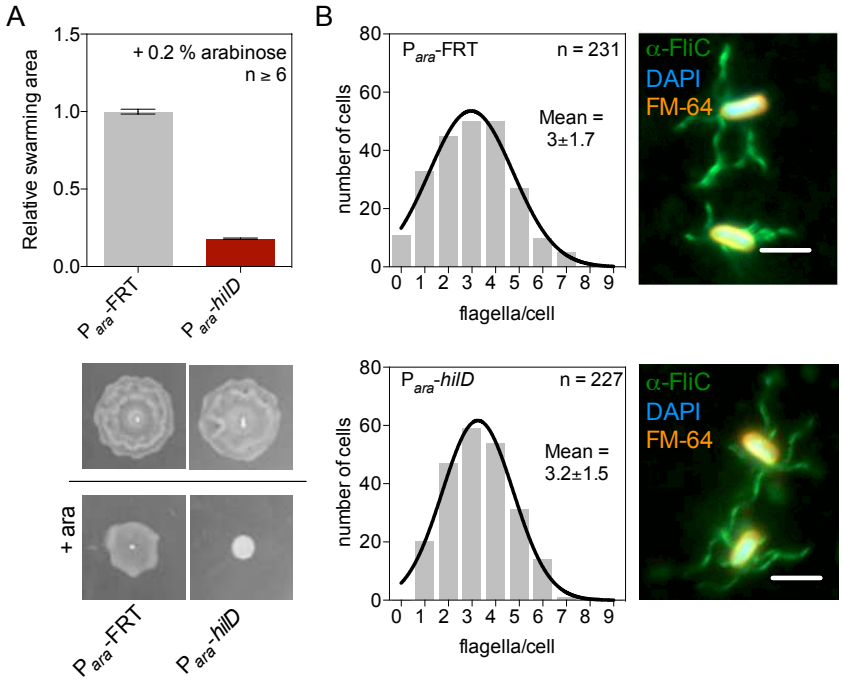


**Figure 3.1: HilD induction influences swarming motility, but not flagellar numbers.** (A) Swarming motility was examined on soft-agar plates containing 0.6 % agar at 37 °C for 8 h. Swarming areas were measured and normalised to the control strain. Bottom: Representative swarming areas of the analysed mutants. Bars represent the mean and error bars indicate the standard error of the mean. (B) Histograms of counted flagella per cell body. Flagella were immunostained using primary $\alpha$-FliC and secondary $\alpha$-rabbit Alexa488 antibody (green). DNA was stained with DAPI (blue) and membranes with FM-64 (red). Flagella were counted and average flagella numbers were calculated by Gaussian non-linear regression analysis (black line). Scale bars = 3 µm.

(Fig.3.4A). Therefore, it was analysed, which region within Spi-1 was responsible for the motility defect. Five segments within Spi-1 were deleted and their contribution to swimming motility was monitored after HilD overexpression (summarised in Fig. 3.4B). A Δ*orgA*-STM05625 mutation restored 30 % of WT motility, whereas deletions of Δ*sprB-prgI*, Δ*sptP-spaS*, Δ*sicA-invB*, and Δ*invI-invH* did not influence motility (Fig. 3.4C). This recovery was narrowed down to deletion of *hilA* (Fig. 3.4C). Notably, overexpression of the downstream transcriptional regulator HilA also resulted in decreased motility [Deditius, 2013]. HilD and HilA share many transcriptional activation sites within Spi-1, e.g. the *prg* operon [Petrone et al., 2014, Thijs et al., 2007], which could explain only a 30 % increase of swimming motility when *hilA* was deleted. Therefore, HilA induced strains with mutations in Spi-1 were investigated for motility. Deletions of *sprB*-STM05625 exhibited 75 % of WT motility (Fig. 3.4D). Within this region, structural components of the Spi-1 injectisome (*prg*/*org* operon) are encoded. However, deletions of genes that code for structural proteins (Δ*orgA*, Δ*prgI*, Δ*prgJ*, and Δ*spaPQR*) did not rescue motility upon HilD

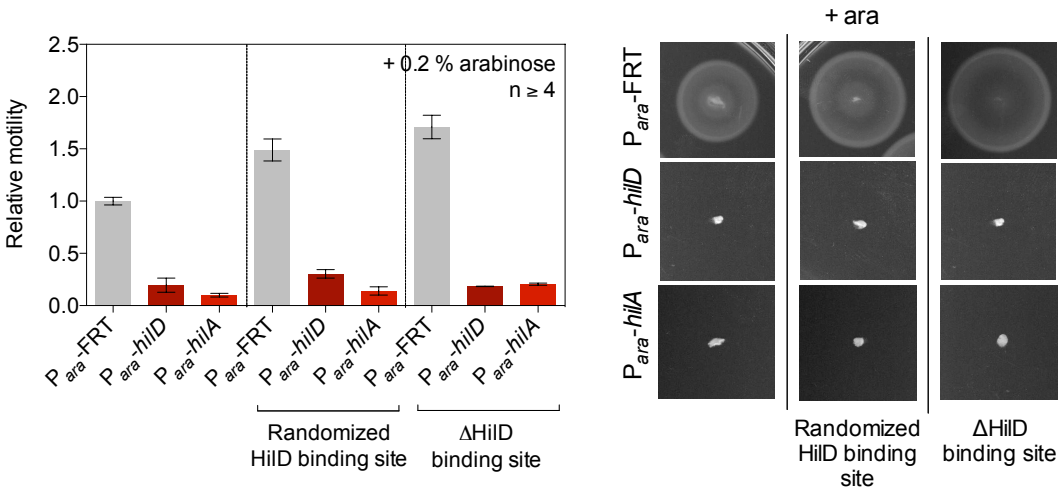


**Figure 3.2: The HilD-dependent motility defect is independent on transcription of *flhDC*.** Swimming motility was monitored as described before using HilD binding site mutations. Representative swimming halos are shown in the right panels. Bars represent the mean and error bars indicate the standard error of the mean.

overexpression (Fig. 3.4E). Also the effector protein regulator InvF and the effector proteins SipBCD were not involved in the HilD-mediated motility decrease (Fig. 3.4E). To get a better understanding of the long-term impact of HilD overexpression on Spi-1, the total RNA was analysed by sequencing. Principle component analysis (PCA) revealed that the transcriptome of the HilD-induced mutant was distinct to the control strain $P_{ara}$-FRT (Fig. 3.5A). Differentially regulated genes were determined as genes with log2 fold changes >1 (downregulation) or <-1 (upregulation). HilD overexpression led to downregulation of 751 genes and upregulation of 833 genes (Fig. 3.5B). Mainly, HilD overexpression resulted in increased levels of genes related to Spi-1 (Tab. 3.1), but also of the Spi-2 operons *sse* and *ssa*. Moreover, flagellar genes were positively regulated (e.g. *flhD*, *fljB*). Especially genes located between *sprB* and *sicA* were highly upregulated, which is in agreement with the observed motility rescue in a HilA induced strain (Tab. 3.1).

It was described previously that Spi-1 induction affects growth of *Salmonella* [Sturm et al., 2011]. Therefore, excessive expression of injectisome structural components, e.g. Prg and Org proteins, might result in a collapse of proton motive force (PMF) and in a loss of motility. Consequently, only a deletion of multiple genes would restore motility. Bacterial growth was monitored upon HilD induction. As expected, HilD induction resulted in reduced growth when entering stationary growth phase (Fig. 3.6 small panels). This might be due to increasing relative oxygen and ATP consumption rates after overexpression of HilD (Fig. 3.6 major panels).

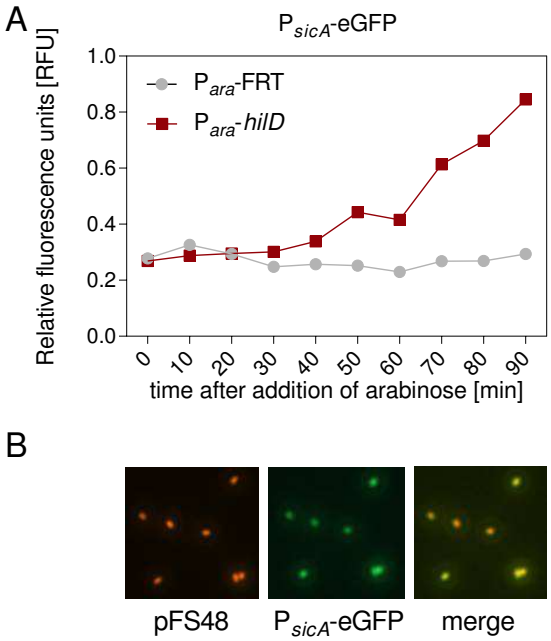


**Figure 3.3: HilD-induction increases Spi-1 effector protein transcription homogenously.** (A) Fluorescence intensities of a P$_{sicA}$-eGFP fusion after HilD-induction. Samples were taken every 10 min after HilD-induction. The $OD_{600}$ and the fluorescence units were measured in a Varioskan Flash Plate Reader. (B) Representative fluorescence images of a P$_{sicA}$-eGFP fusion strain constitutively expressing mCherry on a plasmid (pFS48) after 3 h HilD-induction.

## 3.3 HilD regulates expression of adhesive systems in *Salmonella*

Interestingly, the transcriptome analysis revealed increased levels of genes coding for adhesive structures (Fig. 3.7A). These structures belong to the Spi-4 (STM4257-STM4262), curli (*csgC*, *csgEFG*, and *csgD*), Pef, or Saf adhesive systems. Moreover, a previously described multiprotein immunoglobulin adhesion system ZirSTU (STM1667-STM1669), whose function is still unknown, was upregulated (Fig. 3.7A). Consistently, also transcript levels of major structural subunits of the described fimbriae were highly increased after HilD induction as determined by qRT-PCR analysis (Fig. 3.7B). Preliminary flow cytometry analyses showed that Pef and Saf fimbrial proteins were also present on the bacterial surface (Data not shown). Thus, epithelial cell adhesion was analysed after HilD- and HilA-induction in a Δ*spi-1* background. HilD-overexpression led to increased adhesion to MODE-K murine epithelial cells, which is independent of Spi-1 (Fig. 3.7C).

## 3.4 Discussion

During Infection, *Salmonella* has to quickly adapt to changing environmental conditions to ensure successful infection of the host epithelium. One important virulence factor that has to be tightly regulated and enables bacteria-host interactions is the flagellum. Previously, the Spi-1 transcriptional activator HilD was described to induce flagellar gene expression [Singer et al., 2014], but overexpression also caused a loss of swimming motility independently of flagella assembly [Deditius, 2013]. In this chapter, the motility defect was shown to be dependent on Spi-1, but not on its structural components. Transcriptomic analyses revealed high expression of Spi-1 genes, especially between the *sprB* and *sicA* loci on the chromosome. Excessive expression of injectisome-related proteins might therefore contribute to a collapse of proton motive force (PMF). This would lead to a loss of motility since flagellar rotation is driven by PMF. A defect in bacterial growth as a response to Spi-1 expression was already described earlier [Sturm et al., 2011]. Interestingly, oxygen and ATP consumption rates were increased, indicating that changes in metabolism contribute to the observed motility defect.

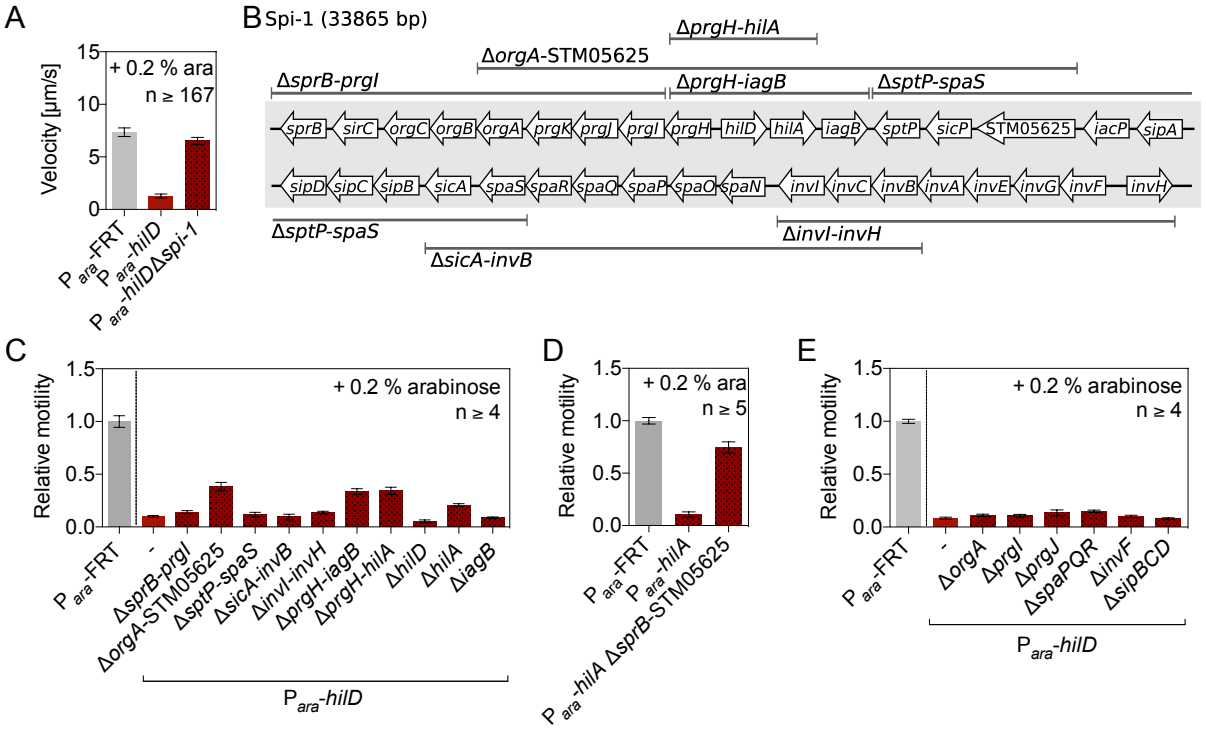


**Figure 3.4: The HilD-mediated motility defect is Spi-1-dependent.** (A) Single cells of a Δ*spi-1* mutant upon HilD-induction were recorded and trajectories were analysed to measure bacterial swimming velocities. (B) Scheme of *Salmonella* pathogenicity island 1 (Spi-1) and the respective mutations analysed in (C). (C-E) Swimming motility was analysed in semi-solid agar plates as described before. Bars represent the mean and error bars indicate the standard error of the mean.

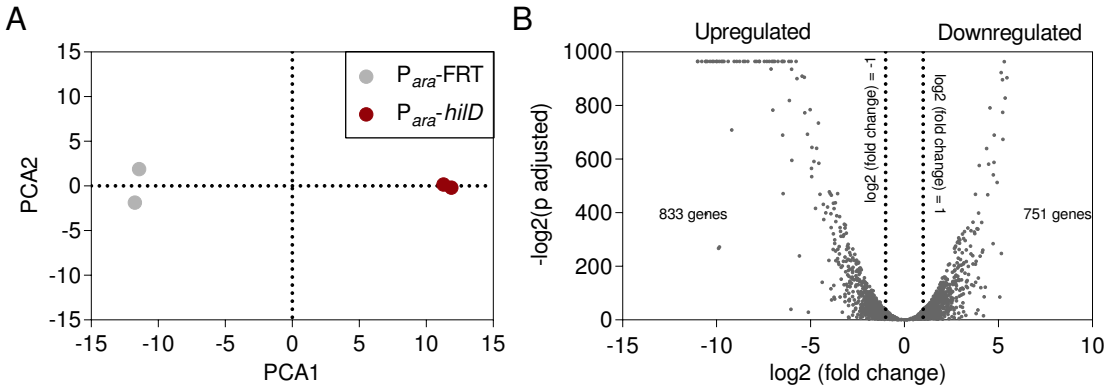


**Figure 3.5: Transcriptome analysis upon HilD overexpression.** Transcriptome data analysis was performed by Abilash Chakravarthy Durairaj (HZI). (A) PCA plot for P$_{ara}$-FRT and P$_{ara}$-*hilD* conditions. Within-sample normalisation was done based on the Transcripts Per Million (TPM). The TPM values of genes less than one variance were removed. The log2 of the TPM values were used to make the PCA plot. (B) Volcano plot showing all differentially expressed genes. DESeq2 was used to calculate the log2(fold change) and the corresponding adjusted p values for the genes, by comparing the expression profile of P$_{ara}$-FRT samples against P$_{ara}$-*hilD* samples.

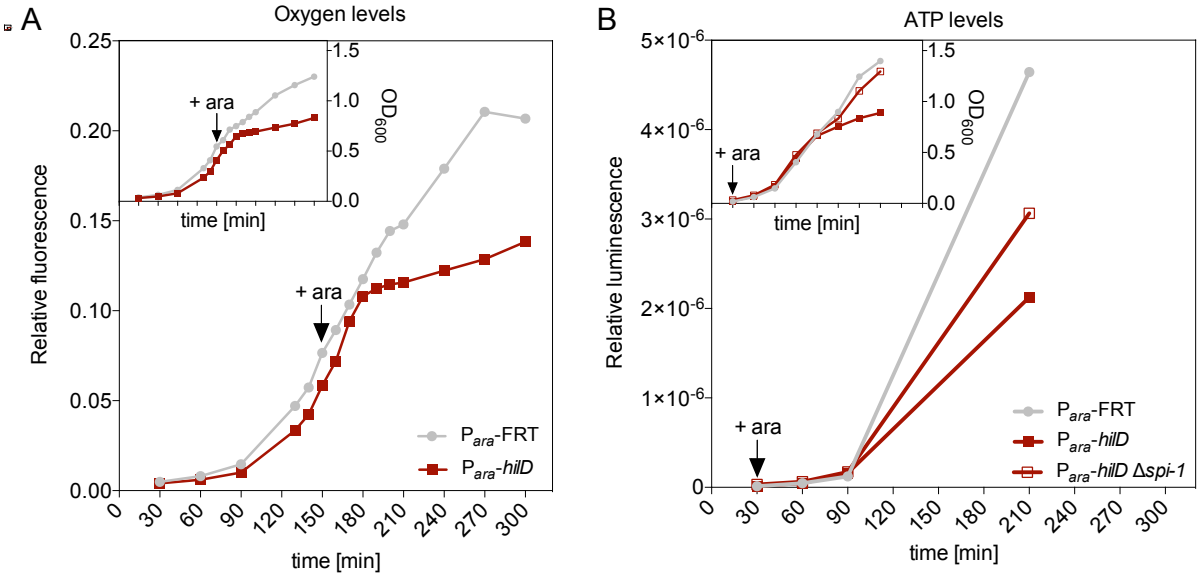


**Figure 3.6: Oxygen and ATP levels.** (A) Oxygen levels were measured using the fluorescent dye ruthenium tris(2,2'-dipyridyl) dichloride hexahydrate (RTDP) after HilD induction within different growth phases (small panel). (B) ATP levels were analysed after HilD induction using the BacTiter-Glo$^{TM}$ Reagent and measurement of luminescence intensities. Relative oxygen and ATP levels were calculated by normalising the absolute fluorescence and luminescence intensities to the $OD_{600}$ (major panels).

**Table 3.1: Transcription of Spi-1 genes upon HilD overexpression.**

| Gene | Transcripts per million (TPM)* | Fold-change* | HilD binding site** | HilA binding site** |
|---|---|---|---|---|
| *sprB* | 1081 | -7.73 | yes | - |
| *sirC* | 7159 | -7.11 | yes | - |
| *orgC* | 3153 | -7.96 | - | - |
| *orgB* | 4560 | -7.45 | - | - |
| *orgA* | 4335 | -9.38 | - | - |
| *prgK* | 7664 | -9.67 | - | - |
| *prgJ* | 10,681 | -9.98 | - | - |
| *prgI* | 16,922 | -10.35 | - | - |
| *prgH* | 13,872 | -10.28 | yes | yes |
| *hilD* | 29,167 | -8.57 | yes | yes |
| *hilA* | 1709 | -9.06 | yes | yes |
| *iagB* | 738 | -8.34 | - | - |
| *sptP* | 4282 | -6.57 | - | - |
| *sicP* | 6405 | -6.73 | - | - |
| STM05625 | 20,226 | -6.49 | - | - |
| *iacP* | 10,142 | -7.87 | - | - |
| *sipA* | 8679 | -9.67 | - | - |
| *sipD* | 5427 | -10.02 | - | - |
| *sipC* | 15,201 | -10.58 | - | - |
| *sipB* | 12,184 | -10.79 | - | - |
| *sicA* | 17,385 | -11.00 | - | yes |
| *spaS* | 1087 | -8.94 | - | - |
| *spaR* | 318 | -8.49 | - | - |
| *spaQ* | 594 | -9.19 | - | - |
| *spaP* | 2901 | -9.87 | - | - |
| *spaO* | 1733 | -9.61 | - | - |
| *spaN* | 2304 | -9.95 | - | - |
| *invI* | 11,599 | -10.49 | - | - |
| *invC* | 956 | -9.77 | - | - |
| *invB* | 6301 | -10.33 | - | - |
| *invA* | 2054 | -9.95 | yes | yes |
| *invE* | 1247 | -10.15 | - | - |
| *invG* | 2451 | -10.15 | - | - |
| *invF* | 6893 | -10.34 | yes | yes |
| *invH* | 1778 | -7.72 | yes | yes |

* All values are relative to the control strain.

** Binding sites according to [Petrone et al., 2014, Thijs et al., 2007].

The HilD regulon was extensively studied before [Petrone et al., 2014, Colgan et al., 2016, Smith et al., 2016]. Spi-1, Spi-2, and Spi-4 are upregulated by HilD [Main-Hester et al., 2008, Saini and Rao, 2010], which was confirmed in this study. Further, Spi-4-related transcript

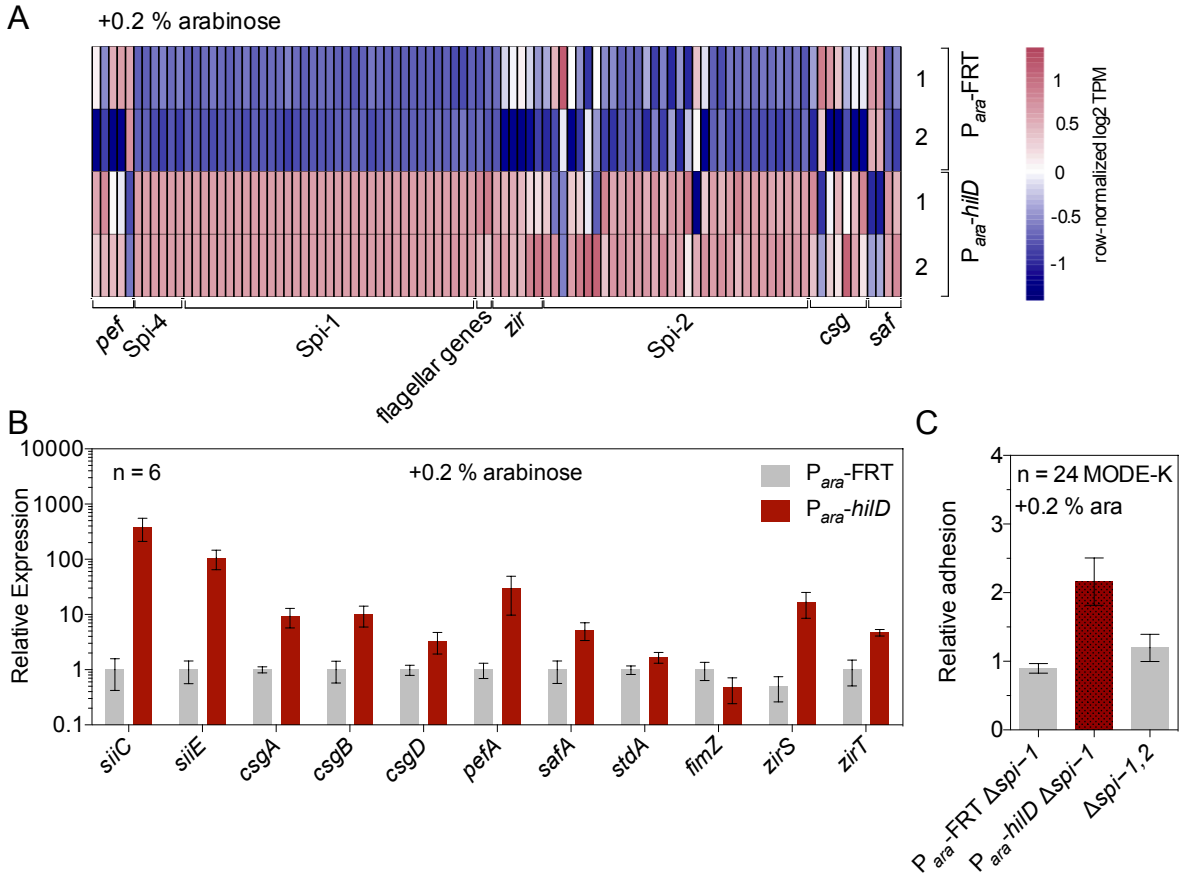


**Figure 3.7: HilD activates expression of adhesive structures in *Salmonella* Typhimurium.** (A) Heatmap of selected differentially expressed genes. The expression profile of selected genes of interest for this study was compared. The TPM values of these selected genes of interest were row normalised across the samples belonging to both the P$_{ara}$-FRT and P$_{ara}$-*hilD* conditions. (B) Relative *siiC*, *siiE*, *csgA*, *csgB*, *csgD*, *pefA*, *safA*, *stdA*, and *fimZ* gene expression of a P$_{ara}$-*hilD* mutant compared to the P$_{ara}$-FRT control strain was analysed using qRT-PCR. Experiments were performed with 6 biological replicates. (C) MODE-K murine epithelial cells were infected with Δ*spi-1 Salmonella* strains at a MOI of 10 for 1 h at 37 °C. After extensive washing, cells were lysed and plated for CFU assessment. Bars represent the mean and error bars indicate the standard error of the mean.

levels were increased after HilD expression. The conducted transcriptomic screen supports a regulatory link between HilD and *Salmonella*-specific methyl-accepting chemotaxis proteins, McpA and McpC [Colgan et al., 2016]. Also uncharacterised genes (STM05010, STM1329, STM1330, STM1600, STM1854, STM2585, STM4079.s, STM4310, STM4312 and STM4313) were upregulated by HilD, as already described before [Colgan et al., 2016, Smith et al., 2016]. However, in this thesis numerous additional genes were differentially expressed, due to different experimental conditions. Colgan et al. used a Δ*hilD* deletion strain, whereas Smith et al. expressed HilD from a plasmid for a very short time period. This enabled the authors to

identify direct regulatory effects of HilD. Here, HilD was overexpressed for longer time periods to ensure a broad overview of up- and downregulated pathways. Notably, this allowed to determine genes indirectly regulated via HilD, for instance upregulation of various adhesion operons was observed and confirmed by qRT-PCR. HilD overexpression led to upregulation of curli and Pef fimbriae, Saf pili, and a recently described multiprotein immunoglobulin adhesion system ZirSTU [Gal-Mor et al., 2008, Prehna et al., 2012]. Curli fimbriae are amyloid-like proteinaceous substances that are ultimately controlled by the master regulator CsgD [Prigent-Combaret et al., 2001, Barnhart and Chapman, 2006]. The *pef* operon is located on the *Salmonella* virulence plasmid [Ledeboer et al., 2006] and repressed by the histone-like protein H-NS [Nicholson and Low, 2000]. H-NS also represses Spi-2 expression by direct binding. HilD displaces H-NS from its binding region in target promoters and enables transcription of the SsrAB two-component system [Martínez et al., 2014, Bustamante et al., 2008]. The contribution of HilD to activation of *pef* genes might resemble this mechanism and needs further investigation. Upon colonisation of the host's epithelium, HilD induction does not only enable expression of the Spi-1 injectisome, but also abolishes bacterial motility. In a separate process, HilD activates expression of adhesion factors that ensure initial contact with the host. This might facilitates injection of effector proteins into eukaryotic cells and contribute to efficient colonisation of the host's intestine.

# 4 Flagellin Phase-dependent Swimming on Cell Surfaces Contributes to Host Cell Invasion in *Salmonella* Typhimurium

The flagellar filament consists out of approximately 20 000 subunits of a single protein, flagellin. In *Salmonella* Typhimurium, two antigenically distinct flagellin proteins, FliC or FljB, are expressed in a process termed "flagellar phase variation" (Fig. 4.1). Each of the flagellin encoding genes is located at distinct chromosomal loci. The *fliC* locus resides within a cluster of operons that code for structural components of the flagellum and that is orthologous to the *Escherichia coli fliC* gene [Macnab, 1992]. Since *fliC* is found in all *Salmonella* species, it was suggested that *fliC* is the ancestral flagellin-encoding gene. The *fljB* gene is part of the *fljBA* operon, which was acquired by a *Salmonella enterica* ancestor [Porwollik et al., 2002]. Flagellar phase variation depends on the orientation of a 996 bp DNA fragment, the H segment. This segment harbours a $\sigma^{28}$-dependent promoter of the acquired *fljBA* operon [Silverman et al., 1979, Zieg et al., 1977, Zieg and Simon, 1980]. In the *fljB*$^{\mathrm{ON}}$ phase, transcription of *fljBA* occurs resulting in expression of FljB flagellin and FljA. FljA interacts with *fliC* mRNA and posttranscriptionally inhibits *fliC* translation [Bonifield and Hughes, 2003, Aldridge et al., 2006]. The H segment is flanked by two 26 bp inverted repetitive sequences, *hixL* and *hixR*, and encodes the DNA invertase Hin [Kutsukake and Iino, 1980, Silverman and Simon, 1980]. Hin targets *hixL* and *hixR* and inverts the H segment through site-specific recombination [Johnson and Simon, 1985]. In this *fliC*$^{\mathrm{ON}}$ phase, the *fljBA* operon is not transcribed due to an inverted promoter, which leads to derepression of *fliC* mRNA translation and expression of the second flagellin, FliC.

The FliC monomer structure was solved and shows a hairpin-like structure with four connected domains, D0, D1, D2, and D3 [Yonekura et al., 2003]. The N- and C-termini form the D0 and D1 domains. Those domains are highly conserved between FliC and FljB and are rich in hydrophobic residues. This enables the formation of a coiled-coil structure and flagellin polymerisation [Yonekura et al., 2003, Beatson et al., 2006]. The central part is highly variable and builds up the D2 and D3 domains.

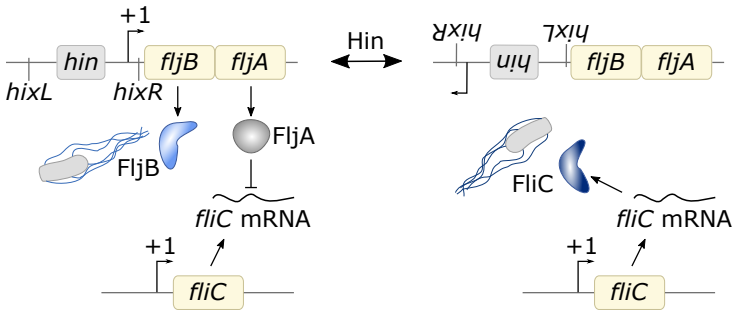


**Figure 4.1: Schematic representation of flagellar phase variation.** In the *fljB*$^{\mathrm{ON}}$ phase, the *fljBA* operon is expressed, leading to FljB filament assembly and inhibition of *fliC* mRNA translation by FljA. The promoter of *fljBA* is located within an invertible segment between *hixL* and *hixR*. In the *fliC*$^{\mathrm{ON}}$ phase, this segment is inverted by the recombinase Hin, disabling expression of the *fljBA* operon and thus allowing translation of *fliC* mRNA.

Besides the well-characterised genetic switch between both flagellin phases, the biological relevance of the two distinct flagellins remains unknown. It was described that FljB-expressing *Salmonella* strains were less virulent in orally and intravenously infected mice [Ikeda et al., 2001]. In contrast, strains constitutively expressing FliC were attenuated in the mouse model [Miao et al., 2010]. Since flagellar phase variation plays a major role during systemic infection and in modulating the host immune defence, this chapter focuses on the contribution of flagellar phase variation during early stages of gastrointestinal infection.

## 4.1 Flagellar phase variation and its impact on colonisation of the intestinal tract

For elucidating the contribution of flagellar phase variation in *Salmonella* virulence, it was determined which *Salmonella* isolate was most suitable for infection experiments. The frequently used *Salmonella* background LT2 is highly attenuated for virulence in the mouse model due to a mutation in *rpoS* [Swords et al., 1997, Bearson et al., 1996]. Together with the virulent strains ATCC14028s and SL1344, the avirulent LT2 strain was tested for their efficacy to infect C57BL/6 mice in the gastroenteritis model. Bodyweights were recorded and the health condition of each mouse was monitored daily (see Chapter 7.8.1). Accordingly, the strain background LT2 caused only slight changes in bodyweight (Fig. 4.2A). Infection with *Salmonella* Typhimurium ATCC14028s led to rapid decrease of bodyweights, which was even more pronounced for infection with SL1344 after 2 days post infection (Fig. 4.2A). Also analysis of mouse survival showed that only 50 % of mice died 10 days after infection with LT2 (Fig. 4.2B). Infection with ATCC14028s and SL1344 killed all mice after 8 and 5 days post infection, respectively. Therefore, for following infection experiments the virulent SL1344 strain background was used.

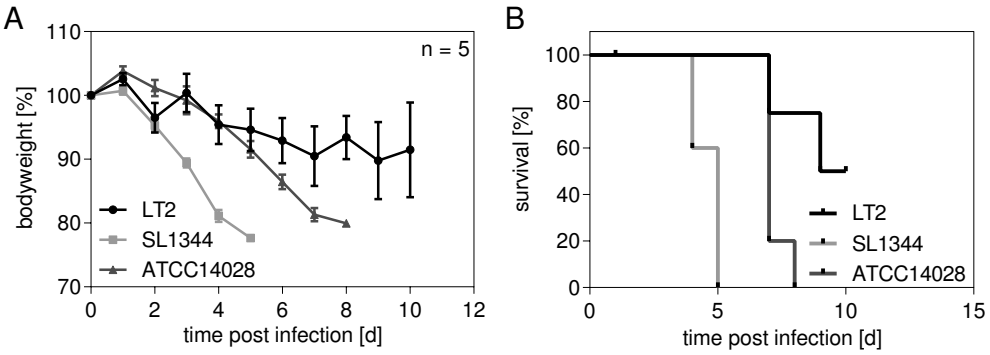


**Figure 4.2: Bodyweights and survival of mice after infection with various *Salmonella enterica* isolates.** Streptomycin pre-treated C57BL/6 mice were infected with $10^7$ CFU of different *Salmonella enterica* isolates. Bodyweights were measured once a day and mice were classified according their behaviour (see Chapter 7.8.1). Mice were sacrificed upon 20 % loss of bodyweight. Adapted from [Horstmann et al., 2017].

The impact of flagellar phase variation on *Salmonella* pathogenesis was investigated using strains that were locked in either FliC or FljB expression via deletion of the recombinase-encoding gene *hin*. Flagellin secretion into the culture supernatant confirmed the presence of only one flagellin in comparison to the WT (Fig. 4.3A). Deletion of *hin* had no effect on bacterial growth in LB or TB medium (Fig. 4.3C) and did not affect growth in co-cultures (Fig. 4.3B).

Colonisation of the intestine in the murine gastroenteritis model was assessed after oral infection with FliC- or FljB-expressing phase variation mutants. Streptomycin pre-treated mice were infected with a 1:1 mixture of both strains harbouring distinct resistance cassettes. The bacterial load in intestinal organ tissues and the luminal content was examined after 6 h, 24 h, and 48 h post infection (p.i.). The competitive indices within the mesenteric lymph nodes, small intestine,

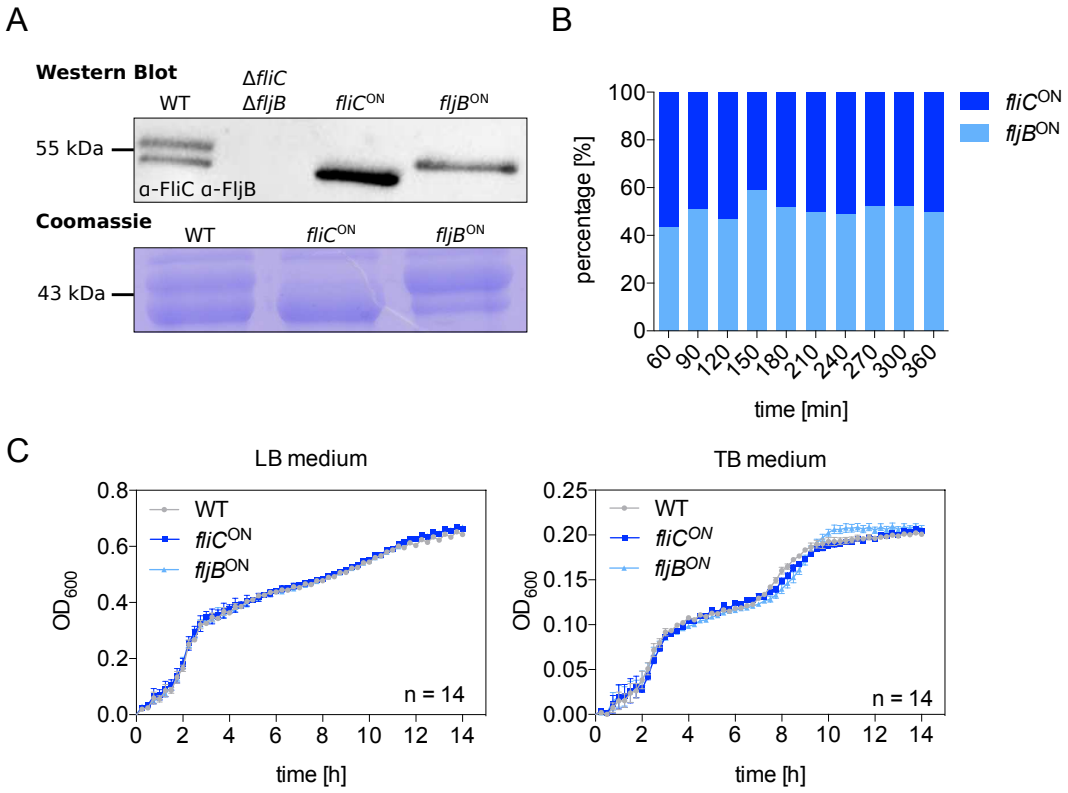


**Figure 4.3: Flagellin secretion and growth of flagellar phase variants.** (A) Proteins were precipitated from the culture supernatant using 10 % TCA. Flagellin variants were detected using $\alpha$-FliC and $\alpha$-FljB antibodies or by Coomassie staining. (B) Growth competition assay. Growth in co-culture was monitored to avoid growth-dependent phenotypes in mouse competition experiments using strains with different antibiotic resistance cassettes in LB medium. Bacteria were plated in serial dilutions with appropriate antibiotics at defined time points. The proportion of each strain was calculated. (C) Bacterial growth was determined by measuring the optical density at 600 nm under agitation conditions every 15 min for 13 h with 14 biological replicates of each strain. Data show the mean and the standard error of the mean. Adapted from [Horstmann et al., 2017].

ceacum, and colon tissue indicated that FliC-expressing bacteria significantly outcompeted FljB-expressing strains more than 2-fold (Fig. 4.4A-C). The strongest competition effect was seen 6 h post infection in the small intestine with a 7-fold increase for the *fliC*$^{ON}$ strain (Fig. 4.4A), indicating that flagellar phase variation plays an important role during early infection. Within the luminal content, no significant difference was observed between both strains (Fig. 4.4C). Effects of the streptomycin-treatment on invasion of the small intestine were excluded using the typhoid infection model without streptomycin pre-treatment. The overall bacterial load in the gastrointestinal tissue was lower than in the gastroenteritis model. However, a colonisation advantage of the FliC-expressing strain was confirmed in the small intestine (Fig. 4.4D).

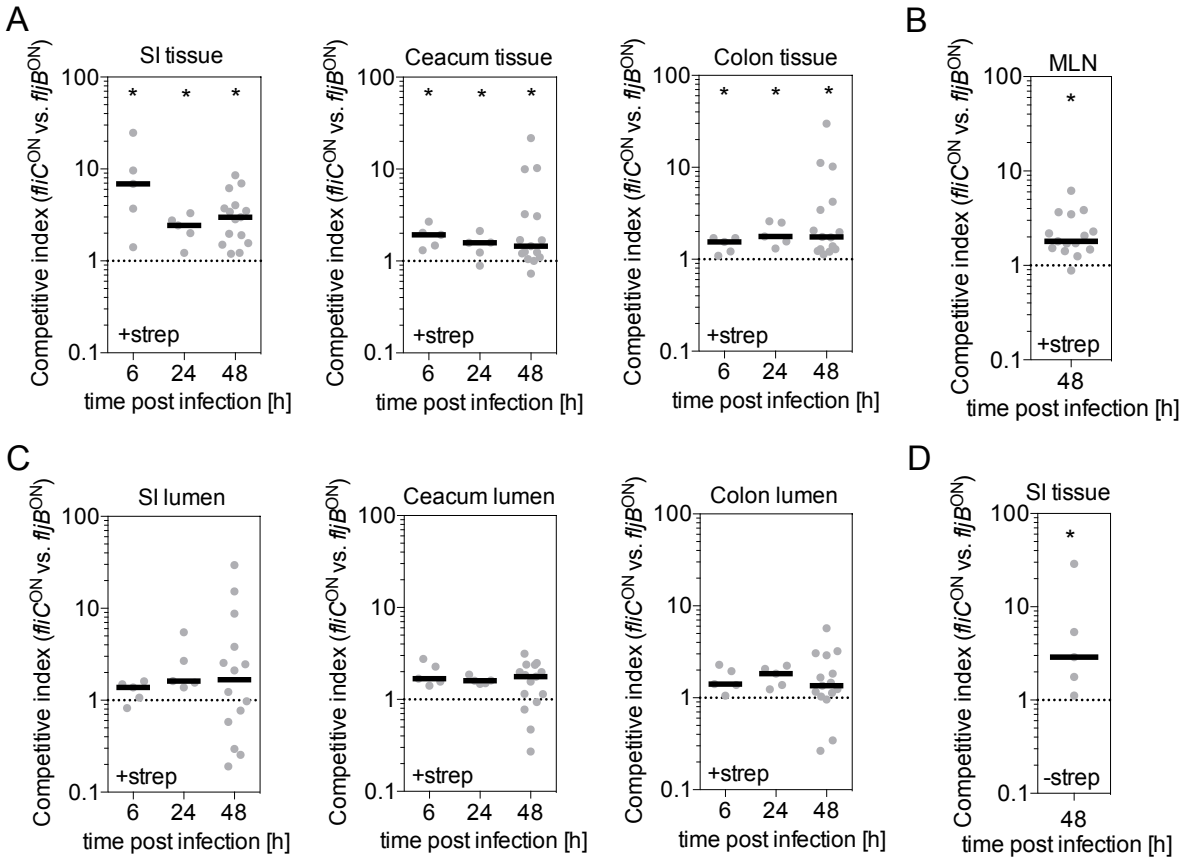


**Figure 4.4: Flagellar phase variation influences *Salmonella* virulence *in vivo*.** (A-C) Streptomycin pre-treated C57BL/6 mice were infected with $10^7$ CFU of phase locked mutants with distinct antibiotic resistance cassettes. (A) 6 h, 24 h, and 48 h post infection (p.i.), organs (small intestine (SI), colon, and ceacum) were taken and washed to collect the luminal content (C). (B) 48 h p.i., mesentheric lymph nodes (MLN) were isolated. (D) C57BL/6 mice without streptomycin treatment were infected with $10^8$ CFU. The SI was isolated 48 h p.i. and all samples were homogenised and plated on appropriate antibiotic resistance plates. Colonies were counted and competitive indices (CI) were calculated. Replicates are shown as individual data points and analysed by the Student's *t*-test. Asterisks indicate a significantly different phenotype to the value 0 (* = P<0.05). Adapted from [Horstmann et al., 2017].

The described competitive advantage of FliC-expressing bacteria might be due to alterations in the innate immune response. To address this question, the role of flagellar phase variation during later steps of infection, such as macrophage survival or cell death, was assessed. Macrophage cell death and survival depended on the presence of flagellin, but no differences between infections with *fliC*$^{ON}$ or *fljB*$^{ON}$ strains were observed (Fig. 4.5).

## 4.2 FliC-expressing bacteria invade eukaryotic cells more efficiently dependent on motility

Previously, it was described that flagellar motility and swimming on host cell surfaces is important for selection of invasion sites [Misselwitz et al., 2012]. However, stopping at particular entry sites was shown to be independent of the Spi-1 injectisome and fimbriae [Misselwitz et al., 2012]. Therefore, the impact of flagellar phase variation on selection of invasion sites was analysed *in vitro* via infection of eukaryotic cells. Invasion of MODE-K murine epithelial cells revealed that the *fliC*$^{ON}$ mutant was approximately 2-fold more invasive than the *fljB*$^{ON}$ mutant (Fig. 4.6A left panel). However, invasion of FljB-expressing bacteria increased upon forced contact with the

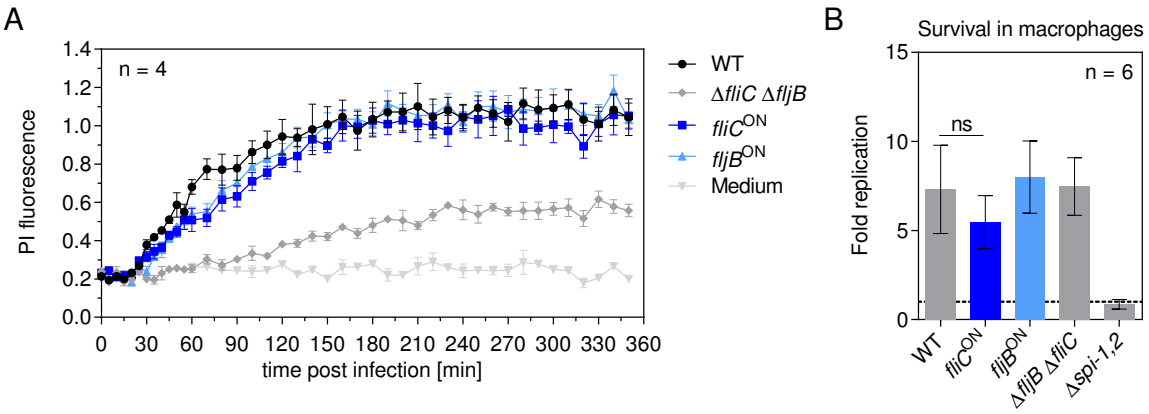


**Figure 4.5: Effect of flagellar phase variation on macrophage cell death and survival.** (A) Bone-marrow derived macrophages were pre-treated with propidium iodide (PI) and infected with flagellin phase variants at a MOI of 50 with centrifugation. PI fluorescence was measured every 10 min. The data represents the mean of 4 biological replicates and error bars show the standard error of the mean. (B) J774 murine macrophage-like cells were infected with flagellin phase variants at a MOI of 10 for 30 min at 37 °C after centrifugation of *Salmonella* onto the cells. Extracellular bacteria were killed by addition of gentamicin for 1 h and incubated with a decreased concentration of gentamicin for 21 h. J774 cells were lysed and serial dilutions were plated on LB agar for CFU assessment. All values are normalised to the macrophage uptake (dotted line). Bars represent the mean and error bars show the standard error of the mean. A Student's *t* test was applied to determine statistical significance (ns = not significant, P>0.05). Adapted from [Horstmann et al., 2017].

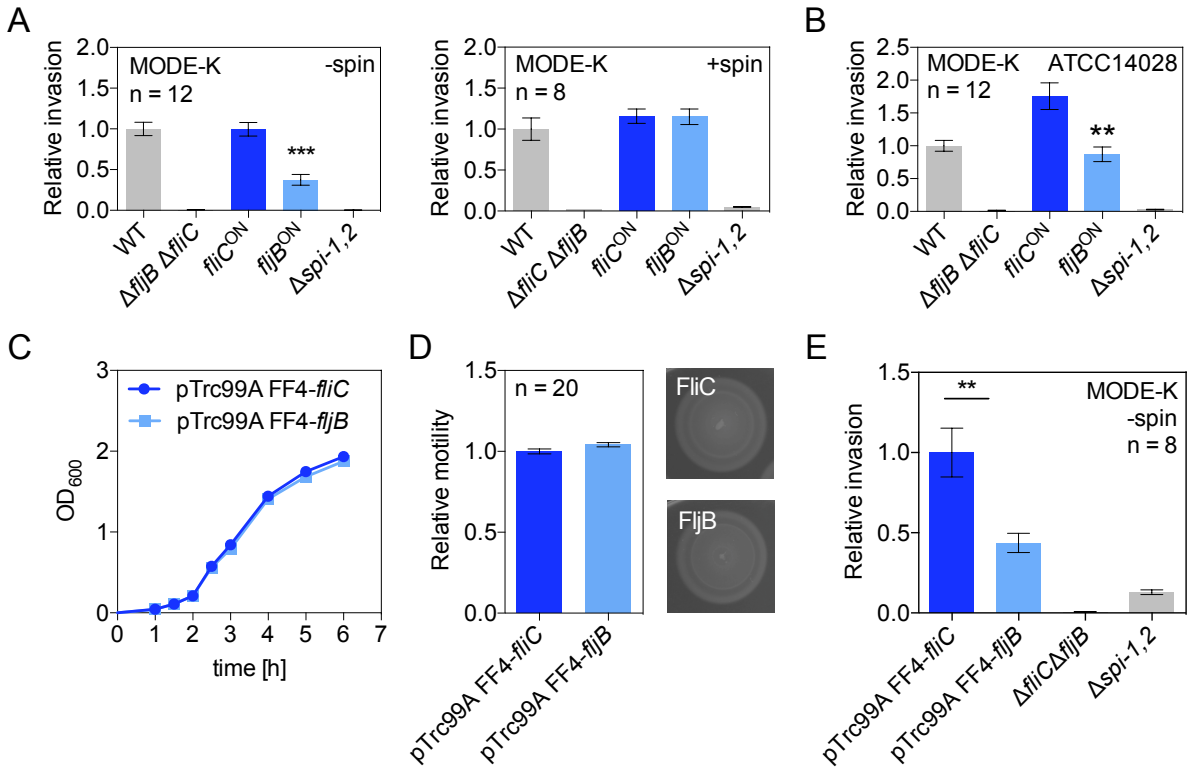


**Figure 4.6: Flagellin phase has an impact on MODE-K epithelial cell invasion.** MODE-K murine epithelial cells were infected with flagellin phase variants at a MOI of 10 for 1 h at 37 °C without (A left panel) and with (A right panel) centrifugation of *Salmonella* onto the epithelial cells. Extracellular bacteria were killed by addition of gentamicin for 1 h. Cells were lysed and serial dilutions were plated on LB agar for CFU assessment. All values were normalised to the inoculum and WT invasion. (B) MODE-K epithelial cell invasion after infection with flagellar phase variants of *Salmonella* Typhimurium ATCC14028s. (C-E) Episomal expression of flagellin has no effect on bacterial growth (C) and swimming motility (D). (E) Invasion of MODE-K cells using strains that express flagellin episomally. A Student's *t*-test was applied to determine statistical significance (** = P<0.01; *** = P<0.001). Adapted from [Horstmann et al., 2017].

host cell surface by centrifugation (Fig. 4.6A right panel). Residual invasion of a Δ*spi-1,2* mutant might be due to injectisome-independent cell invasion as described in [Hänisch et al., 2010]. Invasion experiments using strains derived from the ATCC14028s background also showed increased invasion for the *fliC*$^{ON}$ strain (Fig. 4.6B). To exclude side effects due to the different genomic loci of *fliC* and *fljB*, flagellins were expressed episomally from a plasmid. Both pTrc99A FF4-*fliC* and pTrc99A FF4-*fljB* mutants exhibited the same growth and motility behaviour, but displayed a disadvantage of FljB-expressing strains in eukaryotic cell invasion (Fig. 4.6C-E). Moreover, host cell adhesion was monitored after infection with flagellin phase variants in a Δ*spi-1* background to inhibit injectisome-dependent invasion. After extensive washing, the same number of bacteria remained attached to the MODE-K epithelial cell surface (Fig. 4.7A). A

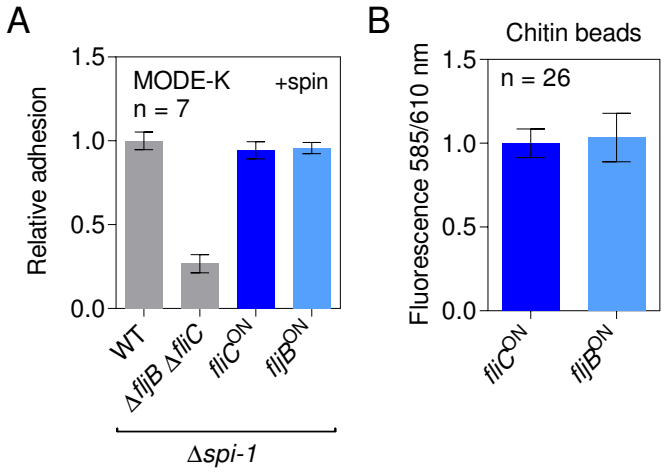


**Figure 4.7: Eukaryotic cell adhesion is not affected by flagellin phase.** (A) MODE-K murine epithelial cells were infected with various flagellin mutants lacking Spi-1 at a MOI of 10 for 1 h at 37 °C. The deletion of Spi-1 genes prevents injectisome-dependent invasion and allows for quantitative analysis of bacteria adhering to the epithelial cell surface. After extensive washing, cells were lysed and plated for CFU assessment. (B) Magnetic chitin beads were incubated with fluorescent, exponentially grown bacterial cultures ($OD_{600}$=0.5) for 1 h at 37 °C. After washing, fluorescence of adhering bacteria was measured. The bars represent the mean and the standard error of the mean are given. Adapted from [Horstmann et al., 2017].

flagellin double knockout strain (Δ*fliC* Δ*fljB*) served as negative control and showed a reduction in adhesion (Fig. 4.7A) consistent with the role of the flagellar filament as important adhesive structure. Adhesion to chitin beads supported that flagella made of FliC or FljB have similar adhesive properties (Fig. 4.7B).

In order to characterise the mechanism by which *fliC*$^{\mathrm{ON}}$ bacteria invade more efficiently than *fljB*$^{\mathrm{ON}}$ bacteria, eukaryotic host cell specificity was analysed using multiple eukaryotic cell lines. The novel Cl10 cell line was developed from immortalised primary murine gut epithelial goblet-like cells and thus mimics the native intestinal environment *in vitro*. Additionally, a variety of established epithelial cell lines, such as E12, HeLa, HEp-2, T84, IPEC-J2, and CACO-2 cells were used. In agreement with the invasion advantage of the *fliC*$^{\mathrm{ON}}$ mutant for MODE-K cells, FliC-expressing bacteria exhibited an advantage in cell invasion for the majority of the analysed cell lines (Fig. 4.8). However, differential invasion was not observed for the human epithelial cell line CACO-2, the porcine epithelial cell line IPEC-J2, and the murine fibroblast cell line NIH 3T3 (Fig. 4.8F-H). No correlation between mucus production and differential invasion of the tested mutants was found (Fig. 4.9). Scanning electron microscopy revealed that CACO-2, IPEC-J2, and NIH 3T3 cell lines showed less prominent cell topologies, whereas especially Cl10, HeLa, HEp-2, and E12 cells exhibited numerous microvilli and membrane ruffles (Fig. 4.10).

This indicated that the topology of the host cell surface mediates flagellin-dependent invasion and contributes to the observed invasion advantage for FliC-expressing bacteria.

## 4.3 Contribution of the Spi-1 injectisome and flagellar rotation to epithelial cell invasion

Recently, it was described that cell invasion can occur independently of the Spi-1 injectisome [Rivera-Chávez et al., 2016]. Therefore, host cell invasion was monitored using flagellar phase variants in a Δ*spi-1* background. Upon deletion of Spi-1, FliC- and FljB-expressing bacteria

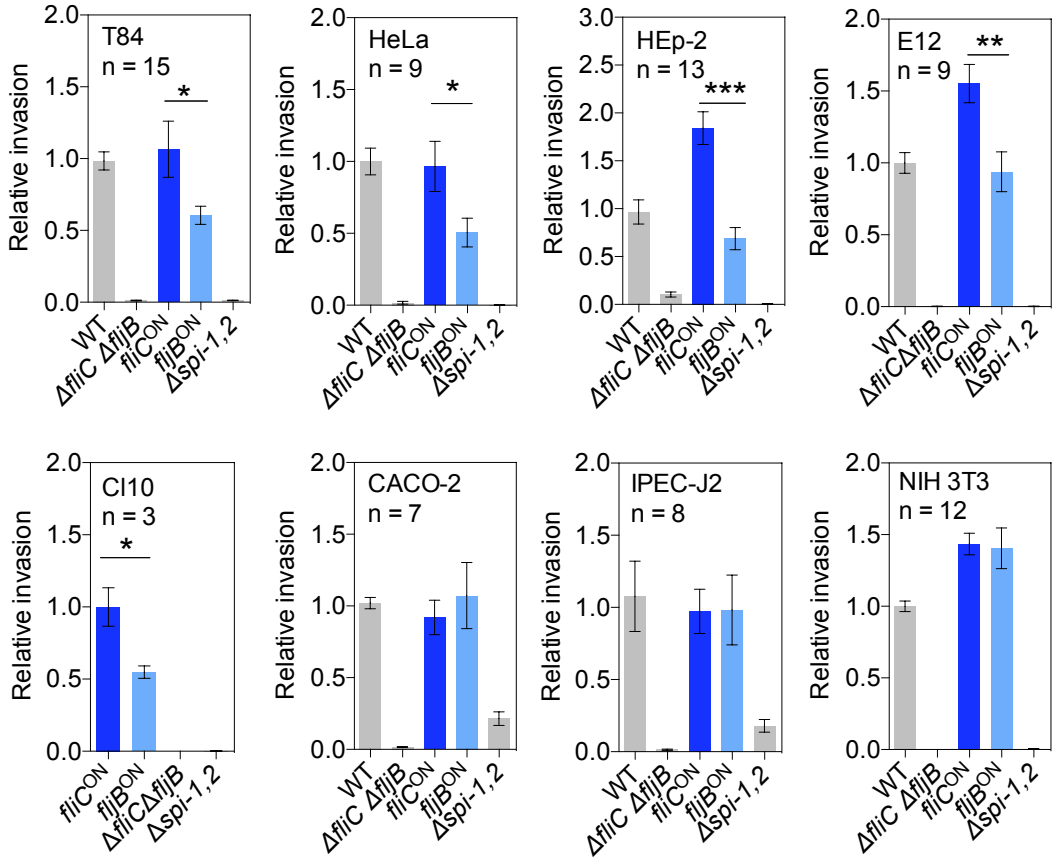


**Figure 4.8: Eukaryotic cell invasion of flagellar phase variants is cell type specific.** The human epithelial cell lines T84, HeLa, HEp-2, E12, and CACO-2, the murine epithelial cell line Cl10, the porcine epithelial cell line IPEC-J2, and the murine fibroblast cell line NIH 3T3 were infected with flagellar phase variants at a MOI of 10 for 1 h at 37 °C. Extracellular bacteria were killed by addition of gentamicin for 1 h. Cells were lysed and serial dilutions were plated on LB agar for CFU assessment. All values were normalised to the inoculum. Data from Cl10 invasion assays were normalised to the *fliC*$^{\mathrm{ON}}$ strain in WT background. A Student's *t*-test was applied to determine statistical significance (* = P<0.05; ** = P<0.01; *** = P<0.001). The bars represent the mean and the standard error of the mean. Adapted from [Horstmann et al., 2017].

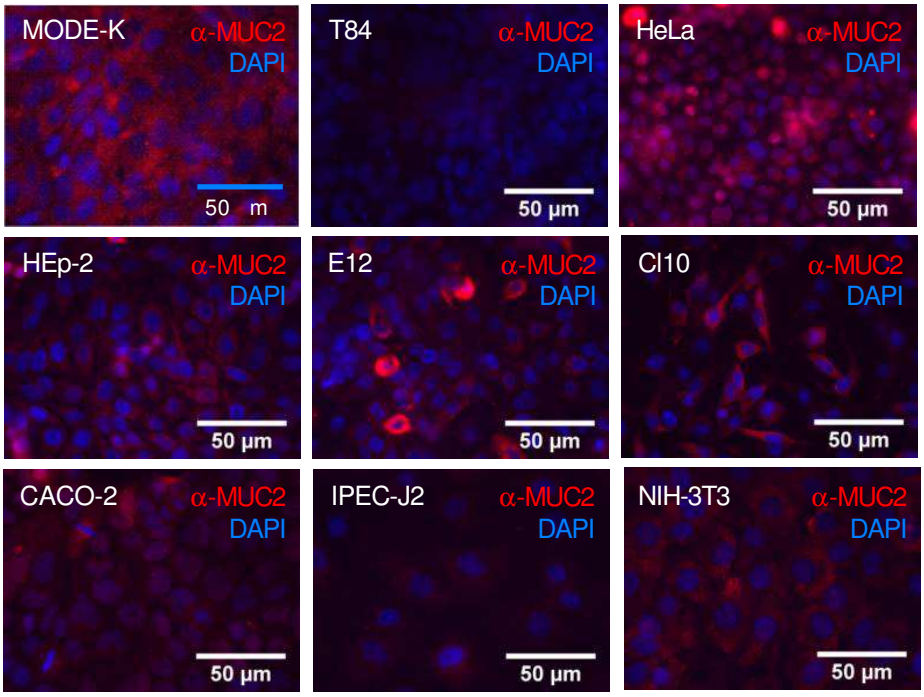


**Figure 4.9: MUC2 staining of eukaryotic cell lines.** MUC2 mucin expression was analysed using a primary $\alpha$-MUC2 antibody and a Cy3-labelled secondary $\alpha$-rabbit antibody. Cell nuclei were stained using DAPI. Adapted from [Horstmann et al., 2017].

exhibited similar invasion rates (Fig. 4.11A+B), indicating that the flagellin-mediated invasion phenotype is dependent on efficient injection of Spi-1 effectors into host cells. Differences in Spi-1 effector secretion into the culture supernatant were not detected (Fig. 4.11B).
As already mentioned, active swimming motility was necessary for the FliC-mediated advantage in cell invasion. The contribution of the flagellar filament was analysed using a $\Delta motA$ mutant background. Due to deletion of the flagellar motor protein MotA, the bacteria are flagellated, but paralysed. Both $fliC^{\mathrm{ON}}$ and $fljB^{\mathrm{ON}}$ strains were equally invasive upon deletion of $motA$ (Fig. 4.12). This suggests that rotation of the flagellum is crucial for eukaryotic cell invasion. The filament as an adhesion factor therefore played a minor role in the observed invasion phenotype.

## 4.4 FliC expression facilitates productive target site selection during swimming on host cell surfaces

In order to characterise the motility-dependent invasion phenotype of the flagellin phase variants, the flagellation patterns were analysed by transmission electron microscopy (TEM) and fluorescence microscopy. Both FliC- and FljB-expressing bacteria showed equal flagellation and displayed approximately 2 flagella per cell body (Fig. 4.13). However, TEM analysis revealed alterations in the filament diameter. FljB flagella had a diameter of 28.9 nm, whereas filaments made of FliC monomers exhibited a smaller diameter of 25.5 nm (Fig. 4.14A). Major structural

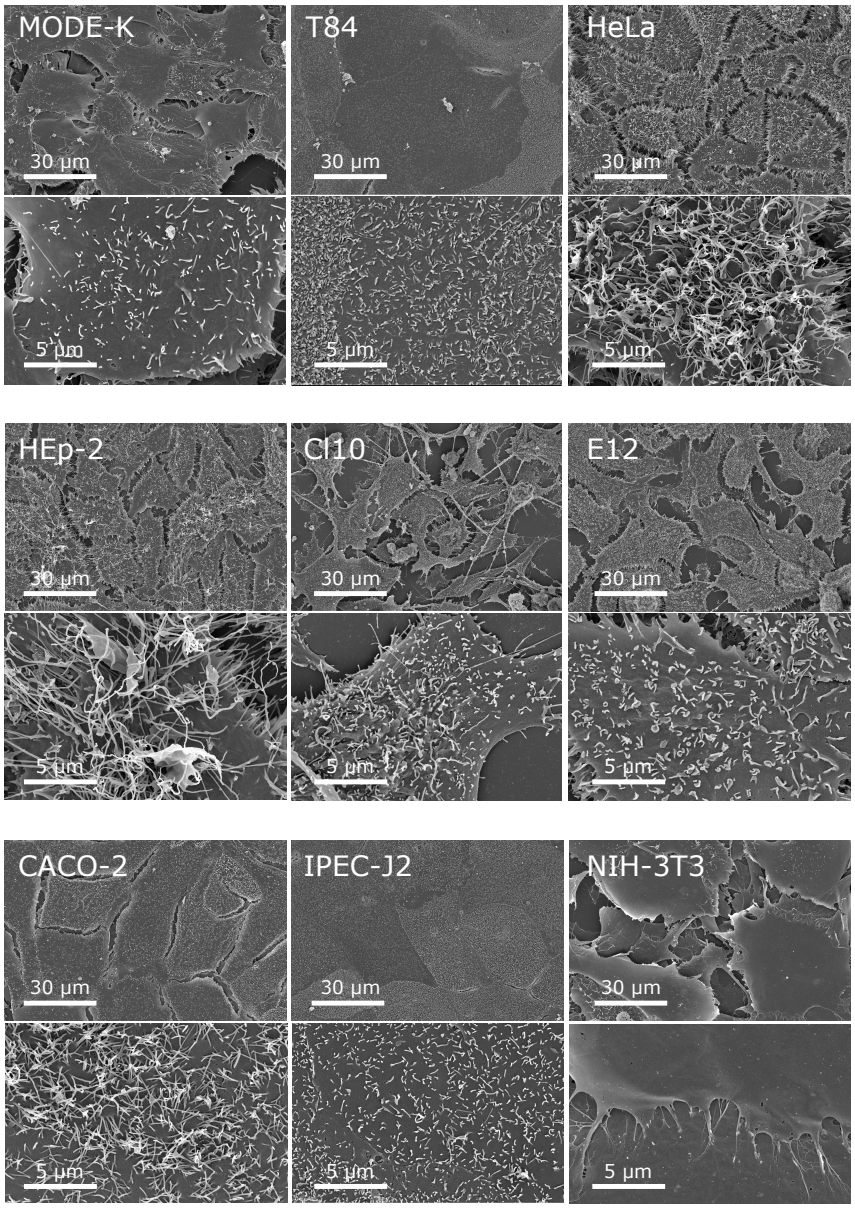


**Figure 4.10: Cell surface topologies of eukaryotic cell lines.** Cell surface topologies of cell lines grown on coverslips were analysed performing Field Emission Scanning Electron Microscopy (FESEM). Microscopy pictures were taken by Prof. Manfred Rohde (HZI). Adapted from [Horstmann et al., 2017].

re-arrangements of the D2 and D3 domains might result in differential depolymerisation kinetics. Purified flagella were incubated at various conditions including pH, temperature, and altered SDS detergent concentrations. Both FliC and FljB flagella depolymerised at pH 3, 60 °C, or 100 µg/ml SDS (Fig. 4.14B-D).

Alternatively, different filament structures might have an impact on the overall bundle formation needed for efficient swimming motility. Consequently, distinct physical properties of rotating

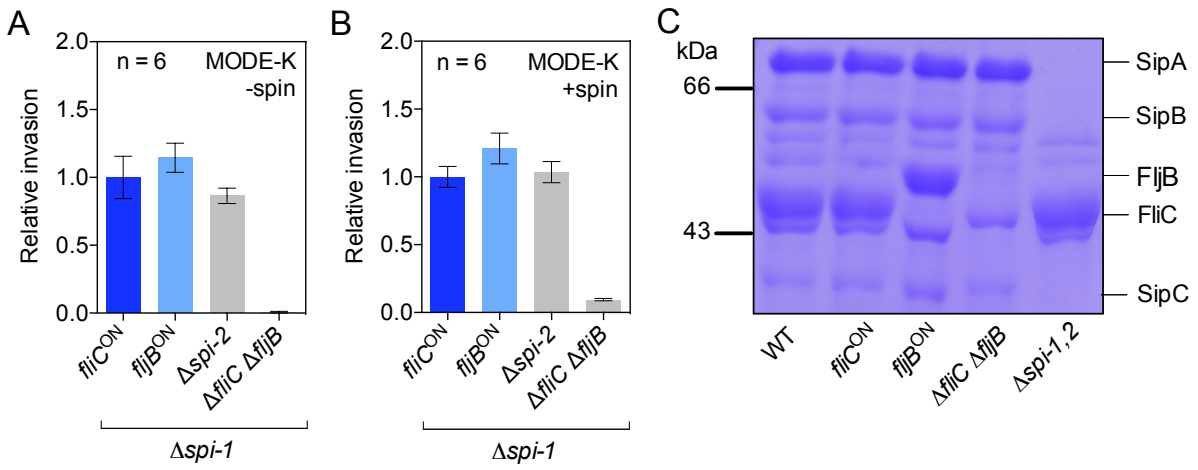


**Figure 4.11: The Spi-1 injectisome is involved in flagellin phase-dependent invasion.** MODE-K murine epithelial cells were infected with flagellin mutants lacking Spi-1 genes at a MOI of 10 for 1 h at 37 °C without (A) or with (B) centrifugation of *Salmonella* onto the epithelial cells. Bars represent the mean and error bars display the standard error of the mean. (C) Spi-1 effector protein secretion was analysed by precipitation from the culture supernatant using 10 % TCA. Secreted proteins were detected by Coomassie staining. Adapted from [Horstmann et al., 2017].

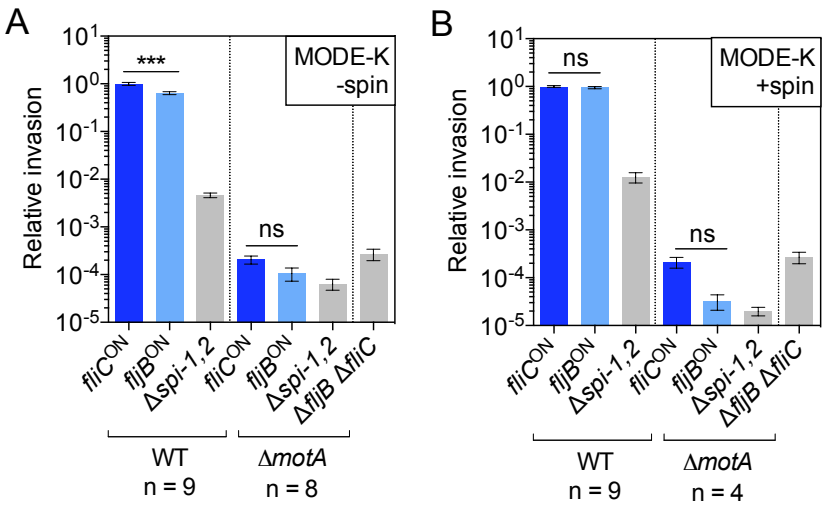


**Figure 4.12: Cell invasion is dependent on flagellar motility, but not on the filament itself.** MODE-K epithelial cells were infected with WT bacteria and paralysed strains (Δ*motA*) without (A) and with (B) centrifugation. Infection was performed at a MOI of 10 for 1 h at 37 °C. Extracellular bacteria were killed by addition of gentamicin for 1 h. MODE-K cells were lysed and serial dilutions were plated on LB agar for CFU assessment. All values were normalised to the inoculum and to the *fliC*$^{\mathrm{ON}}$ strain in WT background. A Student's *t*-test was applied to determine statistical significance (ns = not significant, P>0.05; *** = P<0.001). The bars represent the mean and error bars represent the standard error of the mean. Adapted from [Horstmann et al., 2017].

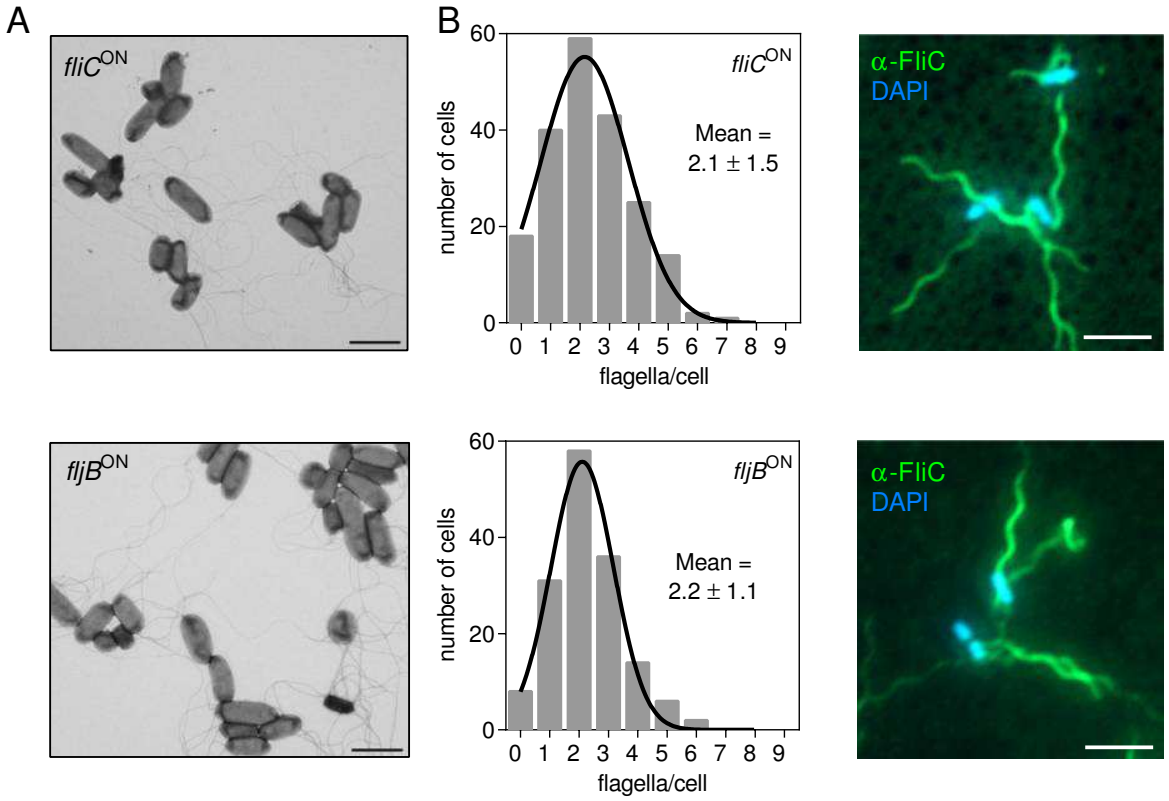


**Figure 4.13: Characterisation of flagellation phenotypes of the flagellin variants.** (A) Negative staining of phase locked mutants. Both strains are flagellated. Scale bars = 2 µm. (B) Flagella numbers per cell were determined using anti-flagellin immunostaining and DNA was stained using DAPI (right panel). The histograms display the number of counted flagella per cell body (left panel). Average flagella numbers and standard deviations were determined by Gaussian non-linear regression analysis (black line). Scale bars = 5 µm. Adapted from [Horstmann et al., 2017].

filaments could lead to differences in surface interactions and result in varying cell invasion. To address this question, population-based agar plate assays were performed for assessment of motility behaviours. Swimming and swarming motility was not influenced by the flagellin phase (Fig. 4.15A+B). The formation of swimming halos or swarming areas is not only dependent on functional flagella, but also on chemotaxis and bacterial growth. Slight differences in motility might therefore be masked by the other parameters. As a consequence, single cell tracking was monitored by time-lapse microscopy in liquid culture on a glass surface at the Max-Planck Institute Berlin. A Δ*fliC* Δ*fljB* double knockout strain was complemented with each flagellin variant and trajectories were statistically interpreted. The fluorescence-based approach revealed that FljB-expressing bacteria exhibit longer run phases between tumbling events compared to the *fliC*$^{ON}$ strain (Fig. 4.15C). Moreover, bacterial motility on the host cell surface was investigated.

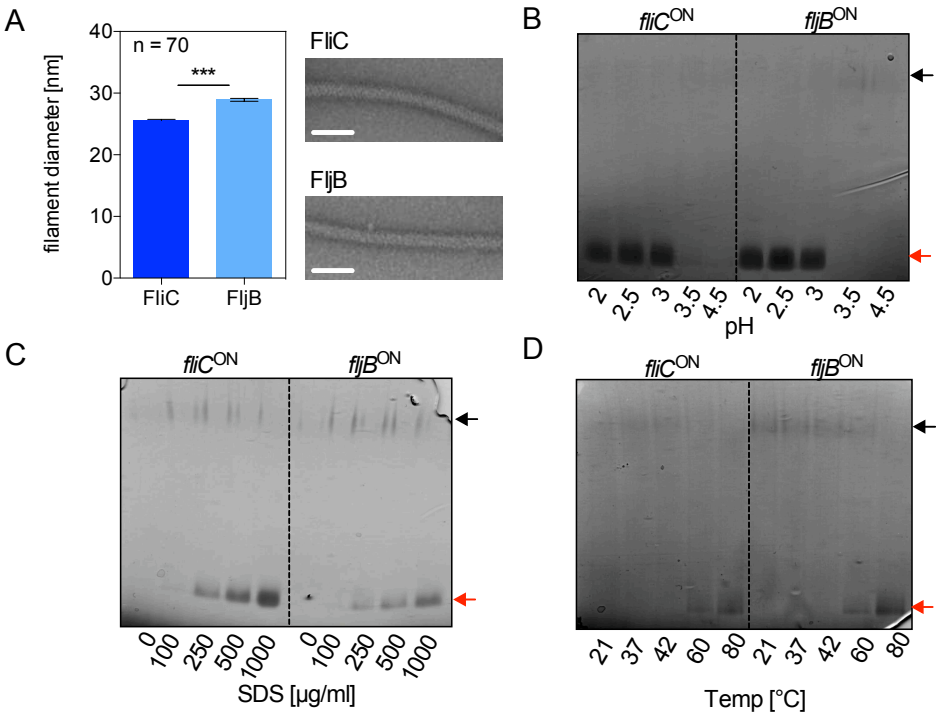


**Figure 4.14: Flagellar phase variants influence filament diameters, but not stability.** (A) Filament diameters of phase-locked strains were analysed using TEM. 70 flagella were measured in three individually performed experiments. Scale bar = 40 nm. Data shown represent the mean with standard error of the mean and a Student's *t*-test was applied to determine statistical significance (*** = P<0.001). (B) Purified flagella of flagellin phase-locked strains were treated in different conditions (pH, SDS, or temperature) for 10 min and analysed by Native-PAGE. Proteins were stained by Coomassie. Black arrow: filamentous state; red arrow: monomeric state. Adapted from [Horstmann et al., 2017].

Near surface swimming was performed on confluently grown MODE-K epithelial cells using fluorescent bacteria via time-lapse microscopy as described in [Misselwitz et al., 2012]. Four phases during near surface swimming were observed: (i) landing of the bacteria on the host cell surface, (ii) near surface swimming, (iii) stopping of bacteria, and (iv) taking off. The durations of each phase were calculated and the stops per bacterium during near surface swimming were counted after infection with either *fliC*$^{ON}$ or *fljB*$^{ON}$ strains. FliC-expressing bacteria stopped more frequently and for longer time periods, whereas *fljB*$^{ON}$ bacteria displayed prolonged near surface swimming phases (Fig. 4.16).

As mentioned before, swimming motility highly contributes to target site selection independently of chemotaxis. Therefore, it was hypothesised that distinct surface interactions, due to structural filament variations and different hydrodynamic forces, maintain differential formation of flagella bundles and altered tumble frequencies. This results in FliC-dependent more frequent and longer stopping phases, especially on cells with prominent cell topologies. Therefore, Spi-1 injectisome-

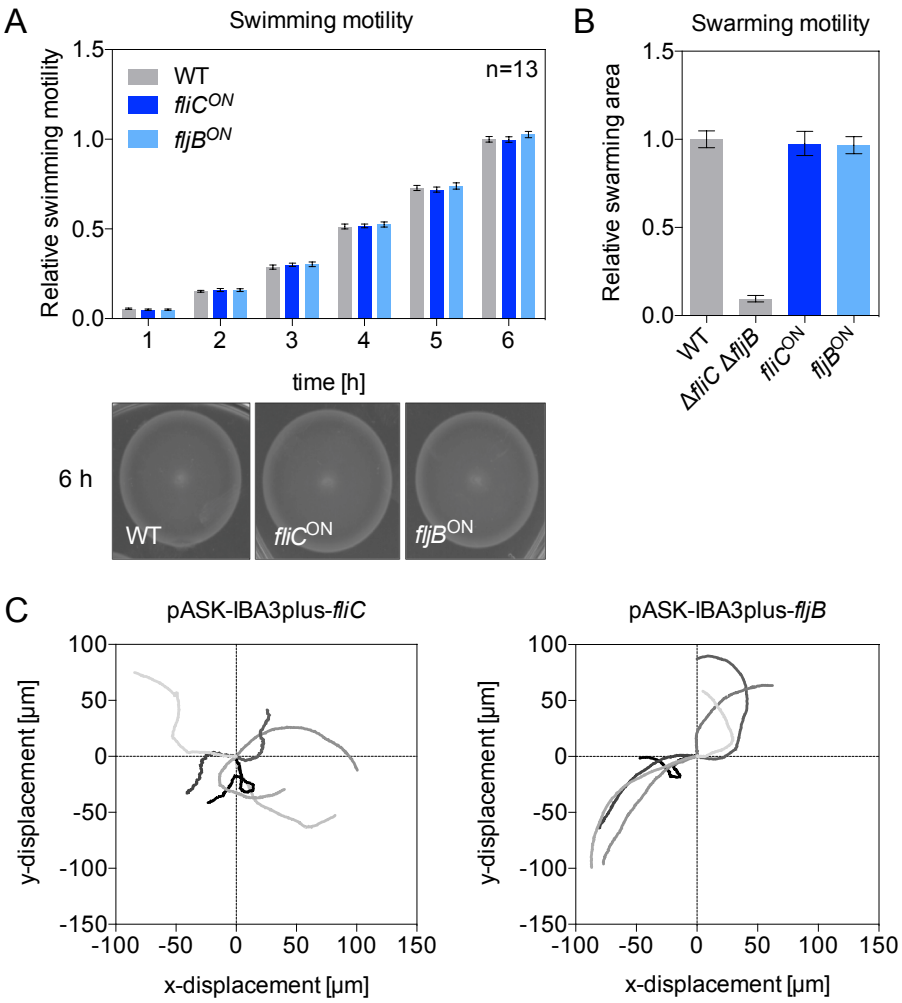


**Figure 4.15: Flagellin phase affects swimming on surfaces.** (A) Swimming motility was monitored in soft-agar plates containing 0.3 % agar at 37 °C and the swarm diameter was measured at the indicated time points. Representative motility swarm halos are shown. (B) Swarming motility was determined using swarm agar plates containing 0.6 % agar and incubated for 8 h at 37 °C. The swarming area was measured and normalised to the WT (WT: n=24; Δ*fliC* Δ*fljB* and *fliC*$^{ON}$: n=21; *fljB*$^{ON}$: n=17). (C) Single cell tracking of flagellin phase-locked mutants. Representative trajectories of the near surface motion profile of single SL1344 GFP-labelled bacteria episomally expressing the indicated flagellin variants in the double-knockout background (Δ*fliC* Δ*fljB*) are shown. Each line depicts the trajectory of a single bacterium tracked over a time period of 5 s (p-*fliC*: n=233; p-*fljB*: n=117). Tracking experiments were performed by Erik Zschieschang (Max-Planck Institute). Adapted from [Horstmann et al., 2017].

mediated invasion might be facilitated, which leads to a competitive advantage in colonisation of the intestinal epithelium.

## 4.5 Discussion

Besides directed movement towards host cells, pathogenic bacteria exploit the flagellum for multiple additional functions during infection. It mediates adhesion to cell surfaces [Crawford et al., 2010, Erdem et al., 2007, Girón et al., 2002], invasion of the epithelial cell barrier [Rivera-Chávez et al., 2016, Elhadad et al., 2015], and immune recognition and evasion [Schreiber et al., 2015, Finlay and McFadden, 2006]. Misselwitz et al. described a new mechanism by which flagellar motility facilitates near surface swimming and enables target site selection on host cell surfaces [Misselwitz et al., 2012]. However, the exact mode of action remained unknown. In this thesis, the contribution of the flagellin phase on *Salmonella* pathogenesis during the initial phase of infection in the gastrointestinal lumen was assessed. Many bacteria express more than one flagellin type from distinct genomic loci [Belas, 1994, Guerry et al., 1991, Ren et al., 2005]. However, *Salmonella* exploits a unique system of switching between alternating flagellins, FliC and FljB, in a process termed flagellar phase variation [Silverman and Simon, 1980]. The genetic mechanism underlying this switch is well characterised, but the biological relevance is still unknown. Previous studies reported that a *fljB*$^{\mathrm{ON}}$ mutant was attenuated in mice after oral and intravenous infection, indicating a role in enteric and systemic pathogenesis [Ikeda et al., 2001]. Moreover, Ikeda et al. observed increased bacterial numbers in blood and spleen 2 days p.i. when infected with FliC-expressing strains [Ikeda et al., 2001]. This is consistent with a study of Koskiniemi et al., in which *Salmonella* evolved towards FliC expression after serial passage in mice [Koskiniemi et al., 2013]. Constitutive expression of FliC, however, resulted in less killing of infected mice and thus was disadvantageous for infection [Miao et al., 2010].

In this chapter, it was revealed that FliC-expressing bacteria outcompeted FljB-expressing bacteria during gastrointestinal colonisation in the murine gastroenteritis and typhoid infection models. A contribution of differential host immune responses was excluded, since the observed colonisation phenotype in the small intestine was more pronounced at early infection time points. In agreement with Ikeda et al., swimming motility was not impaired in agar plate assays [Ikeda et al., 2001]. However, single cell tracking of bacteria displayed more frequent and longer stopping phases of FliC-expressing bacteria during near surface swimming on glass and epithelial cell surfaces. Near surface swimming is enabled by physical and hydrodynamic forces on the surface and is extensively studied in *Escherichia coli* [Frymier et al., 1995, Lauga et al., 2006, Li et al., 2011, Vigeant et al., 2002, Berke et al., 2008]. It facilitates selection of infection sites and subsequent stopping at prominent surface topologies like membrane ruffles, microvilli, or the bases of rounded-up cells. This near surface behaviour is independent of the Spi-1 injectisome, fimbrial expression, or chemotaxis [Misselwitz et al., 2012]. Here, the contribution of flagella and filament rotation was analysed. The experimental results propose a mechanism by which different rotational forces generated by distinct structural filaments of FliC and FljB flagella facilitate

altered host cell interactions. The more frequent and prolonged stops during near surface swimming of *fliC*$^{ON}$ strains then might enhance invasion of epithelial cells dependent on Spi-1-related injection of effector proteins and motility. Distinct surface topologies of cells that showed a flagellin-dependent invasion phenotype supported this hypothesis. Host cell species and mucin production of the host cell were not attributable to this phenotype. In the proposed mechanism, the involvement of flagellin phase-specific cell surface receptors, such as sugar residues, still has to be investigated.

*Salmonella enterica* was divided into diphasic and monophasic subspecies by evolutionary acquisition of the *fljB* flagellin locus [Porwollik et al., 2002]. *Salmonella enterica* subsp. *enterica* is predominantly diphasic. However, monophasic serovars like *Salmonella enterica* subsp. *enterica* serovar Typhi or Paratyphi A exist. These serovars are primarily found in humans and lost the *fljB* locus again [Herikstad et al., 2002]. The preservation of the *fliC* locus still raises questions, since it was thought that two antigenically distinct flagellins contribute to evasion of the host immune system. The disadvantage of FljB-expressing bacteria to efficiently invade the host might explain the selection towards FliC flagella. WT *Salmonella enterica* subsp. *enterica* serovar Typhimurium expresses FliC or FljB in subpopulations. Therefore, one might speculate that phenotypic heterogeneity represents a bet-hedging strategy, in which a FliC-expressing subpopulation ensures efficient invasion of the host epithelium and a FljB-expressing subpopulation is advantageous in other environmental niches.

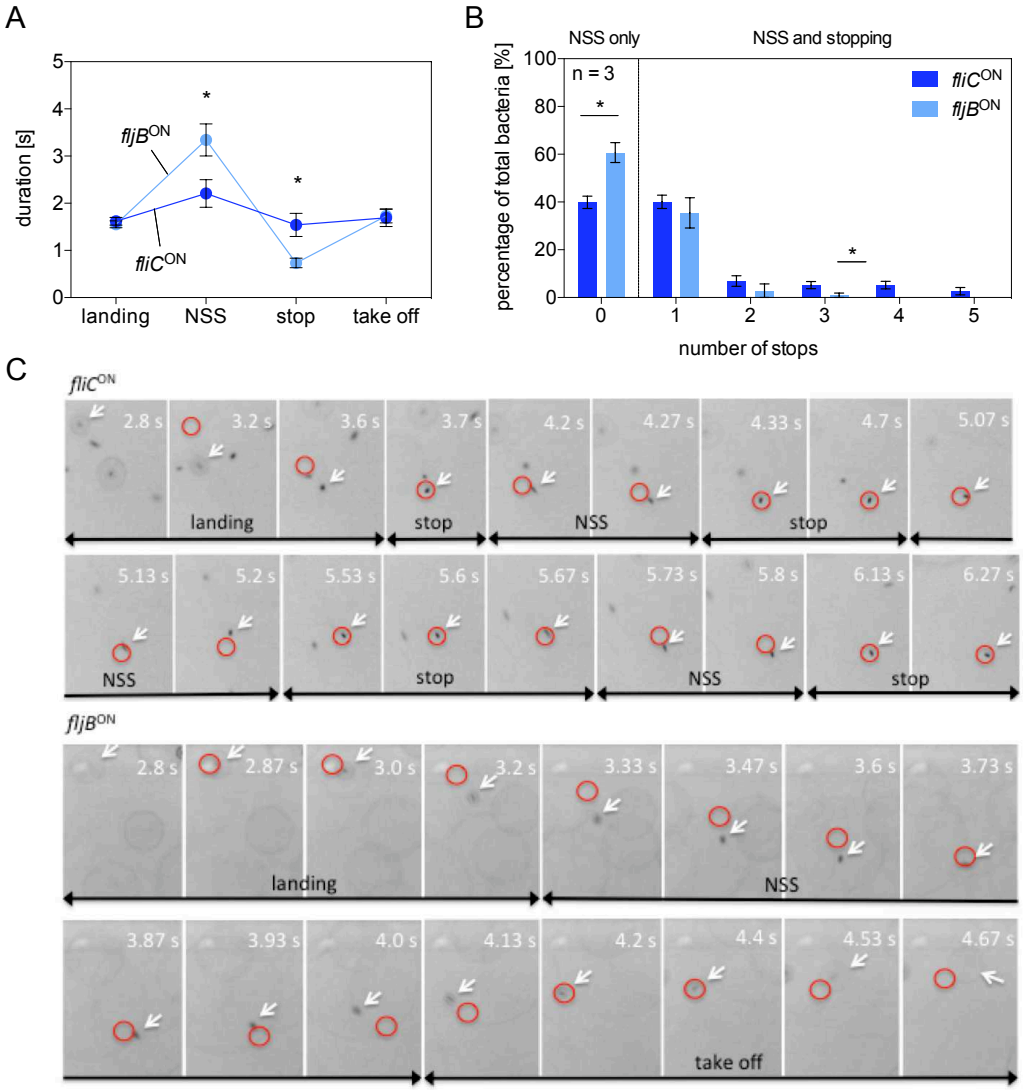


**Figure 4.16: Near surface swimming of flagellin phase-locked *Salmonella* on cell surfaces.** (A) Durations of near surface swimming (NSS) phases. MODE-K murine epithelial cells were grown to confluency and infected with flagellar phase variants at a MOI of 10. Videos were recorded immediately after addition of bacteria and durations of motility phases were determined with a frame rate of 3 frames/s. The data show the median duration in seconds with standard error of the mean of the different NSS phases of individual bacteria from three individual experiments (cumulative number of analysed individual bacteria: landing phase: *fliC*$^{ON}$ n=87, *fljB*$^{ON}$ n=80; NSS phase: *fliC*$^{ON}$ n=118, *fljB*$^{ON}$ n=102; stop phase: *fliC*$^{ON}$ n=54, *fljB*$^{ON}$ n=43; take off phase: *fliC*$^{ON}$ n=33, *fljB*$^{ON}$ n=54). (B) Quantification of the fraction of bacteria stopping for the indicated number of times during NSS on the host cell surface. The bars represent the mean with standard error of the mean of three individual experiments (cumulative number of analysed individual bacteria: *fliC*$^{ON}$ n=95, *fljB*$^{ON}$ n=72). A Student's *t*-test was applied to determine statistical significance (* = P<0.05). (C) Representative frames illustrating the near surface swimming behaviour of *fliC*$^{ON}$ and *fljB*$^{ON}$ mutants. White arrows indicate the observed bacterium. Red circles show the positions of the bacterium in the previous frame. Adapted from [Horstmann et al., 2017].

# 5 Flagellin Methylation is Crucial for Mannose-dependent Cell Adhesion of *Salmonella* Typhimurium

Surface exposed domains of a flagellin monomer are highly variable and immunogenic, leading to recognition by host receptors and triggering of innate and adaptive immune responses [Josenhans and Suerbaum, 2002, Hayashi et al., 2001, Reid et al., 1999]. Many flagellated bacteria thus evolved mechanisms to prevent flagellin recognition, for example by posttranslational modifications of flagellin. Recently, De Maayer et al. showed that glycosylation, which means the addition of sugar chains to the flagellin protein, is relatively common among *Enterobacteriaceae* [De Maayer and Cowan, 2016]. Flagellin glycosylation has already been described in a variety of bacteria, such as *Campylobacter*, *Aeromonas* or *Pseudomonas* species [Logan, 2006, Miller et al., 2008, Szymanski et al., 2003]. It is also involved in adhesion, biofilm formation, or mimicry of host cell surface glycans [Power and Jennings, 2003, Merino and Tomás, 2014].

In *Salmonella enterica*, posttranslational glycosylation of flagellin has not been described so far. However, *Salmonella* harbours a methylase, FliB, that is known to posttranslationally methylate flagellin proteins at lysine (Lys) residues to form $\epsilon$-N-methyl-lysine [Ambler and Rees, 1959, Tronick and Martinez, 1971, Stocker et al., 1961]. The gene *fliB* is located adjacent to the *fliC* gene on the chromosome. This region also contains the gene coding for the flagellum capping protein FliD and the flagellum-specific sigma factor encoding gene, *fliA* [Morimoto and Minamino, 2014]. Although flagellin methylation was first reported in 1959, the role of the methylation remains elusive. Previously, it was reported that deletion of *fliB* did not affect swimming and swarming motility [Frye et al., 2006] (see Chapter 2). Due to the predominance of the *fliB* gene in clinical *S. enterica* isolates, it was suggested that flagellin methylation is required for virulence of *Salmonella* [Frye et al., 2006]. To gain a better insight into the biological function of the FliB-dependent methylation of flagellin, we analysed a *fliB* knockout mutant for effects concerning flagellar assembly and function, motility, and virulence *in vivo* and *in vitro*.

## 5.1 Flagellin methylation in *Salmonella* Typhimurium

To elucidate if posttranslational methylation varies between FliC and FljB flagellins, secretion into the culture supernatant was assessed. Fractionation on a SDS-gel showed that non-methylated flagellin from a Δ*fliB* mutant strain migrated slightly faster independently of the flagellin phase, suggesting posttranslational modification (Fig. 5.1).

Mass spectrometry analyses of purified FliC and FljB from WT and *fliB* knockout strains in either *fliC*$^{ON}$ or *fljB*$^{ON}$ backgrounds revealed 14 and 15 *fliB*-dependent methylated Lys residues, respectively (Fig. 5.2A+B; mass spectrometry performed in collaboration with Michael Kolbe). These methylation sites were found mainly in the surface-exposed D2 and D3 domains (Fig. 5.2B), indicating posttranslational modification of Lys before export in a partially folded state. Interestingly, two Lys in FliC and one lysine in FljB were methylated independently of the methylase FliB (Fig. 5.2), suggesting the presence of a second flagellin methylase in *Salmonella* Typhimurium.

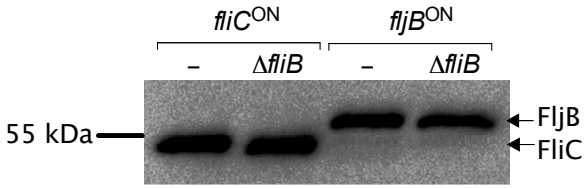


**Figure 5.1: Flagellin secretion into the culture supernatant.** Secreted proteins were precipitated by addition of 10 % TCA and fractionated according to their molecular weight by SDS-PAGE. Immunoblotting was performed using $\alpha$-FliC/FljB antibodies.

## 5.2 Swimming motility is not influenced by flagellin methylation

Since posttranslational modifications of the filament through glycosylation were already described to have an effect on flagellar assembly, the influence of methylated flagellin on motility was assessed (Fig. 5.3A). As described before (see Chapter 2)[Frye et al., 2006], swimming motility was not affected (Fig. 5.3A). Immunostaining of flagella from WT and a $\Delta$*fliB* mutant strain showed no alterations in flagella assembly and flagella numbers per cell body (mean = 2.2) (Fig. 5.3B).

To better understand to which extent Lys methylation plays a role in flagella assembly and filament stability, several Lys substitution mutants were constructed. Methylation of Lys residues removes the positive charge of Lys. Similar to Lys, arginine (Arg) also exhibits a positively charged side chain, but is not methylated by FliB and therefore remains charged. Asparagines (Asp) are structurally similar to Lys and harbour an uncharged side chain, mimicking a methylated flagellin state. Lys were exchanged with Asp or Arg and mutant strains were analysed regarding their swimming behaviour, flagellin secretion, and filament structure (summarised in Tab. 5.1). Neither Asp nor Arg substitutions in both FliC and FljB did affect flagellin secretion (Fig. 5.4B and 5.5B), but migration on a SDS-gel was increasingly altered the more Lys were exchanged to asparagines (Fig. 5.4B and 5.5B). This indicated that the flagellin surface charge or the flagellin monomer structure was influenced. Swimming motility was not influenced for mutants with up to four substitutions in both FliC (K204N, K216N, K233N, K252N = K4N; K222N, K229N = K2N; K222N = K1N) and FljB (K189N, K288N = K2Na; K319N, K369N = K2Nb)(Fig. 5.4A and 5.5B). Consistently, immunostaining of filaments showed WT flagellation for the FliC K4N, K2N, and K1N variants and for the FljB K2Na and K2Nb variants (Fig. 5.4C). Interestingly, a mutant harbouring a FliC K204N, K216N, K222N, K229N, K233N, K293N, K309N, K319N, and K327N variant (K9N) was less motile (50 % of control strain)(Fig. 5.4A). The flagella numbers per cell body were similar to WT flagellation, however, filaments observed by fluorescent labelling were shorter (Fig. 5.4C), indicating a role of methylated Lys residues in filament stability or assembly. A strain that expressed a FljB K182N, K189N, K209N, K227N, K234N, K249N, K271N, K288N, K319N, K355N, K357N, K369N, and K390N variant (K12N) showed an even more pronounced swimming motility defect (Fig. 5.5A) and was not flagellated

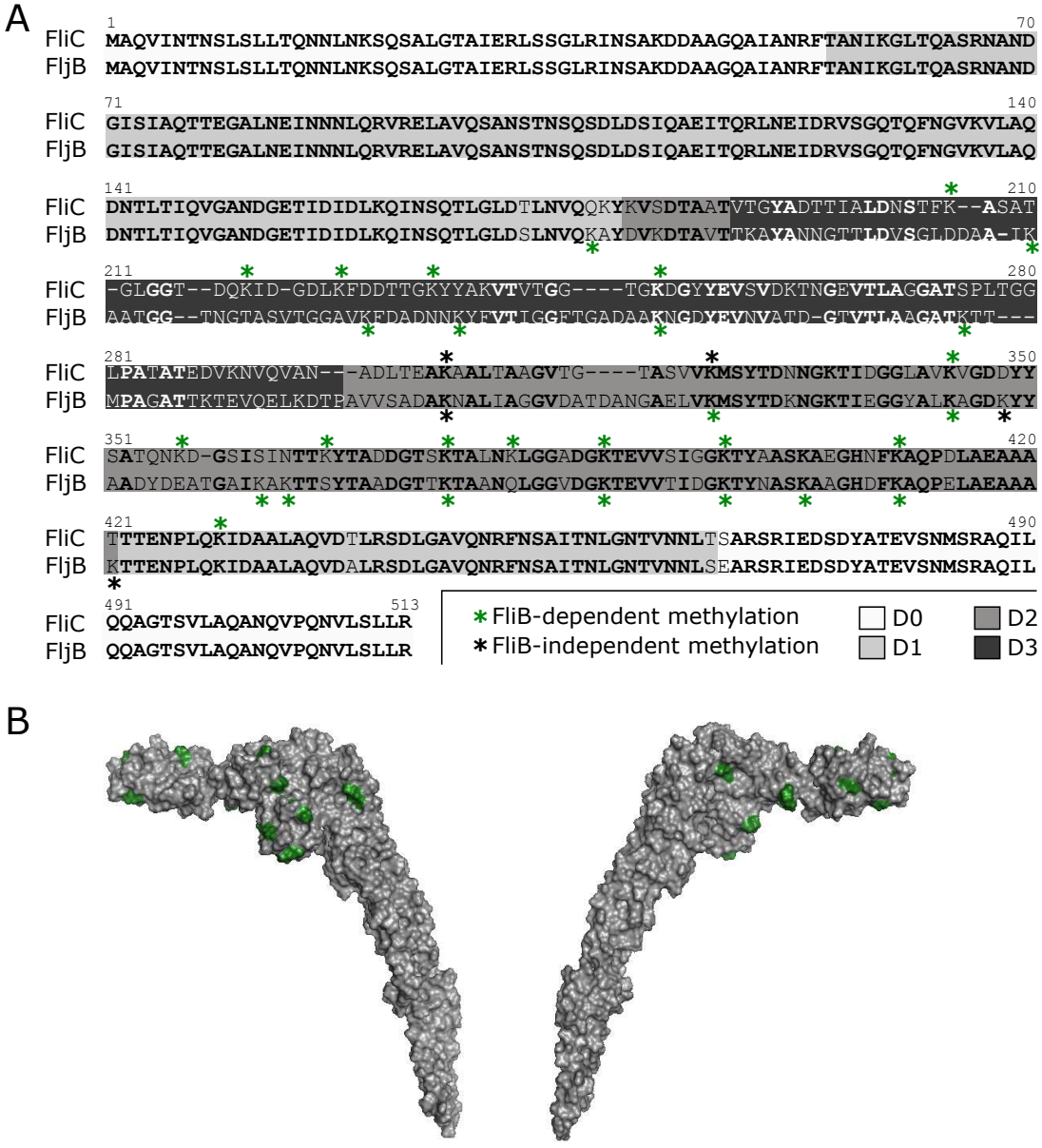


**Figure 5.2: Flagellar lysine methylation in *Salmonella* Typhimurium.** Lysine (Lys) methylation was assessed via mass spectrometry of WT flagellin and non-methylated flagellin (Δ*fliB*; performed in collaboration with Michael Kolbe). (A) FliC and FljB were aligned and grey parts represent distinct flagellin domains. Green asterisks show Lys that are methylated dependent on FliB. Black asterisks highlight FliB-independent methylation sites. (B) Structure of a FliC monomer with surface-exposed methylation sites highlighted in green.

(Fig. 5.5C). Upon substitutions of Lys to Arg in FliC (K9R and K4R), migration of secreted FliC was not influenced (Fig. 5.4B). Swimming motility was reduced to 75 % of the control strain (Fig. 5.4A). Immunostaining of filaments revealed that the filament structure strongly varied between the Arg mutant and the control (Fig. 5.4C). The helical structure was tightened and the

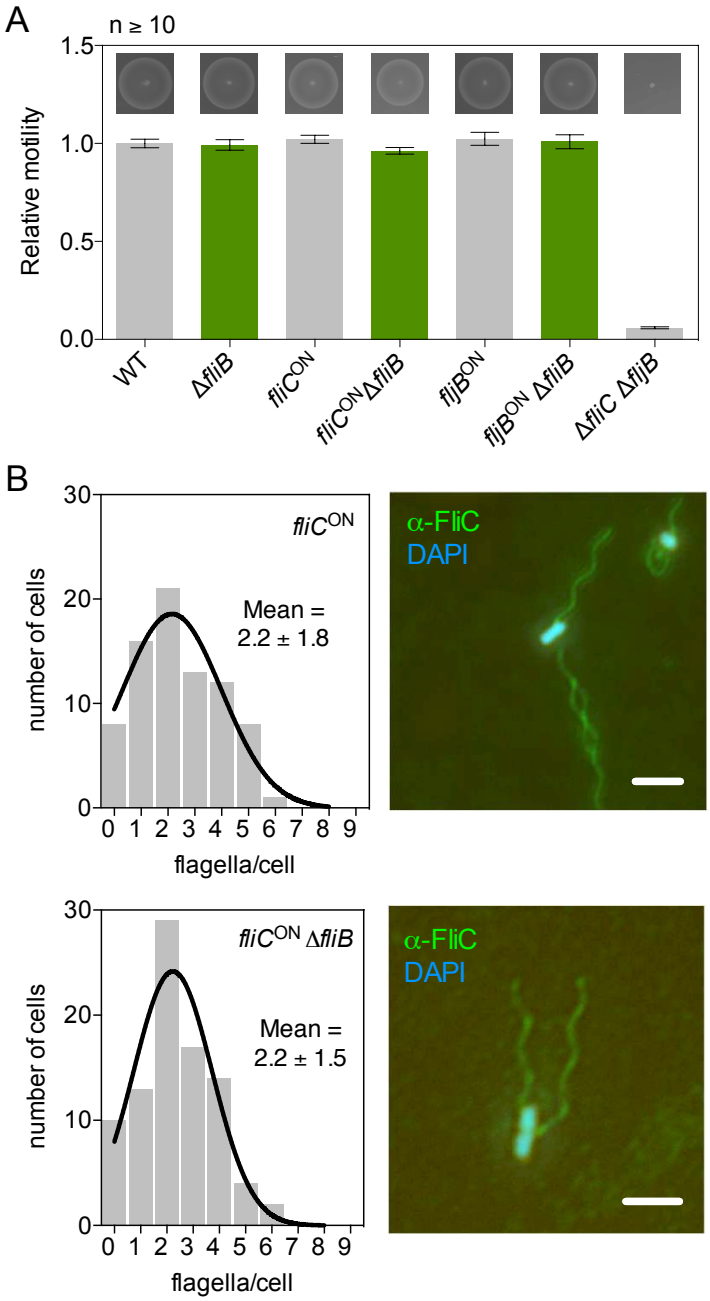


**Figure 5.3: Swimming motility and flagellar assembly are independent on flagellin methylation.** (A) Motility phenotypes were analysed in soft-agar plates containing 0.3 % agar after 4 h incubation at 37 °C. The diameters of the motility swarm were measured and normalised to the control strain. Bar graphs show the mean and standard error of the mean. Biological replicates are analysed by the Student's $t$ test. (B) Left: Histograms of counted flagella per bacterium of *fliC*-locked strains with and without *fliB*. Average flagella numbers were calculated by Gaussian non-linear regression analysis (black line). Right: Flagella filaments were immunostained using $\alpha$-FliC primary and $\alpha$-rabbit conjugated Alexa488 secondary antibodies (green). DNA was stained with DAPI (blue). Scale bar = 5 µm.

filaments appeared stiff, suggesting a different motility behaviour through less flexible filaments and a defect in bundle formation.

**Table 5.1: Characterisation of constructed lysine substitutions.**

| Name | Exchanged lysine residues | Motility | Flagellin secretion | Filament staining |
|---|---|---|---|---|
| FliC | | | | |
| K9N | K204N, K216N, K222N, K229N, K233N, K293N, K309N, K319N, K327N | 50 % | Yes; migrates slower | Shorter filaments |
| K4N | K204N, K216N, K233N, K252N | 100 % | Yes; migrates slower | WT flagellation |
| K2N | K222N, K229N | 100 % | Yes | WT flagellation |
| K1N | K222N | 100 % | Yes | WT flagellation |
| K9R | K204R, K216R, K222R, K229R, K233R, K293R, K309R, K319R, K327R | 75 % | Yes | Helical filament structure tightened; stiff |
| K4R | K293R, K309R, K319R, K327R | 75 % | Yes | Helical filament structure tightened; stiff |
| FljB | | | | |
| K12N | K182N, K189N, K209N, K227N, K234N, K249N, K271N, K288N, K319N, K355N, K357N, K369N, K390N | 0 % | Yes; migrates slower | No |
| K2Na | K189N, K288N | 100 % | Yes | WT flagellation |
| K2Nb | K319N, K369N | 100 % | Yes | WT flagellation |

## 5.3 Flagellin methylation has an impact on virulence *in vivo* and *in vitro*

Next, the role of flagellin methylation in virulence of *Salmonella* was investigated. Organ burden analysis in the gastroenteritis mouse model 2 days post-infection revealed that the Δ*fliB* strain was outcompeted by the WT, especially in the ceacal tissue (Fig. 5.6). This indicated that methylated flagella are crucial for organ colonisation. To test if epithelial cell invasion was affected, MODE-K epithelial cells were infected with strains deficient in flagellin methylation (Δ*fliB*). Invasion was reduced about 50 % for the Δ*fliB* mutant strain independent on the flagellin type and centrifugation of the bacteria onto the host cells (Fig. 5.7A). This indicates that bacterial motility does not contribute to the Δ*fliB* invasion phenotype.

To complement this phenotype, *fliB* was fused to an inducible $P_{tet}$ promoter at its native chromosomal locus. This enabled induction of *fliB* expression upon anhydrotetracycline (AnTc) addition. After AnTc-mediated induction, *fliB* trancripts were detected by qRT-PCR (Fig. 5.7B)

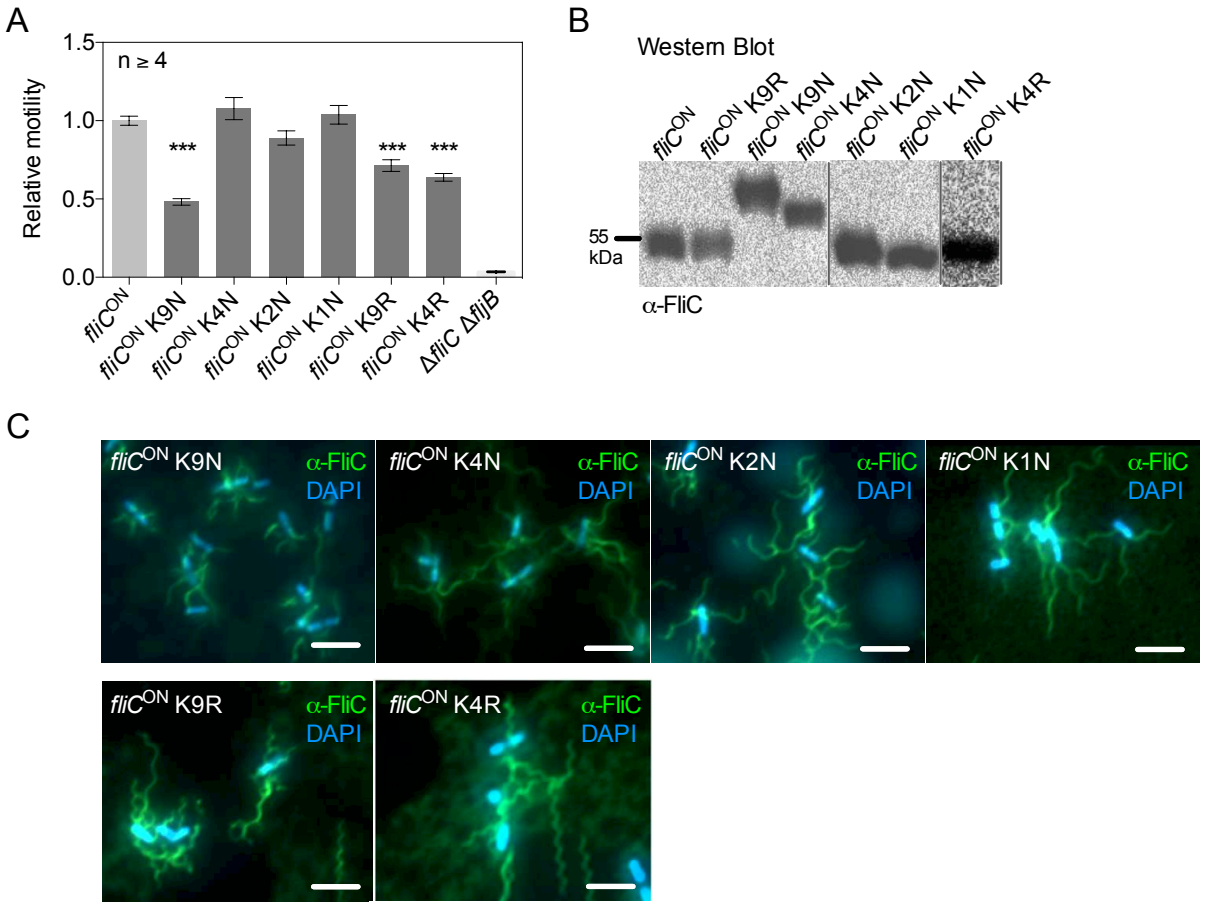


**Figure 5.4: Lysine substitutions in FliC and their impact on motility, flagellin secretion, and flagella assembly.** (A) Motility phenotypes of lysine substitution mutants were analysed in soft-agar plates as described before. Bar graphs show the mean and standard error of the mean. Biological replicates are analysed by the Student's $t$ test. (B) Flagellin secretion into the culture supernatant. Secreted proteins were precipitated by addition of 10 % TCA and fractionated by SDS-PAGE. Immunoblotting was performed using $\alpha$-FliC antibodies. (C) Flagella filaments were immunostained using $\alpha$-FliC primary and $\alpha$-rabbit conjugated Alexa488 secondary antibodies (green). DNA was stained with DAPI (blue). Scale bar = 5 µm.

and WT invasion levels were observed (Fig. 5.7C). Furthermore, the FliB-mediated invasion phenotype was completely flagella-dependent, since deletions of the hook ($\Delta$*flgE*) or hook-filament junction proteins ($\Delta$*flgKL*) abolished the observed invasion phenotype (Fig. 5.8A). In agreement with the finding that the flagellin D3 domain is predominantly methylated, a D3 deletion variant also exhibited reduced cell invasion (Fig. 5.8C). This invasion rate was comparable to invasion of a $\Delta$*fliB* mutant (Fig. 5.8C), although motility was not impaired in the absence of D3 (Fig. 5.8B). The methylation-dependent invasion phenotype was further analysed in a variety of eukaryotic cell lines. The human epithelial cell line E12 and the cell line Cl11, which was developed from primary murine intestinal epithelial cells, were tested for

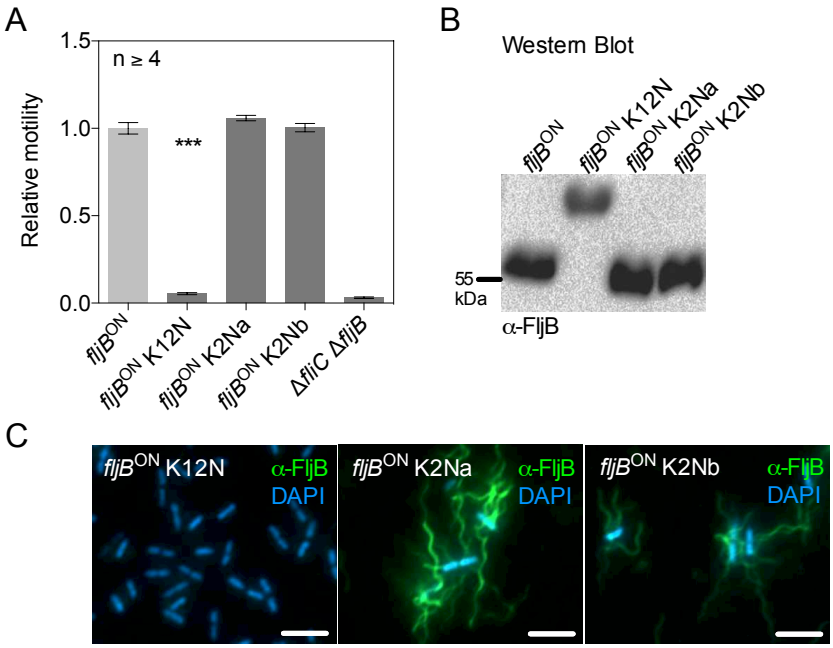


**Figure 5.5: Lysine substitutions in FljB and their impact on motility, flagellin secretion, and flagella assembly.** (A) Motility phenotypes of lysine substitution mutants were analysed in soft-agar plates as described before. Bar graphs show the mean and standard error of the mean. Biological replicates are analysed by the Student's $t$ test. (B) Flagellin secretion into the culture supernatant. Secreted proteins were precipitated by addition of 10 % TCA and fractionated by SDS-PAGE. Immunoblotting was performed using $\alpha$-FljB antibodies. (C) Flagella filaments were immunostained using $\alpha$-FljB primary and $\alpha$-rabbit conjugated Alexa488 secondary antibodies (green). DNA was stained with DAPI (blue). Scale bar = 5 µm.

bacterial cell invasion. These cell lines mimic the native intestinal environment *in vitro* and comparable to MODE-K cells, a Δ*fliB* mutant strain showed reduced invasion (50 % of WT) (Fig. 5.9A+B). Notably, invasion of murine fibroblast NIH 3T3 cells was independent of flagellin methylation (Fig. 5.9C), suggesting that the observed invasion phenotype is cell type-specific and does only occur on epithelial-like cells.

## 5.4 Flagellin methylation is crucial for adhesion to glycostructures

Epithelial cell adhesion was investigated using MODE-K cells. Interestingly, cell adhesion was reduced for strains deficient in flagellin methylation (Fig. 5.10A), suggesting that flagellin methylation promotes adherence to glycostructures or an unknown receptor on the cell surface. Since binding to extracellular matrix (ECM) proteins was not significantly altered (Fig. 5.10B), invasion of genetically modified CHO cells was monitored in collaboration with Guntram Grassl at the Hannover Medical School (Fig. 5.10C). The hamster epithelial-like cell line was mutated for genes necessary to build up specific glycostructures on the cell surface. A Δ*xylT* mutation lacks proteoglycans, whereas a Δ*lec2* cell line has a defect in forming sialic acid. Invasion of

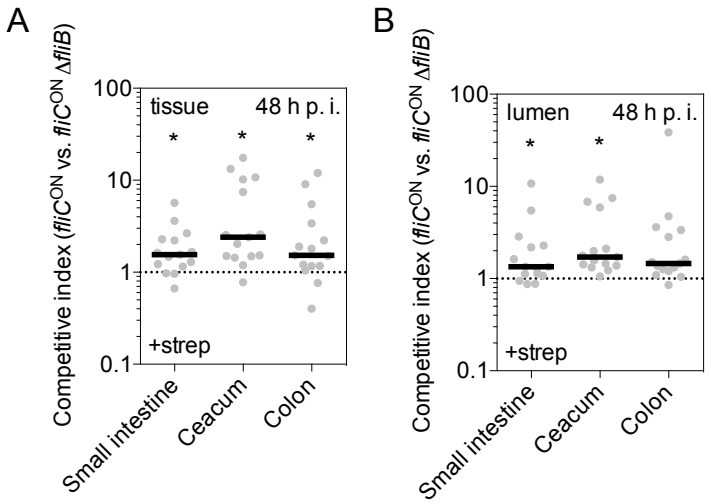


**Figure 5.6: Colonisation of the gut is affected by flagellin methylation in the gastroenteritis mouse model.** Streptomycin pre-treated C57BL/6 mice were infected with $10^7$ CFU of each bacterial strain harbouring distinct antibiotic resistant cassettes. Two days post-infection, organs (small intestine, colon, and ceacum) were isolated and the luminal content was collected for CFU assessment and for calculation of the competitive indices (CI). Replicates are shown as individual data points and analysed by the Wilcoxon Signed Rank test. Asterisks indicate a significant different phenotype to the value 0 (* = $P<0.05$).

both cell lines was not altered between the control strain and the Δ*fliB* mutant (Fig. 5.10C), which was in agreement with the invasion behaviour using WT CHO cells (Fig. 5.10C). This indicated that CHO cells lack surface markers or receptors that enable binding of methylated flagella. Importantly, cell invasion of the Δ*fliB* strain was significantly reduced using CHO Δ*lec1* cells (Fig. 5.10C). These cells lack complex N-glycans, which results in exposed terminal mannose residues. To test if methylated flagella bind predominantly to mannose, a competition cell culture assay was performed. Prior to infection of MODE-K cells, 2.5 % mannose was added to the bacterial cultures and the cells. Invasion rates decreased for the control strain to the same extent than a Δ*fliB* mutant (Fig. 5.10D). This suggested that methylated filaments bind to soluble mannose and therefore binding to cell-surface exposed mannose residues was inhibited.

## 5.5 Discussion

Flagella-dependent motility is crucial for *Salmonella* pathogenesis as it enables a directed swimming behaviour towards host epithelial cells. However, it has been shown previously that flagella not only play a role in bacterial motility, but also in colonisation, adhesion, and biofilm formation [Josenhans and Suerbaum, 2002, Pratt and Kolter, 1998a, Danese et al., 2000b, Danese et al., 2000a]. Moreover, flagella mediate attachment to sites within the epithelial landscape that are inaccessible due to ruffling of the host cell membrane. Primary

direct adhesion to epithelial tissue is predominantly conferred by the filament structure. Its surface-exposed filament made of thousands of identical flagellin proteins represents an excellent adhesion molecule. Here, a new mechanism of flagella-dependent adhesion to mannose is described. This adhesion phenotype was dependent on methylation of flagellin via the FliB

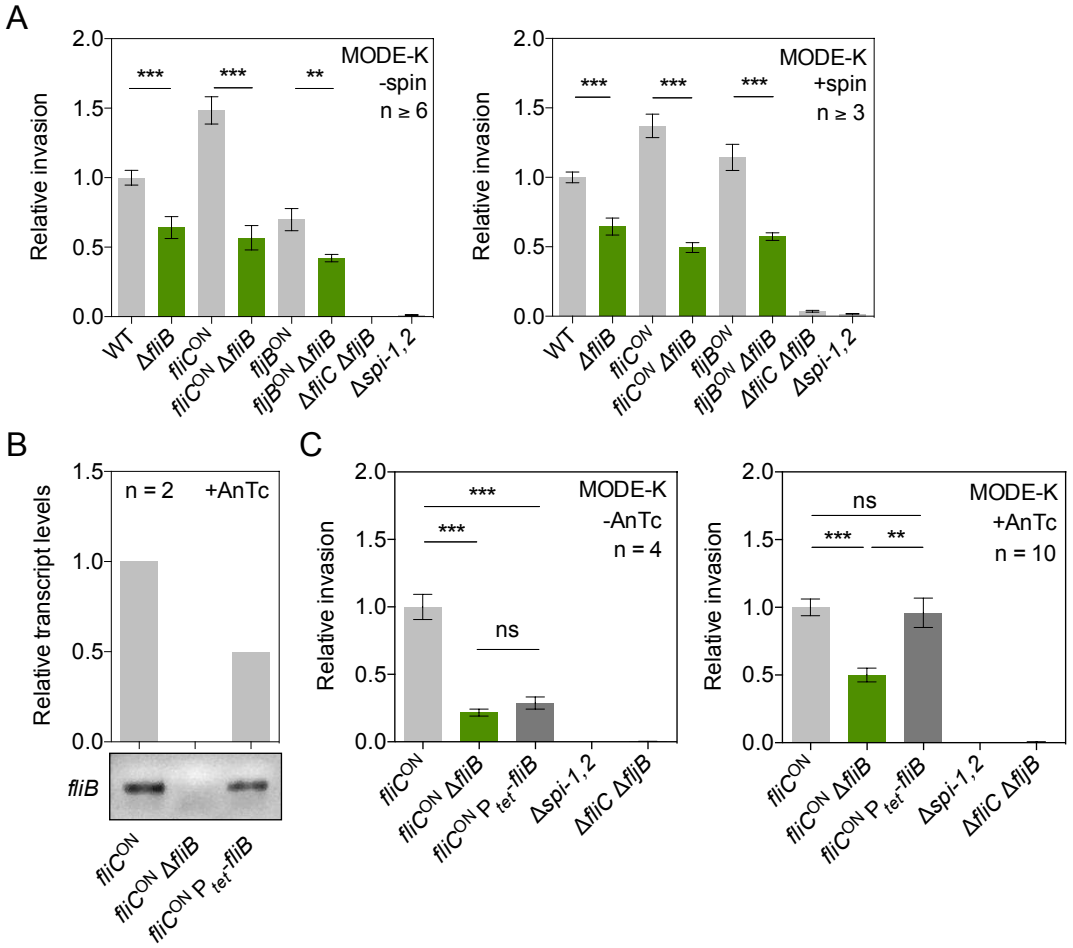


**Figure 5.7: Flagellin methylation is crucial for epithelial cell invasion.** (A) MODE-K murine epithelial cells were infected with various mutants at a MOI of 10 for 1 h at 37 °C with (right panel; +spin) or without centrifugation (left panel; -spin). Extracellular bacteria were killed by addition of gentamicin for 1 h. MODE-K cells were lysed and serial dilutions were plated on LB agar for CFU assessment. (B) Relative *fliB* gene expression of a *fliC*-locked control strain, a *fliB* deletion strain, and a *fliB*-inducible complementation strain was analysed upon induction with 100 ng/ml anhydrotetracycline (AnTc) using qRT-PCR. Experiments were performed with 2 biological replicates. Amplified PCR products are shown on a representative 1 % agarose gel.(C) Cell invasion was complemented using an inducible $P_{tet}$ promoter chromosomally fused to *fliB*. FliB expression was induced by addition of 100 ng/ml anhydrotetracycline (AnTc). All values were normalised to the inoculum and control strain invasion. Statistical significances were determined by the Student's *t* test (** = P<0.01; *** = P<0.001; ns = not significant, P>0.05).

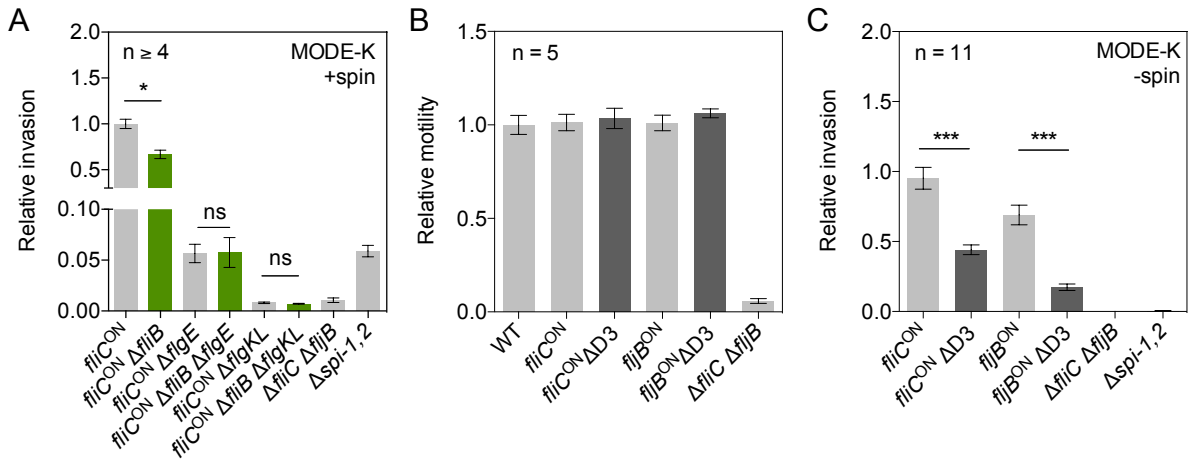


**Figure 5.8: Flagellin methylation enhances invasion in a flagellin D3 domain-dependent manner.** (A) Infection of MODE-K murine epithelial cells was performed with various mutants at a MOI of 10 for 1 h at 37 °C with centrifugation (+spin). Extracellular bacteria were killed by addition of gentamicin for 1 h. Cell lysates were plated in serial dilutions for CFU assessment. Values were normalised to the inoculum and control strain invasion. (B) Motility phenotypes of D3 domain mutants were analysed in soft-agar plates as described before. Bar graphs show the mean and standard error of the mean. (C) Epithelial cell invasion of D3 domain mutants. MODE-K cells were infected at a MOI of 10 for 1 h at 37 °C. Extracellular bacteria were killed by addition of gentamicin for 1 h. Cell lysates were plated in serial dilutions for CFU assessment. Values were normalised to the inoculum and control strain invasion. Statistical significances were determined by the Student's $t$ test (*** = $P<0.001$; * = $P<0.05$; ns = not significant, $P>0.05$).

methylase. It was shown that mainly Lys residues within the surface-exposed D2 and D3 domains of FliC and FljB were methylated, indicating posttranslational modification of Lys before flagellin export and filament assembly. Moreover, flagellin methylation was confirmed to have no effect on swimming motility or flagella assembly as reported previously [Frye et al., 2006] (see Chapter 2). Lys substitutions to Arg or Asp were analysed to investigate the contribution of charged residues in a flagellin monomer to filament stability and flagella function. A low number of Lys substitutions to Asp did not affect flagellin secretion, flagellar assembly, or flagellar motility, whereas a high amount of Lys residue exchanges to Asp or Arg significantly changed filament stability or structure. Further research using strains with an additional Δ*fliB* mutation is required to elucidate how substitutions of one or more lysine residues affect flagellar assembly or filament bundle formation.

Methylation through FliB was crucial for *Salmonella* pathogenesis in the mouse model, as well as in epithelial cell adhesion and invasion *in vitro*. The invasion phenotype was dependent on surface-exposed mannose glycostructures. In *E. coli* [Lillehoj et al., 2002], several strains were reported, in which flagellin acts as an adhesion molecule, including epithelial

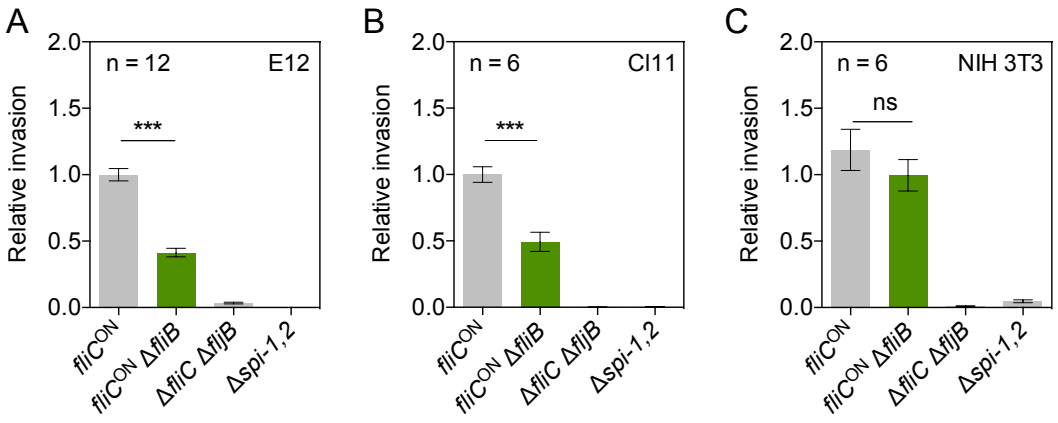


**Figure 5.9: Epithelial cell invasion of flagellin methylation mutants is cell type-specific.** The human epithelial cell line E12 (A), the murine epithelial cell line Cl11 (B), and the murine fibroblast cell line NIH 3T3 (C) were infected with flagellar phase variants at a MOI of 10 for 1 h at 37 °C. Extracellular bacteria were killed by addition of gentamicin for 1 h. Cells were lysed and serial dilutions were plated on LB agar for CFU assessment. All values were normalised to the inoculum and to the *fliC*$^{ON}$ strain in WT background. A Student's *t*-test was applied to determine statistical significance (ns = not significant, P>0.05; *** = P<0.001). The bars represent the mean and the error bars show the standard error of the mean.

cell adhesion of enteropathogenic *E. coli* (EPEC) [Girón et al., 2002] or enterotoxigenic *E. coli* (ETEC) [Roy et al., 2009]. Interestingly, mannose is also present in the epithelial mucus layer and interactions between flagella and mucus have been demonstrated before. The *E. coli* strain O157:H7 adheres with its H7 flagellins to bovine mucus [Mahajan et al., 2009] and both flagellin and the flagellin cap protein FliD were shown to adhere to mucin in *Pseudomonas aeruginosa* [Arora et al., 1998, Lillehoj et al., 2002]. Flagella of the opportunistic pathogen *Stenotrophomonas maltophilia* have been described to bind to mouse tracheal mucus [Zgair and Chhibber, 2011].

Flagellin methylation was first described in *Salmonella* in 1959 [Ambler and Rees, 1959, Stocker et al., 1961, Tronick and Martinez, 1971]. Moreover, flagellin methylation was also recently found in *Shewanella oneidensis* [Sun et al., 2013]. In mass spectrometry analyses of *S. oneidensis* flagellin (FlaB), at least five Lys residues were methylated. Sun et al. also identified a gene, SO4160, that exhibited 24 % identity to the *Salmonella fliB* gene, which encodes for the lysine-N-methylase FliB. In agreement with the observations in this thesis, flagellin methylation was not required for motility and flagellar assembly in *S. oneidensis* [Sun et al., 2013]. Recently, De Maayer and Cowan analysed Flagellin Glycosylation Islands (FGI) and Flagellin Methylation Islands (FMI) in *Enterobacteriaceae*, revealing that flagellin modifications by glycosylation or methylation is relatively common [De Maayer and Cowan, 2016]. Many bacterial species including *Yersinia*, *Enterobacter*, *Franconibacter*, and *Pantoea* contained chromosomal FMI loci, which encode orthologs of FliB. Thus, the contribution of FliB-dependent methylation of flagellin

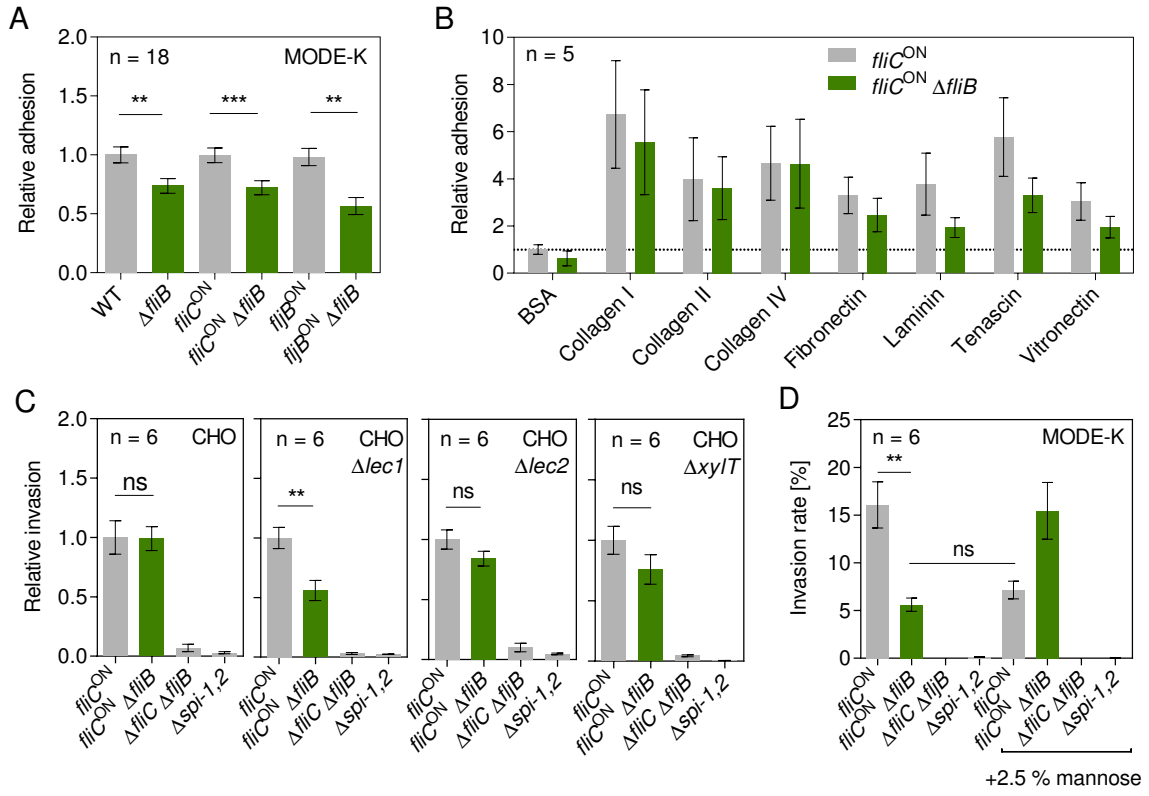


**Figure 5.10: Characterisation of methylation-dependent adhesion.** (A) Epithelial cell adhesion was monitored using strains that lack Spi-1 genes at a MOI of 10 for 1 h at 37 °C. After extensive washing, the CFU were calculated. All values were normalised to the inoculum and control strain adhesion. Statistical significances were determined by the Student's $t$ test (** = P<0.01; *** = P<0.001). (B) Adhesion to extracellular matrix (ECM) proteins. Control and Δ*fliB* strains were added to ECM protein pre-coated 96-well plates and incubated for 1 h at 37 °C. After extensive washing, adherent bacteria were plated in serial dilutions for CFU assessment. Error bars represent the standard error of the mean. (C) Eukaryotic cell invasion was monitored using CHO WT, Δ*lec1*, Δ*lec2*, and Δ*xylT* cells. Cells were infected with various *Salmonella* strains at a MOI of 10 for 1 h at 37 °C. After lysis, serial dilutions were plated on LB agar for CFU assessment. All values were normalised to the inoculum and *fliC*$^{\mathrm{ON}}$ strain in WT background. (D) Mannose competition invasion rates were determined by addition of 2.5 % mannose to the bacterial cultures prior to infection of MODE-K epithelial cells. A Student's $t$-test was applied to determine statistical significance (ns = not significant, P>0.05; ** = P<0.01). The bars represent the mean and error bars represent the standard error of the mean.

to cell adhesion in other genera needs more investigation and could represent a new adhesion mechanism in a broad range of bacterial species.

Posttranslational modifications of flagellin were also shown to be involved in immune evasion [Arora et al., 2005]. Methylation of Lys residues at surface-exposed domains might remove the positive charge, which could help avoiding host immune responses. Flagellin glycosylation has been described to be involved in immune recognition mechanisms for various animal

or phytopathogenic bacteria [Ichinose et al., 2013, Ewing et al., 2009]. *Acidovorax avenae* flagellin regulates specific plant immune responses by glycosylation and flagella stability [Hirai et al., 2011]. Other well characterised species, which use glycosylation of flagellin to evade the immune system, are *Campylobacter jejuni* and *coli* [Logan et al., 1989], *Pseudomonas aeruginosa* [Brimer and Montie, 1998] and *Shewanella oneidensis* [Kerridge, 1966]. The contribution of flagellin methylation in *Salmonella* to immune recognition and evasion needs further investigation. Altogether, the findings of this chapter display a new mechanism how flagellated bacteria efficiently use cell surface-exposed glycostructures for colonisation and successful infection of the host.

# 6 Conclusion and Future Perspectives

The flagellum is a crucial virulence factor of many bacterial pathogens with various functions. Besides its main role as a motility organelle, it plays an important role during adhesion, invasion, and immune system modulation [Rossez et al., 2015]. Flagellar motility is responsible for directed movements dependent on chemotaxis [Sourjik and Wingreen, 2011]. However, a role in flagella-mediated adherence has been reported for many flagellated pathogens and in a variety of animal infection models [Haiko and Westerlund-Wikström, 2013]. Initial flagella interactions enable the formation of bacterial biofilms, which makes the flagellum an early stage colonisation factor [Pratt and Kolter, 1998b]. In *Listeria monocytogenes*, flagella have been described as non-adhesive and to be required for efficient adherence and invasion of CACO-2 cells, suggesting that rotational forces of flagella on the cell surface are needed [Dons et al., 2004]. Apart from flagella-mediated advantages in pathogenesis, biosynthesis of the flagellar system also uses significant parts of the cell's biosynthetic resources and conserved domains of flagellin monomers are recognised by the host's immune system and induce innate immune responses *in vivo*. This recognition leads to clearance of flagellated strains from the intestine of the host [Lai et al., 2013, Lockman and Curtiss, 1990, Olsen et al., 2013].

## 6.1 Flagellar gene regulation and bacterial motility

Due to its numerous functions, bacteria fine-tune flagellar synthesis, assembly, and stability according to diverse environmental stimuli. In *Salmonella* Typhimurium, flagella are highly expressed upon increasing nutrient conditions during colonisation of the small intestine, which is a result of the mucosal defense [Stecher et al., 2008, Wada et al., 2011a]. Inside SCVs and epithelial host cells, flagellar gene expression is downregulated to evade the host's immune system. However, a new round of flagellar biosynthesis occurs at later stages of the infection upon replication inside the host, presumably to facilitate escape from dying macrophages [Sano et al., 2007]. It was reported that approximately 60 % of the bacterial population in the Peyer's patches, which belongs to the gut-associated lymphoid tissue, express flagellin [Cummings et al., 2006]. At systemic sites, e.g. in spleen and mesenteric lymph nodes, flagellin expression is repressed again to evade adaptive immune recognition by $CD4^+$ T-cells [Cummings et al., 2005, Cummings et al., 2006]. Deregulation of flagellar biosynthesis e.g. through overexpression attenuates virulence in the mouse model [Yang et al., 2012, Lai et al., 2013].

In this thesis, multiple levels of flagellar regulation and their impact on *Salmonella* pathogenesis were investigated (summarised in Fig. 6.1). Flagella biosynthesis, assembly, and stability are modulated by numerous regulatory factors [Erhardt and Dersch, 2015]. In Chapter 2, novel motility regulators were identified and characterised in more detail. The negative flagellar regulator RflP was shown to also repress curli fimbrial gene expression. A *rflP* deletion therefore

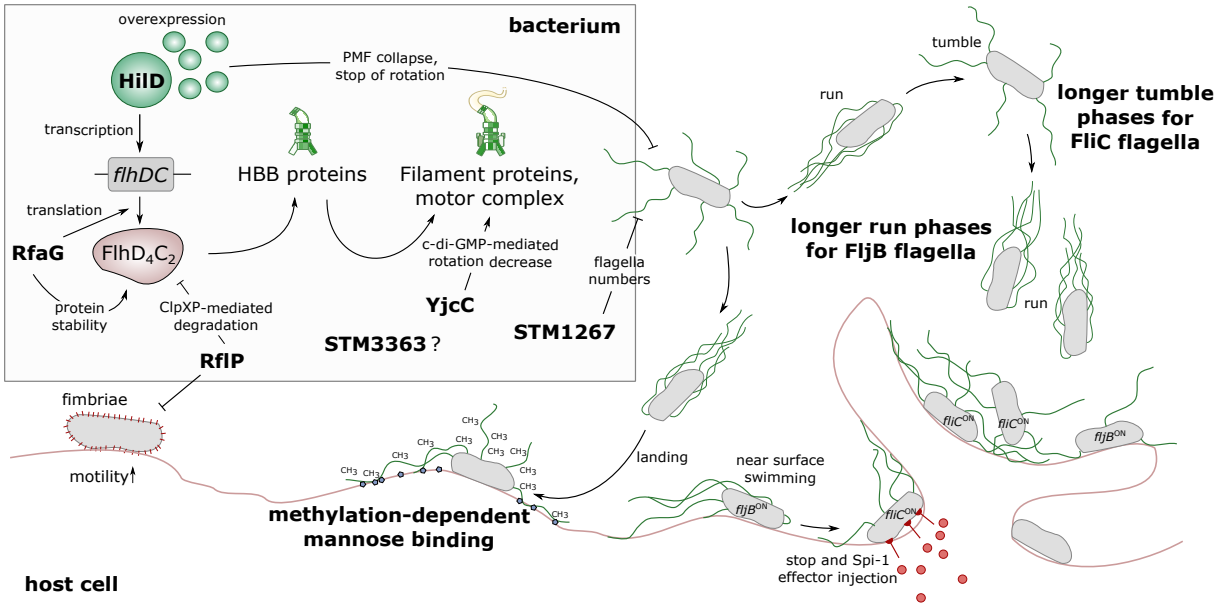


**Figure 6.1: The role of flagella and bacterial motility in *Salmonella* pathogenicity.** Fine-tuning of flagella regulation is crucial within the infection process of *Salmonella*. In this thesis, numerous regulators of flagella biosynthesis, assembly, and functionality, such as HilD, RfaG, RflP, YjcC, STM1267, and STM3363, are described. Additionally, regulation of the flagellar structure influences pathogenicity of *S.* Typhimurium. The alternate expression of flagellin has an impact on swimming on host cell surfaces favouring FliC-flagella in contrast to FljB-flagella. Adhesion to glycostructures on the eukaryotic cell surface is affected by flagellin methylation enabling successful colonisation of the gut epithelium.

might lead to reduced swarming motility of *Salmonella* due to high fimbrial gene expression and increased adhesive structures on the bacterial surface. Curli fimbriae are often associated with biofilm formation and the master regulator CsgD is known to repress flagellar-mediated motility. Biofilm-related cellulose production, EAL-like proteins, and phosphodiesterases are also involved in a decrease of motility [Lamprokostopoulou et al., 2010]. A detailed analysis of curli fimbriae assembly on the bacterial surface, *csgD* expression, or biofilm formation in a Δ*rflP* strain might therefore reveal a new role of fimbrial gene expression and biofilm formation in motility. Moreover, YjcC was shown to repress swimming motility, but not flagellar gene expression. The EAL-motif-containing protein might inhibit motility through modulation of c-di-GMP levels. C-di-GMP is known to bind YcgR, which results in a tightened interaction with flagellar motor proteins to slow down flagellar rotation [Boehm et al., 2010, Paul et al., 2010]. Rotational analyses could help understanding the mode-of-action behind this motility reduction and the contribution of YcgR in this mechanism. Interestingly, swimming and swarming motility was affected upon changes of the LPS structure in a Δ*rfaG* mutant. RfaG connects the inner core with the outer part of LPS. Here, it was shown that RfaG is involved in posttranscriptional regulation of *flhDC* translation or $FlhD_4C_2$ protein complex stability through an unknown

mechanism. Further research on this topic revealed that altered LPS structures trigger a membrane stress response, which ultimately results in RflP-mediated targeting of the $FlhD_4C_2$ complex to ClpXP-dependent degradation and thus result in non-motile bacteria (unpublished data, Imke Spöring and Dr. Sebastian Felgner).
The impact of the transcriptional activator of flagellar gene expression, HilD, on motility was analysed in Chapter 3. Besides activation of *flhDC* expression, motility was fully eradicated upon HilD induction. However, the exact mechanism behind the loss of motility was not determined. Based on the results, it was suggested that HilD overexpression leads to induction of Spi-1 injectisome-related proteins, which might affect the *Salmonella* metabolism and might result in collapse of the PMF. A detailed analysis of flagellar rotation and PMF-measurement after HilD induction would therefore contribute to the understanding of the HilD-mediated motility defect. In *L. monocytogenesis*, overexpression of PrfA, a key regulator of pathogenesis, similarly results in metabolic changes and reduced growth in broth culture [Bruno and Freitag, 2010].
In general, new motility regulators can be identified through random transposon mutagenesis or verification of mutants from Bogomolnaya et al. Careful characterisation of motility phenotypes and the underlying mechanism expand the regulatory network and our knowledge of motility-dependent virulence strategies.

## 6.2 Modification of flagella structures for productive host cell infection

Aside from flagellar gene regulation, flagella structures can be changed or posttranslationally modified to ensure efficient infection of the host. In Chapter 4, the expression of the alternative flagellins FliC and FljB was analysed regarding their function during the initial infection of the host epithelium. Differential flagellin expression resulted in assembly of distinct filament structures and diameters. These structural rearrangements influenced near surface swimming on host cell surfaces. Bacteria that harboured FliC-flagella exhibited more frequent and longer stopping phases, which facilitated Spi-1-dependent invasion. FljB-flagella were detrimental for *Salmonella* strains regarding successful infection of epithelial cells. A more detailed investigation of the filament structure through e.g. fiber diffraction analysis could hint towards the exact mechanism of how different physical and hydrodynamic forces onto the surface result in higher tumble frequencies. Also, it remains elusive at which time points *Salmonella* switches between the two flagellins during infection. Using specific antibodies against FliC and FljB or epitope-tagged flagellins, the dynamics of flagellar phase variation could be analysed *in vivo*.
Posttranslational modification through flagellin methylation at its lysine residues has been described in *Salmonella* species. In Chapter 5, the lysine methylation of FliC and FljB flagellin at specific lysine residues was investigated. Lysine residues within the variable D2 and D3 domains were predominantly methylated and affected epithelial cell adhesion and invasion. A detailed characterisation of adhesion patterns revealed that flagellin methylation was crucial for binding to mannose sugar residues on the surface of eukaryotic cells. *In vitro* binding assays

of filaments to mannose would strongly support the results obtained in this thesis. Further, upon lysine substitutions, a severe effect on filament assembly or stability was observed. To address if filaments are less stable or assemble less efficiently *in vivo*, one could measure the rate of filament formation using sequential maleimide staining [Renault et al., 2017]. Phenotypic analyses of additional flagellin substitution variants in a Δ*fliB* strain background might also contribute to a better understanding of lysine methylation.

Methylation islands were also found in many other bacterial species, such as *Yersinia*. These islands usually contain a gene that encodes a homologous protein to FliB, the methylase in *Salmonella* strains. Consequently, flagellin methylation should be analysed in other species to elucidate if methylation and its impact on cell adhesion is a general mechanism of pathogenic, flagellated bacteria. Posttranslational modification of flagellin in other bacterial species has been extensively studied regarding glycosylation. Glycosylation is involved in flagella stability and immune system evasion. Therefore, investigation of flagellin methylation and its contribution to evasion of the host's immune system is needed in the future.

# 7 Material and Methods

## 7.1 Material

### 7.1.1 Chemicals and equipment

Chemicals and equipment were purchased from Ambion, Amersham Biosciences, AppliChem, B Braun Melsungen GmbH, Beckman Coulter, Becton Dickinson & Company, Bio-Rad, Biochrom, Bioline, Biometra, Biozym, Brand, Corning, CytoOne, Edmund Bühler, eppendorf, Fisher Scientific, Fluka, G. Heinemann, GE Healthcare, Gibco, Grant-bio, Greiner, Heidolph, IDT, IMPLEN, Invitrogen, J. T. Baker, Kern PCB, Kimtech Science, KNF Lab Laboport, Macherey-Nagel, MACS Miltenyi Biotec, Memmert, Merck, Mettler Toledo, Microflex, Milli-Q, New Brunswick Scientific, New England Biolabs, Nunc, Peqlab, Poly Tron, Promega, Qiagen, Roth, Sarstedt, Sartorius, Scientific industries, Sigma-Aldrich, Starlab, Stratagene, Tecan, Thermo Scientific, TPP, VWR international, and Zeiss. Special equipment, consumables, and chemicals are indicated in the corresponding paragraphs.

### 7.1.2 Software and databases

For whole genome sequences of *Salmonella enterica* serovar Typhimurium, the Nucleotide Database from the National Center for Biotechnology Information (NCBI; www.ncbi.nlm.nih.gov) was used. Special software and databases are mentioned in the corresponding paragraphs.

### 7.1.3 Bacterial strains

All *Salmonella* Typhimurium and *Escherichia coli* strains used in this thesis are listed in Tab. 7.1.

**Table 7.1: Strains used in this thesis.**

| Strain | Genotype | Reference |
|---|---|---|
| *Salmonella enterica* serovar Typhimurium LT2 | | |
| TH437 | WT | Lab collection |
| TH13438 | $\Delta araBAD997$::$fimZ^+$ $fimH56$::Mu*dJ* | Lab collection |
| TH13439 | $\Delta araBAD997$::$fimZ^+$ $fimW57$::Mu*dJ* | Lab collection |
| TH13498 | $fimH56$::Mu*dJ* | Lab collection |
| TH13502 | $\Delta araBAD995$::$rflP^+$ $fimH56$::Mu*dJ* | Lab collection |
| TH13505 | $fimW57$::Mu*dJ* | Lab collection |
| TH13509 | $\Delta araBAD995$::$rflP^+$ $fimW57$::Mu*dJ* | Lab collection |

| Strain | Genotype | Reference |
|---|---|---|
| TH13646 | Δ*araBAD*1005::FCF P$_{flhDC}$5451::Tn*10d*Tc (del-25) | This thesis |
| TH16339 | Δ*araBAD*1065::*hilD*$^{+}$ | [Singer et al., 2014] |
| EM89 | Δ*araBAD*1065::*hilD*$^{+}$ P$_{flhDC}$5451::Tn*10d*Tc (del-25) | This thesis |
| EM93 | Δ*araBAD*1065::*hilD*$^{+}$ Δ*invH-sprB*::FRT | This thesis |
| EM584 | *flhC*5213::Mu*dJ* | Lab collection |
| EM808 | Δ*araBAD*1005::FRT | This thesis |
| EM824 | Δ*fliF*7355 | Lab collection |
| EM831 | Δ*araBAD*1182::*hilD*$_{\Delta\text{HTH}}$ | This thesis |
| EM839 | Δ*sseA-ssaU*::FRT (Δ*spi-2*) Δ*invH-sprB*::FRT (Δ*spi-1*) Δ*araBAD*1065::*hilD*$^{+}$ | This thesis |
| EM840 | Δ*sseA-ssaU*::FRT (Δ*spi-2*) Δ*araBAD*1065::*hilD*$^{+}$ | This thesis |
| EM859 | Δ*hin*-5717::FRT Δ*araBAD*1065::*hilD*+ | This thesis |
| EM860 | Δ*hin*-5717::FRT Δ*araBAD*1005::FRT | This thesis |
| EM880 | Δ*fliB*8191 | [Deditius et al., 2015] |
| EM899 | Δ*hutI-H*::P$_{sicA}$-eGFP Δ*araBAD*1065::*hilD*$^{+}$ | This thesis |
| EM900 | Δ*hutI-H*::P$_{sicA}$-eGFP Δ*araBAD*1005::FRT | This thesis |
| EM930 | Δ*araBAD*1183::*hilA*$^{+}$ | This thesis |
| EM1343 | Δ*invF* Δ*araBAD*1065::*hilD*$^{+}$ | This thesis |
| EM1438 | *flhC*::3xFLAG-FRT | [Deditius et al., 2015] |
| EM1480 | ΔSTM0971::FRT | [Deditius et al., 2015] |
| EM1481 | ΔSTM1267::FRT | [Deditius et al., 2015] |
| EM1482 | ΔSTM1896::FRT | [Deditius et al., 2015] |
| EM1484 | ΔSTM3363:FRT | [Deditius et al., 2015] |
| EM1507 | ΔSTM0266::FRT | [Deditius et al., 2015] |
| EM1508 | ΔSTM0295::FRT | [Deditius et al., 2015] |
| EM1509 | ΔSTM1575::FRT | [Deditius et al., 2015] |
| EM1510 | ΔSTM1630::FRT | [Deditius et al., 2015] |
| EM1511 | Δ*yjcC*::FRT | [Deditius et al., 2015] |
| EM1512 | ΔSTM0289::FRT | [Deditius et al., 2015] |
| EM1655 | Δ*araBAD*1065::*hilD*$^{+}$ Δ*siiE*::FKF | This thesis |
| EM1686 | ΔSTM0847::FRT | [Deditius et al., 2015] |
| EM1688 | ΔSTM1131::FRT | [Deditius et al., 2015] |
| EM1689 | ΔSTM1268::FRT | [Deditius et al., 2015] |

| Strain | Genotype | Reference |
|---|---|---|
| EM1690 | ΔSTM3696::FRT | [Deditius et al., 2015] |
| EM1691 | Δ*rygD*::FRT (deletes sRNA) | [Deditius et al., 2015] |
| EM1780 | ΔSTM1267::FRT *flhC*5213::Mu*dJ* | [Deditius et al., 2015] |
| EM1781 | ΔSTM1267::FRT *fliL*5100::Mu*dJ* | [Deditius et al., 2015] |
| EM1783 | ΔSTM3363::FRT *flhC*5213::Mu*dJ* | [Deditius et al., 2015] |
| EM1784 | ΔSTM3363::FRT *fliL*5100::Mu*dJ* | [Deditius et al., 2015] |
| EM1795 | Δ*araBAD*1065::*hilD*$^+$ Δ*sipBCD*::FKF | This thesis |
| EM1933 | Δ*araBAD*1065::*hilD*$^+$ Δ*spaPQR* | This thesis |
| EM2170 | Δ*araBAD*1065::*hilD*$^+$ Δ*prgH-hilA*-7726::*tetRA* | This thesis |
| EM2171 | Δ*araBAD*1065::*hilD*$^+$ Δ*sptP-spaS*::*tetRA* | This thesis |
| EM2172 | Δ*araBAD*1065::*hilD*$^+$ Δ*invI-invH*::*tetRA* | This thesis |
| EM2213 | Δ*araBAD*1065::*hilD*$^+$ Δ*sprB-prgI*::*tetRA* | This thesis |
| EM2214 | Δ*araBAD*1065::*hilD*$^+$ Δ*orgA*-STM05625::*tetRA* | This thesis |
| EM2215 | Δ*araBAD*1065::*hilD*$^+$ Δ*sicA-invB*::*tetRA* | This thesis |
| EM2375 | ΔSTM1267::FRT Δ*hin*-5717::FCF | [Deditius et al., 2015] |
| EM2376 | ΔSTM3363::FRT Δ*hin*-5717::FCF | [Deditius et al., 2015] |
| EM2381 | Δ*fljA*5576::FKF | [Deditius et al., 2015] |
| EM2382 | Δ*rflP*::FKF | [Deditius et al., 2015] |
| EM2383 | Δ*fimZ*::FKF | [Deditius et al., 2015] |
| EM2384 | Δ*sipA*::FKF | [Deditius et al., 2015] |
| EM2385 | Δ*sptP*::FKF | [Deditius et al., 2015] |
| EM2397 | Δ*araBAD*1065::*hilD*$^+$ Δ*hilD*::*tetRA* | This thesis |
| EM2398 | Δ*araBAD*1065::*hilD*$^+$ Δ*hilA*112::FRT | This thesis |
| EM2476 | ΔSTM1267::FRT Δ*hin*-5717::FCF *fliC*5050::Mu*dJ* | [Deditius et al., 2015] |
| EM2477 | ΔSTM3363::FRT Δ*hin*-5717::FCF *fliC*5050::Mu*dJ* | [Deditius et al., 2015] |
| EM2527 | Δ*rflP*252 *fimH*56::Mu*dJ* | [Deditius et al., 2015] |
| EM2528 | Δ*rflP*252 *fimW*57::Mu*dJ* | [Deditius et al., 2015] |
| EM2585 | Δ*hin*-5717::FCF *fliC*5050::Mu*dJ* | [Deditius et al., 2015] |
| EM2586 | *fliL*5100::Mu*dJ* | [Deditius et al., 2015] |
| EM2587 | Δ*yjcC*::FRT Δ*hin*-5717::FCF *fliC*5050::Mu*dJ* | [Deditius et al., 2015] |
| EM2588 | Δ*yjcC*::FRT *fliL*5100::Mu*dJ* | [Deditius et al., 2015] |
| EM2589 | Δ*yjcC*::FRT *flhC*5213::Mu*dJ* | [Deditius et al., 2015] |
| EM2590 | Δ*flgE*7659 | [Deditius et al., 2015] |

| Strain | Genotype | Reference |
|---|---|---|
| EM2591 | Δ*fliH*7363 | [Deditius et al., 2015] |
| EM2596 | Δ*araBAD*1065::*hilD*$^+$ Δ*iagB*::*tetRA* | This thesis |
| EM2597 | Δ*araBAD*1065::*hilD*$^+$ Δ*prgH-iagB*::*tetRA* | This thesis |
| EM2605 | Δ*rfaG*::FRT | [Zenk et al., 2009] |
| EM2606 | Δ*rfaG flhC*5213::Mu*dJ* | [Deditius et al., 2015] |
| EM2607 | Δ*rfaG fliL*5100::Mu*dJ* | [Deditius et al., 2015] |
| EM2608 | Δ*rfaG* Δ*hin*-5718::FCF *fljB*5001::Mu*dJ* | [Deditius et al., 2015] |
| EM2609 | Δ*hin*-5718::FRT *fljB*5001::Mu*dJ* | [Deditius et al., 2015] |
| EM2724 | Δ*araBAD*997::*fimZ*$^+$ *fimH*56::Mu*dJ* *rflP*240::Tn*10d*Tc (del-25) | [Deditius et al., 2015] |
| EM2725 | Δ*araBAD*997::*fimZ*$^+$ *fimW*57::Mu*dJ* *rflP*240::Tn*10d*Tc (del-25) | [Deditius et al., 2015] |
| EM2726 | Δ*araBAD*997::*fimZ*$^+$ *fimH*56::Mu*dJ* Δ*rflP*251::*tetRA* | [Deditius et al., 2015] |
| EM2727 | Δ*araBAD*997::*fimZ*$^+$ *fimW*57::Mu*dJ* Δ*rflP*251::*tetRA* | [Deditius et al., 2015] |
| EM2733 | Δ*araBAD*1065::*hilD*$^+$ Δ*prgI*152::*tetRA* | This thesis |
| EM2739 | Δ*araBAD*1183::*hilA*$^+$ Δ*sprB*-STM05625::*tetRA* | This thesis |
| EM2748 | *flhC*::3xFLAG-FRT Δ*rfaG* | [Deditius et al., 2015] |
| EM3050 | P$_{flhDC}$22343 (-598 to -554 A=C, T=G) (randomised HilD binding site) Δ*araBAD*1005::FRT | This thesis |
| EM3051 | P$_{flhDC}$22343 (-598 to -554 A=C, T=G) (randomised HilD binding site) Δ*araBAD*1065::*hilD*$^+$ | This thesis |
| EM3052 | P$_{flhDC}$22343 (-598 to -554 A=C, T=G) (randomised HilD binding site) Δ*araBAD*1183::*hilA*$^+$ | This thesis |
| EM3059 | ΔP$_{flhDC}$(-598 to -554) (ΔHilD binding site) Δ*araBAD*1005::FRT | This thesis |
| EM3060 | ΔP$_{flhDC}$(-598 to -554) (ΔHilD binding site) Δ*araBAD*1065::*hilD*$^+$ | This thesis |
| EM3061 | ΔP$_{flhDC}$(-598 to -554) (ΔHilD binding site) Δ*araBAD*1183::*hilA*$^+$ | This thesis |
| EM3903 | Δ*araBAD*1065::*hilD*$^+$ Δ*prgJ*157 | This thesis |
| EM3906 | Δ*araBAD*1065::*hilD*$^+$ Δ*orgA* | This thesis |

| Strain | Genotype | Reference |
|---|---|---|
| EM4464 | Δ*araBAD*1065::*hilD*$^{+}$ Δ*spi-5*::FKF | This thesis |
| *Salmonella enterica* serovar Typhimurium ATCC14028s | | |
| TH6622 | WT | Lab collection |
| TH11254 | Δ*hin*-5717::FRT (*fliC*$^{\mathrm{ON}}$) | Lab collection |
| TH11255 | Δ*hin*-5718::FRT (*fljB*$^{\mathrm{ON}}$) | [Horstmann et al., 2017] |
| EM838 | Δ*invH-sprB*::FRT (Δ*spi-1*) Δ*sseA-ssaU*::FRT (Δ*spi-2*) | [Horstmann et al., 2017] |
| EM1025 | Δ*fliC*7716 Δ*fljB*22314 | [Horstmann et al., 2017] |
| *Salmonella enterica* serovar Typhimurium SJW1103 | | |
| TH8362 | WT | Lab collection |
| *Salmonella enterica* serovar Typhimurium SL1344 | | |
| EM774 | WT | Lab collection |
| EM812 | Δ*fliC*7716 Δ*fljB*22314 | [Horstmann et al., 2017] |
| EM1012 | Δ*hin*-5717::FRT (*fliC*$^{\mathrm{ON}}$) | [Horstmann et al., 2017] |
| EM1013 | Δ*hin*-5718::FRT (*fljB*$^{\mathrm{ON}}$) | [Horstmann et al., 2017] |
| EM1014 | Δ*invH-sprB*::FRT (Δ*spi-1*) | [Horstmann et al., 2017] |
| EM1022 | Δ*invH-sprB*::FRT (Δ*spi-1*) Δ*sseA-ssaU*::FCF (Δ*spi-2*) | [Horstmann et al., 2017] |
| EM1398 | Δ*hin*-5717::FRT (*fliC*$^{\mathrm{ON}}$) Δ*attP*22::FKF | [Horstmann et al., 2017] |
| EM1399 | Δ*hin*-5718::FRT (*fljB*$^{\mathrm{ON}}$) Δ*attP*22::FCF | [Horstmann et al., 2017] |
| EM3122 | Δ*invH-sprB*::FKF (Δ*spi-1*) | This thesis |
| EM3123 | Δ*hin*-5717::FRT (*fliC*$^{\mathrm{ON}}$) Δ*invH-sprB*::FKF (Δ*spi-1*) | [Horstmann et al., 2017] |
| EM3124 | Δ*hin*-5718::FRT (*fljB*$^{\mathrm{ON}}$) Δ*invH-sprB*::FKF (Δ*spi-1*) | [Horstmann et al., 2017] |
| EM3125 | Δ*fliC*7716 Δ*fljB*22314 Δ*invH-sprB*::FKF (Δ*spi-1*) | [Horstmann et al., 2017] |
| EM3734 | Δ*fliB*8191 | This thesis |
| EM3755 | Δ*hin*-5717::FRT (*fliC*$^{\mathrm{ON}}$) / pFS48 | [Horstmann et al., 2017] |
| EM3757 | Δ*hin*-5718::FRT (*fljB*$^{\mathrm{ON}}$) / pFS48 | [Horstmann et al., 2017] |
| EM3758 | Δ*fliB*8191 Δ*invH-sprB*::FKF (Δ*spi-1*) | This thesis |
| EM3759 | Δ*fliB*8191 Δ*hin*-5717::FCF (*fliC*$^{\mathrm{ON}}$) Δ*invH-sprB*::FKF (Δ*spi-1*) | This thesis |
| EM3760 | Δ*fliB*8191 Δ*hin*-5718::FCF (*fljB*$^{\mathrm{ON}}$) Δ*invH-sprB*::FKF (Δ*spi-1*) | This thesis |

| Strain | Genotype | Reference |
|---|---|---|
| EM3827 | Δ*hin*-5717::FRT (*fliC*$^{ON}$) *motA*5461::Mu*dJ* | [Horstmann et al., 2017] |
| EM3868 | Δ*hin*-5718::FRT (*fljB*$^{ON}$) *motA*5461::Mu*dJ* | [Horstmann et al., 2017] |
| EM4043 | Δ*invH-sprB*::FRT (Δ*spi-1*) Δ*sseA-ssaU*::FCF (Δ*spi-2*) *motA*5461::Mu*dJ* | [Horstmann et al., 2017] |
| EM4113 | Δ*fliB*8191 Δ*hin*-5717::FRT (*fliC*$^{ON}$) | This thesis |
| EM4114 | Δ*fliB*8191 Δ*hin*-5718::FRT (*fljB*$^{ON}$) | This thesis |
| EM4660 | Δ*fliB*8191 Δ*hin*-5717::FRT (*fliC*$^{ON}$) Δ*attP*22::FCF | This thesis |
| EM4699 | Δ*hin*-5717::FRT (*fliC*$^{ON}$) Δ*flgE*6231(Δaa R106-Q112)::*tetRA* | This thesis |
| EM4700 | Δ*hin*-5717::FRT (*fliC*$^{ON}$) Δ*fliB*8191 Δ*flgE*6231(Δaa R106-Q112)::*tetRA* | This thesis |
| EM4809 | Δ*fliC*7716 Δ*hin*-5717::FRT (*fliC*$^{ON}$) Δ*fljB*22314 / pTrc99A FF4-*fliC* | [Horstmann et al., 2017] |
| EM4949 | Δ*hin*-5717::FRT (*fliC*$^{ON}$) Δ*flgKL*5739::FKF | This thesis |
| EM4950 | Δ*hin*-5717::FRT (*fliC*$^{ON}$) Δ*fliB*8191 Δ*flgKL*5739::FKF | This thesis |
| EM5054 | Δ*fliC*7716 Δ*hin*-5717::FRT (*fliC*$^{ON}$) Δ*fljB*22314 / pTrc99A FF4-*fljB* | [Horstmann et al., 2017] |
| EM5080 | *fliB*22903::Tn*10d*Tc (*tetR* terminator) Δ*hin*-5717::FCF (*fliC*$^{ON}$) | This thesis |
| | Δ*fliC*7716 Δ*fljB*22314 pASK-IBA3plus-*fliC* | [Horstmann et al., 2017] |
| | Δ*fliC*7716 Δ*fljB*22314 pASK-IBA3plus-*fljB* | [Horstmann et al., 2017] |
| *Escherichia coli* K12 | | |
| EM902 | DH10beta F- *endA*1 *recA*1 *galE*15 *galK*16 *nupG* *rpsL* Δ*lacX*74 Φ80*lacZ*Δ*M15* *araD*139 Δ(*ara,leu*)7697 *mcrA* Δ(*mrr-hsdRMS-mcrBC*) λ$^{-}$ | Lab collection |

### 7.1.4 Plasmids, oligonucleotides, and gBlocks®

All plasmids used in this thesis are listed in Tab. 7.2. Oligonucleotides and gBlocks® were purchased from "IDT-Integrated DNA Technologies" (Belgium) and are listed in Tab. 7.3 and 7.4, respectively. All oligonucleotides were adjusted to an end concentration of 200 µM and stored at -20 °C.

**Table 7.2: Plasmids used in this thesis.**

| Plasmid | Genotype | Reference |
|---|---|---|
| pCP20 | Flp expression plasmid; P$\lambda$*pR*-$\lambda$cI857-*FLP*, *repA*101ts; $Cmn^R$, $Amp^R$, 30 °C | B. Wanner |
| pFS48 | PL*tetO*-1-*mCherry*, p15A; $Cmn^R$ | F. Schuster, PhD thesis |
| pKD46 | $\lambda$-Red recombinase plasmid; $P_{araBAD}$-$\lambda$ *red* ($\gamma$, $\beta$, *exo*) tL3, *repA*101ts, *oriR*101, $Amp^R$, 30 °C | B. Wanner |
| pTrc99A FF4-*fliC* | Modified pTrc99A expression vector with *fliC* insertion; *trc* promoter, ColE1 ori, $Amp^R$ | This study |
| pTrc99A FF4-*fljB* | Modified pTrc99A expression vector with *fljB* insertion, *trc* promoter, ColE1 ori, $Amp^R$ | This study |

**Table 7.3: Oligonucleotides used in this thesis.**

| ID | Name | Sequence (5' to 3')* |
|---|---|---|
| Strain construction | | |
| 712 | 3'-STM1668_tetR_fw | AAACATTAATTCGCATCAGAGGTTGCGGT ATTACCCTTAGgtttccatttaggtgggtac |
| 713 | 5'-STM1668_tetA_rv | TAAGATTATGTTTCGACATACGCACTGTT GATCCTTTTTActaagcacttgtctcctg |
| 714 | 3'-STM1669_tetR_fw | TATATCCCCCTGCCTGGCAGAGGGAGTAT TTAAATAAGATgtttccatttaggtgggtac |
| 715 | 5'-STM1669_tetA_rv | TAATGGGTTTTTTAGAAAAAACCACTGTA TTGTCTCCTGCctaagcacttgtctcctg |
| 736 | 3'-STM1668-1669_seq_fw | ccccgatgttccttttggata |
| 737 | 5'-STM1668_seq_rv | cagcgcaattgataggccaa |
| 738 | 5'-STM1669_seq_rv | cgcgaaagccaagctgac |
| 955 | 5'_invF_tetRA_fw | ACTCTGGCCAAAAGAATATGTGTCTTCAT TTGTCTGCCAAttaagacccactttcacatt |
| 956 | 3'_invF_tetRA_rv | GACGTGTTCCGCGCAAAAGCTGCATATGT CATTTTCTGaactaagcacttgtctcctg |
| 957 | 5'_invF_seq_fw | cgggggttcgctactgacaa |
| 958 | 3'_invF_seq_rv | cagaagaatgaggcgccatg |
| 961 | 5'_invF_clean_fw | cagcgttatggtttgataat |
| 962 | 3'_invF_clean_rv | ACTCTGGCCAAAAGAATATGTGTCTTCAT TTGTCTGCCAAttcagaaaatgacatatgca |

| ID | Name | Sequence (5' to 3')* |
|---|---|---|
| 1137 | 5'-STM0699-FKF_fw | AACCGCCTCCAGGCCGGATAAGGCGCTTG TGATATCTGACgtgtaggctggagctgcttc |
| 1138 | 3'-STM0699-FKF_rv | GTAGTCCGGGCATTTTCACTCTTTGAATA AGATAATAGAAcatatgaatatcctccttag |
| 1139 | 5'-STM0971-FKF_fw | CATCCTGTAAAAAAGCGGTACTGCGAGCG TAAATTTTGGAgtgtaggctggagctgcttc |
| 1140 | 3'-STM0971-FKF_rv | ATCAGCCTGGGTTTAGAAATGACATCAGA TTTACACCTGAcatatgaatatcctccttag |
| 1141 | 5'-STM1267-FKF_fw | CTTGCCGCCTTTAAGCAACTCGAATTATTT TGGGTATATAgtgtaggctggagctgcttc |
| 1142 | 3'-STM1267-FKF_rv | CAGGGAGATCGGCTTCAATTTACATCGAA TATGGTGAAATcatatgaatatcctccttag |
| 1143 | 5'-STM1896-FKF_fw | GCTGGCGTCAGCTAATAGCCTCACGGAAA CACGGGAAAGAgtgtaggctggagctgcttc |
| 1144 | 3'-STM1896-FKF_rv | AATTAATGCTGTGCATTAAACTGTGATGG TAATCTGGCAAcatatgaatatcctccttag |
| 1145 | 5'-STM2901-FKF_fw | ATGCCTGGAATGAATGGCAAACAGTCTAT AAGGTGATTGAgtgtaggctggagctgcttc |
| 1146 | 3'-STM2901-FKF_rv | TCACGGAAGAGTGCTAACACCTCTTGCTG AATTGTGTCCAcatatgaatatcctccttag |
| 1147 | 5'-STM3363-FKF_fw | ACGACTTGCCCCCGCCTGCCGGGGGCTTT TTTATGCTTTTgtgtaggctggagctgcttc |
| 1148 | 3'-STM3363-FKF_rv | AGTAAAACAGACAATTGTCTGTCGGGGAT GGTGGCTGGCTcatatgaatatcctccttag |
| 1149 | 5'-spaPQR-tetRA_fw | CATGAATGGCTGAGCGAGTCTGGTAATGG GGAATGATATCttaagacccactttcacatt |
| 1150 | 3'-spaPQR-tetRA_rv | CCGTTTTTTAGTCGGTTTTTCTGTTTTATT CGAGGACATGctaagcacttgtctcctg |
| 1151 | 5'-spaPQR_clean_fw | ctctgcctggcttgaatcaa |
| 1152 | 3'-spaPQR_clean_rv | CCGTTTTTTAGTCGGTTTTTCTGTTTTATT CGAGGACATGgatatcattccccattacca |
| 1153 | 5'-spaPQR_seq_fw | gacaatcaatgcgcaagcaa |
| 1154 | 3'-spaPQR_seq_rv | aatcggtagcagtgatacgc |
| 1181 | 5'-STM0699-seq_fw | aaagcttcctgggggaagaa |
| 1182 | 5'-STM0971-seq_fw | agtgaatgcgaccaataacc |
| 1183 | 5'-STM1267-seq_fw | cttcatacttcaagttgcttatgtg |

| ID | Name | Sequence (5' to 3')* |
|---|---|---|
| 1184 | 5'-STM1896-seq_fw | gtccagatacgcattatcac |
| 1185 | 5'-STM2901-seq_fw | ctatcgtctcgtatatcgcg |
| 1186 | 5'-STM3363-seq_fw | gtctcgcagattggtagtac |
| 1312 | 5'-sipBCD-FKF-fw | CTTACACTTGTAACCATTATTAATATCCTC TTCTGTTATCgtgtaggctggagctgcttc |
| 1313 | 3'-sipBCD-FKF-rv | ACAGAGCAGCACAGTGAACAAGAAAAGGA ATAATTATGGTcatatgaatatcctccttag |
| 1314 | 5'-sipD_seq-fw | acatatcaagcgcctcaaca |
| 1752 | 5'-orgA_seq_fw | ggatggtcgaccgcagctga |
| 1753 | 5'-DprgI-tetRA_fw | ATAGTTGCAATCGACATAATCCACCTTATA ACTGATTAACtaagacccactttcacatt |
| 1754 | 5'-prgI_seq_fw | cgtcaccagattagggtcct |
| 1755 | 3'-DorgA-tetRA_rv | CCATTATGCCCGCAATAAGAAAGGCATAA CGGCTGATGATctaagcacttgtctcctg |
| 2039 | 5'-DprgI-clean_fw | atcgtctgtaatgactgttc |
| 2040 | 3'-DprgI-clean_rv | ATTTAACGTAAATAAGGAAGTCATTATGG CAACACCTTGGgttaatcagttataaggtgg |
| 2041 | 3'-DprgI-seq_rv | agagctcgaggtgttaagtc |
| 2042 | 5'-DorgA-clean_fw | tgcgatctgatcgccgcaac |
| 2043 | 3'-DorgA-clean_rv | CCATTATGCCCGCAATAAGAAAGGCATAA CGGCTGATGATgctttcgcctgttgaggggga |
| 2044 | 3'-DorgA-seq_rv | tattgaacagcgactggaac |
| 2045 | 5'-DprgK-tetRA_fw | GGGCTGTTGAAACGCTATTACGCTCATGA TTCGTCGATAttaagacccactttcacatt |
| 2046 | 3'-DprgK-tetRA_rv | TTGCCAGATAATGGGTAATGGCTGCCTAT TCATTTGACgactaagcacttgtctcctg |
| 2047 | 5'-DprgK-seq_fw | gtctatggaaacggacattg |
| 2048 | 3'-DprgK-seq_rv | cggcgccttattgcagacag |
| 2049 | 5'-DprgK-clean_fw | caggtctatggaaacggaca |
| 2050 | 3'-DprgK-clean_rv | TTGCCAGATAATGGGTAATGGCTGCCTAT TCATTTGACGAatatcgacgaatcatgagcg |
| 2051 | 5'-DprgJ-tetRA_fw | CCGTTAATCAGTTATAAGGTGGATTATGT CGATTGCAACttaagacccactttcacatt |
| 2052 | 3'-DprgJ-tetRA_rv | AGAAAAGTATATAGATATCGACGAATCAT GAGCGTAATagctaagcacttgtctcctg |
| 2053 | 5'-DprgJ-seq_fw | gtaaataaggaagtcattat |

| ID | Name | Sequence (5' to 3')* |
|---|---|---|
| 2054 | 3'-DprgJ-seq_rv | tccatcgtctgtaatgactg |
| 2055 | 3'-DprgJ-clean_rv | AGAAAAGTATATAGATATCGACGAATCAT GAGCGTAATAGagttgcaatcgacataatcc |
| 2084 | 5'-fliC-Dlysine_KanR_fw | GGGAACTGGTAAAGATGGCTATTATGAAG TTTCCGTTGATagggttttcccagtcacgac |
| 2085 | 3'-fliC-Dlysine_KanR_rv | GGGAAGTCGCACCGCCAGCAAGAGTCACC TCACCGTTCGTtgcttccggctcgtatgttg |
| 2086 | 3'-fliC-KtoN4x_seq_rv | tcgtattatcaacggaaact |
| 2087 | 5'-fliC-K204N_fw | TGCCGATACTACGATTGCTTTAGACAATA GTACTTTTAACgcctcggctactggtcttgg |
| 2088 | 5'-fliC-K216N_fw | TAAAGCCTCGGCTACTGGTCTTGGTGGTA CTGACCAGAACattgatggcgatttaaaatt |
| 2089 | 5'-fliC-K233N_fw | TTTAAAATTTGATGATACGACTGGAAAAT ATTACGCCAACgttaccgttacgggggggaac |
| 2090 | 5'-fliC-K252N_fw | AACTGGTAAAGATGGCTATTATGAAGTTT CCGTTGATAATacgaacggtgaggtgactct |
| 2091 | 3'-fliC-KtoN_singledel_rv | ggtaatagcggagttgaaac |
| 2092 | 3'-fliC-K204N_seq_rv | tagccgaggcgttaaaagta |
| 2093 | 3'-fliC-K216N_seq_rv | atcgccatcaatgttctggt |
| 2094 | 3'-fliC-K233N_seq_rv | cgtaacggtaacgttggcgt |
| 2095 | 3'-fliC-K252N_seq_rv | gttcgtattatcaacggaaa |
| 2228 | 5'-DfljB_DD3-tetRA_fw | GTATGATGTGAAAGATACAGCAGTAACAA CGAAAGCTAGctaagacccactttcacatt |
| 2229 | 3'-DfljB_DD3-tetRA_rv | TTTTAGCATCTGCTGAAACAACTGCCGGT GTATCTTTTaactaagcacttgtctcctg |
| 2230 | 5'-DfliC_DD3-tetRA_fw | ATATAAGGTCAGCGATACGGCTGCAACTG TTACAGGAAGCtaagacccactttcacatt |
| 2231 | 3'-DfliC_DD3-tetRA_rv | ATGCGGCTTTAGCCTCTGTCAAATCAGCA TTTGCAACTtgctaagcacttgtctcctg |
| 2474 | 5'-fliCK222N-rth_fw | TCTTGGTGGTACTGACCAGAAAATTGATG GCGATTTAAActttgatgatacgactggaaa |
| 2475 | 3'-fliCK222N-rth_rv | ccagtagccgaggctttaaa |
| 2482 | 5'-fliCLysKtoNall_tetRA_fw | ATATGCCGATACTACGATTGCTTTAGACA ATAGTACTTTttaagacccactttcacatt |
| 2483 | 3'-fliCLysKtoNall_tetRA_rv | CATCTTTATTTTGAGTTGCAGAATAGTAA TCATCGCCTacctaagcacttgtctcctg |

| ID | Name | Sequence (5' to 3')* |
|---|---|---|
| 2484 | 5'-fliCK222-229N_tetRA_fw | TGGTCTTGGTGGTACTGACCAGAAaATTGA TGGCGATTTataagacccactttcacatt |
| 2485 | 3'-fliCK222-229N_tetRA_rv | CTTTACCAGTTCCCCCCGTAACGGTAACTT TGGCGTAAtactaagcacttgtctcctg |
| 2486 | 5'-fliCK222-229N_fw | ACTTTTAAAGCCTCGGCTACTGGTCTTGG TGGTACTGACCagaaaattgatggcgattta |
| 2487 | 3'-fliCK222-229N_rv | GGAAACTTCATAATAGCCATCTTTACCAGT TCCCCCCGTAacggtaactttggcgtaata |
| 2488 | 5'-fliCK293-309-319-327N_tetRA_fw | GAAAAATGTACAAGTTGCAAATGCTGATT TGACAGAGGCttaagacccactttcacatt |
| 2489 | 3'-fliCK293-309-319-327N_tetRA_rv | CATCTTTATTTTGAGTTGCAGAATAGTAA TCATCGCCTacctaagcacttgtctcctg |
| 2490 | 5'-fliCK293-309-319-327N_fw | GCGACAGCAACTGAGGATGTGAAAAATGT ACAAGTTGCAAatgctgatttgacagaggct |
| 2491 | 3'-fliCK293-309-319-327N_rv | AGTATTAATACTTATGGAACCATCTTTATT TTGAGTTGCAgaatagtaatcatcgcctac |
| 2492 | 5'-fljBLysKtoNall_tetRA_fw | GGGTCTGGACTCACTGAACGTGCAGAAAG CGTATGATGTgtaagacccactttcacatt |
| 2493 | 3'-fljBLysKtoNall_tetRA_rv | CTTTGAAATCATGACCAGCGGCTTTGCTG GCATTGTAGgtctaagcacttgtctcctg |
| 2498 | 5'-fljBK189-288N_tetRA_fw | GCAGAAAGCGTATGATGTGAAAGATACAG CAGTAACAACgtaagacccactttcacatt |
| 2499 | 3'-fljBK189-288N_tetRA_rv | AGGCATTTTTAGCATCTGCTGAAACAACT GCCGGTGTAtcctaagcacttgtctcctg |
| 2500 | 5'-fljBK189-288N_fw | GCAGAAAGCGTATGATGTGAAAGATACAG CAGTAACAACGAacgcttatgccaataatgg |
| 2501 | 3'-fljBK189-288N_rv | AGGCATTTTTAGCATCTGCTGAAACAACT GCCGGTGTATCgtttaactcctgtacttctg |
| 2502 | 5'-fljBK189-209N_tetRA_fw | GCAGAAAGCGTATGATGTGAAAGATACAG CAGTAACAACgtaagacccactttcacatt |
| 2503 | 3'-fljBK189-209N_tetRA_rv | CTGTACCGTCAGTAGCAACGTTAACTTCAT AATCGCCAttctaagcacttgtctcctg |
| 2504 | 5'-fljBK189-209N_fw | GAAAGCGTATGATGTGAAAGATACAGCAG TAACAACGAAcgcttatgccaataatggtac |
| 2505 | 3'-fljBK189-209N_rv | TTACAGAAGCCGTACCATTCGTACCACCCG TAGCCGCGTTaatagctgcatcatcaagac |

| ID | Name | Sequence (5' to 3')* |
|---|---|---|
| 2506 | 5'-fljBK249N_fw | TGTTACTATTGGTGGCTTTACTGGTGCTG ATGCCGCCAAcaatggcgattatgaagttaa |
| 2507 | 3'-fljBK249N_rv | ctgttttagttgtcgcacca |
| 2508 | 5'-fljBK182-319-355-357-369N_tetRA_fw | CGGCGTTGACGCTACCGATGCTAATGGCG CTGAGTTGGTctaagacccactttcacatt |
| 2509 | 3'-fljBK182-319-355-357-369N_tetRA_rv | CGGTTTTACCGTCTACGCCACCCAGTTGGT TAGCCGCTgtctaagcacttgtctcctg |
| 2510 | 5'-fljBK182N_fw | ctggcgcaggacaacaccct |
| 2511 | 3'-fljBK182N_rv | CGTTGTTACTGCTGTATCGTTCACATCATA CGCTTTCTGCA |
| 2512 | 5'-fljBK319-355-357-369N_fw | CTAATGGCGCTGAGTTGGTCAACATGTCT TATACCGATAAAAA |
| 2513 | 3'-fljBK319-355-357-369N_rv | CGGTTTTACCGTCTACGCCACCCAGTTGGT TAGCCGCTGTGTTGGTAGTGCCGTCAGCA G |
| 2539 | 5'-fliB_tetRA_fw | TCGCTGCCTTGATTGTGTACCACGTGTCG GTGAATCAAtcctaagcacttgtctcctg |
| 2540 | 3'-fliB_tetRA_rv | GAACCAGGTTCCGCAAAACGTCCTCTCTTT ACTGCGTtaaagagtagggaactgcca |
| 2541 | 5'-fliB_seq_fw | cggcgctggggaattgccct |
| 2587 | 3'-fliC-tetRA_204-233_rv | CATAATAGCCATCTTTACCAGTTCCCCCCG TAACGGTAACctaagcacttgtctcctg |
| 2588 | 3'-fliC_seq_rv | taagcggggaagtcgcaccg |
| qRT-PCR | | |
| 531 | 5'-flagellin_qPCR-60C-fw | aacgacggtatctccattgc |
| 532 | 3'-flagellin_qPCR-60C-rv | atttcagcctggatggagtc |
| 533 | 5'-fljB_qPCR-60C-fw | tacaccggcagttgtttcag |
| 534 | 3'-fljB_qPCR-60C-rv | ccgccttcaattgtcttacc |
| 535 | 5'-fliC_qPCR-60C-fw | tgataagacgaacggtgagg |
| 536 | 3'-fliC_qPCR-60C-rv | aacacctgctgctgtcaatg |
| 537 | flhDC-qPCR-fw | gtaggcagctttgcgtgtag |
| 538 | flhDC-qPCR-rv | tccagcagttgtggaataatatcg |
| 539 | flgE-qPCR-fw | aacgtctattttgtgaaaaccaaag |
| 540 | flgE-qPCR-rv | agactccagaatcccgttttc |
| 716 | gyrB_qPCR_new-fw | acgctctgtcgcaaaaactg |

| ID | Name | Sequence (5' to 3')* |
|---|---|---|
| 717 | gyrB_qPCR_new-rv | accatcgtgccggttttatc |
| 718 | gmk_qPCR_new-fw | ttttgccgccgtcaaagatc |
| 719 | gmk_qPCR_new-rv | atggctcatttctgcaaccg |
| 720 | rpoD_qPCR_new-fw | acaccatcaaagcgaaaggc |
| 721 | rpoD_qPCR_new-rv | tcatcacgcgcatactgttg |
| 1129 | 5'-lrhA_qPCR_fw | ttcagacagtccagcgaatg |
| 1130 | 3'-lrhA_qPCR_rv | cagctcggtttatccgaaac |
| 1131 | 5'-sopE2_qPCR_fw | agcataggccggatctttac |
| 1132 | 3'-sopE2_qPCR_rv | ccgactacccattttcatcg |
| 1133 | 5'-sopB_qPCR_fw | tcatgataggggggaaagcac |
| 1134 | 3'-sopB_qPCR_rv | tatgagggaaagggcgtatg |
| 1135 | 5'-sipA_qPCR_fw | cgtgaccacctttccatctt |
| 1136 | 3'-sipA_qPCR_rv | ccattcgactaacagcagca |
| 1302 | 5'-STM1668_qPCR-fw | accgtcgggatgttttctcc |
| 1303 | 3'-STM1668_qPCR-rv | ctcgcaatagtcattcccgga |
| 1304 | 5'-STM1669_qPCR-fw | ccccttgcttgaggtcagag |
| 1305 | 3'-STM1669_qPCR-rv | cgccggttagtcgtattcga |
| 1756 | 5'-csgB_qPCR_fw | attgagcaaacgggcaatgc |
| 1757 | 3'-csgB_qPCR_rv | actgctgttttctgcgtacc |
| 1758 | 5'-csgA_qPCR_fw | agcattcgcagcaatcgtag |
| 1759 | 3'-csgA_qPCR_rv | aatgctcaacgtggaatccg |
| 1760 | 5'-fimZ_qPCR_fw | ggcgcaaacggatttgtaag |
| 1761 | 3'-fimZ_qPCR_rv | tttgggggtacgggtattactg |
| 1762 | 5'-fimW_qPCR_fw | atttgccactactgcacgac |
| 1763 | 3'-fimW_qPCR_rv | aaagtaaagcggccgtttcg |
| 1764 | 5'-fimH_qPCR_fw | taacgtgtcgcagcaaaagc |
| 1765 | 3'-fimH_qPCR_rv | aacattgtctggcgagggatc |
| 1766 | 5'-pefA_qPCR_fw | agcgtgaactccaaaaaccc |
| 1767 | 3'-pefA_qPCR_rv | tcagcttggctttgaactgc |
| 1768 | 5'-siiC_qPCR_fw | tgtctcaggaggttgtgacaac |
| 1769 | 3'-siiC_qPCR_rv | tacaccggaagataccagcaac |
| 1770 | 5'-siiE_qPCR_fw | agcgctcaatgaagcgtttg |
| 1771 | 3'-siiE_qPCR_rv | attttgctgggaagcatcgc |
| 1772 | 5'-stdA_qPCR_fw | aataccgccaatgcaaccac |
| 1773 | 3'-stdA_qPCR_rv | atctgctgtgccactgaaag |

| ID | Name | Sequence (5' to 3')* |
|---|---|---|
| 2569 | 5'-safA-qPCR_fw | tttgccgaactcagagcaac |
| 2570 | 3'-safA-qPCR_rv | tcgcgctaggagcatttttc |
| 2571 | 5'-csgD-qPCR_fw | tgggtgcgatttttgacagc |
| 2572 | 3'-csgD-qPCR_rv | cactcatcgcgaaaaagagatcc |

* Recombination sites are indicated in capital letters.

**Table 7.4: gBlocks® used in this thesis.**

| Name | Sequence (5' to 3')* |
|---|---|
| fliC Lys KtoR all | cgatacggctgcaactgttacaggatatgccgatactacgattgctttagacaatagtactttta<br>**ga**gcctcggctactggtcttggtggtactgaccaga**ga**attgatggcgatttaa**ga**tttgatga<br>tacgactggaa**ga**tattacgcca**ga**gttaccgttacgggggggaactggtaaagatggctattat<br>gaagtttccgttgataagacgaacggtgaggtgactcttgctggcggtgcgacttccccgcttac<br>aggtggactacctgcgacagcaactgaggatgtgaaaaatgtacaagttgcaaatgctgatttg<br>acagaggcta**ga**gccgcattgacagcagcaggtgttaccggcacagcatctgttgtta**ga**atgt<br>cttatactgataataacggta**ga**actattgatggtggtttagcagtta**ga**gtaggcgatgattac<br>tattctgcaactcaaaataaagatggttccataagtattaatactacga |
| fljB Lys KtoN all | aagcagatcaactctcagaccctgggtctggactcactgaacgtgcagaaagcgtatgatgtga<br>a**c**gatacagcagtaacaacgaa**c**gcttatgccaataatggtactacactggatgtatcgggtct<br>tgatgatgcagctattaa**c**gcggctacgggtggtacgaatggtacggcttctgtaaccggtggtg<br>cggttaa**c**tttgacgcagataataacaa**c**tactttgttactattggtggctttactggtgctgatg<br>ccgccaa**c**aatggcgattatgaagttaacgttgctactgacggtacagtaacccttgcggctggc<br>gcaactaa**c**accacaatgcctgctggtgcgacaactaaaacagaagtacaggagttaaa**c**gat<br>acaccggcagttgtttcagcagatgctaaaaatgccttaattgctggcggcgttgacgctaccga<br>tgctaatggcgctgagttggtcaa**c**atgtcttataccgataaaaatggtaagacaattgaaggc<br>ggttatgcgcttaaagctggcgataagtattacgccgcagattacgatgaagcgacaggagcaa<br>ttaa**c**gctaa**c**actacaagttatactgctgctgacggcactaccaa**c**acagcggctaaccaact<br>gggtggcgtagacggtaaaaccgaagtcgttactatcgacggtaa**c**acctacaatgccagcaaa<br>gccgctggtcatgatttcaaagcacaaccagagctggcggaa |

| Name | Sequence (5' to 3')* |
|---|---|
| fliC Lys KtoN all | cgatacggctgcaactgttacaggatatgccgatactacgattgctttagacaatagtactttta a**c**gcctcggctactggtcttggtggtactgaccagaa**c**attgatggcgatttaaa**c**tttgatgat acgactggaaa**c**tattacgccaa**c**gttaccgttacgggggggaactggtaaagatggctattatg aagtttccgttgataagacgaacggtgaggtgactcttgctggcggtgcgacttccccgcttaca ggtggactacctgcgacagcaactgaggatgtgaaaaatgtacaagttgcaaatgctgatttga cagaggctaa**c**gccgcattgacagcagcaggtgttaccggcacagcatctgttgttaa**c**atgtct tatactgataataacggtaa**c**actattgatggtggtttagcagttaa**c**gtaggcgatgattacta ttctgcaactcaaaataaagatggttccataagtattaatactacga |

* Mutations or mutated nucleotides are highlighted in bold.

### 7.1.5 Antibodies

Antibodies used in this thesis are listed in Tab. 7.5 and were stored at 4 °C. All antibodies were diluted in 5 % milk/TBS and stored at -20 °C.

**Table 7.5: Antibodies for Western Blot and immunostaining.**

| Target | Host | Dilution | Company |
|---|---|---|---|
| Primary antibodies | | | |
| FliC | rabbit | 1:5000 (WB)<br>1:1000 (I) | Becton Dickinson & Company |
| FljB | rabbit | 1:5000 (WB)<br>1:1000 (I) | Becton Dickinson & Company |
| FLAG | mouse | 1:1000 (WB) | Sigma |
| DnaK | mouse | 1:10,000 (WB) | abcam |
| MUC2 | rabbit | 1:100 (I) | Thermo Fisher (Theresa Truschel, InSCREENeX GmbH) |
| Secondary antibodies | | | |
| GAM-HRP | goat | 1:20,000 | Bio-Rad |
| GAR-HRP | goat | 1:20,000 | Bio-Rad |
| GAR-Alexa488 | goat | 1:1000 | Invitrogen |
| GAR-Cy3 | goat | | Thermo Fisher (Theresa Truschel, InSCREENeX GmbH) |

WB = Western Blot, I = Immunostaining

### 7.1.6 Eukaryotic cell lines

Eukaryotic cell lines used in this study are listed in Tab. 7.6 and were stored in liquid nitrogen containers at -196 °C.

**Table 7.6: Eukaryotic cell lines used in this thesis.**

| Name | Source | Reference/ATCC number |
|---|---|---|
| CACO-2 | Human, colon epithelial cells | ATCC® HTB-37TM |
| CHO-K1 | Hamster, ovary epithelial-like cells | ATCC® CCL-61TM |
| CHO-K1 Δ*lec1* | No complex N-glycans, lots of terminal mannose exposed | Guntram Grassl, Hannover Medical School |
| CHO-K1 Δ*lec2* | no sialic acids | Guntram Grassl, Hannover Medical School |
| CHO-K1 Δ*xylT* | no proteoglycans | Guntram Grassl, Hannover Medical School |
| Cl10 | Mouse, colon epithelial cells | Theresa Truschel, InSCREENeX GmbH |
| Cl11 | Mouse, colon epithelial cells | Theresa Truschel, InSCREENeX GmbH |
| HT29-MTX-E12 (E12) | Human, colon epithelial cells | [Navabi et al., 2013] |
| HeLa | Human, cervical epithelial cells | ATCC® CCL-2TM |
| HEp-2 | Human, HeLa derivative (cervical epithelial cells) | ATCC® CCL-23TM |
| IPEC-J2 | Porcine, small intestinal epithelial cells | [Brosnahan and Brown, 2012] |
| J774 | Mouse, macrophage cells | ATCC® TIB-67 |
| MODE-K | Mouse, small intestinal epithelial cells | [Vidal et al., 1993] |
| NIH-3T3 | Mouse, embryonic fibroblast cells | ATCC® CRL-1658TM |
| T84 | Human, colon epithelial cells | ATCC® CCL-248TM |

### 7.1.7 Mice

All animal experiments were performed according to guidelines of the German Law for Animal Protection and with permission of the local ethics committee and the local authority LAVES (Niedersächsisches Landesamt für Verbraucherschutz und Lebensmittelsicherheit) under permission number 33.19-42502-04-13/1191. For infection experiments the laboratory inbred strain C57BL/6 was used.

### 7.1.8 Media and supplements

All media and their compositions are listed in Tab. 7.7 and were autoclaved before usage. Media supplements are listed in Tab. 7.8. Heat-sensitive components were sterile-filtered and added to the autoclaved medium.

**Table 7.7: Media compositions.**

| Medium | Composition (in $ddH_2O$) |
|---|---|
| LB (lysogeny broth) medium [Bertani, 2004] | 10 g/l tryptone, 5 g/l yeast extract, 5 g/l NaCl, (12 g/l agar) |
| TB (tryptone broth) medium | 10 g/l tryptone, 5 g/l NaCl |
| Swimming motility agar [Gillen and Hughes, 1991] | 10 g/l tryptone, 5 g/l NaCl, 3 g/l Bacto-agar |
| Swarming motility agar | 10 g/l tryptone, 5 g/l yeast extract, 5 g/l NaCl, 5 g/l Bacto-agar |
| Green plate agar | 7.4 g/l D-glucose, 7.9 g/l tryptone, 1 g/l yeast extract, 4.9 g/l NaCl, 12 g/l agar, 65 mg/l methyl blue, 0.6 g/l alizarin yellow G |
| Minimal E agar (EDEX) | 2 % Ex50, 12 g/l agar, 0.2 % D-glucose; Ex50: 9.6 g/l $MgSO_4$ x $7H_2O$, 100 g/l citric acid, 655 g/l $K_2HPO_4$ x $3H_2O$, 175 g/l $NaNH_4PO_4$ x $4H_2O$, 2.5 % chloroform |
| Minimal NCE agar | 2 % NCEx50, 12 g/l agar, 1 mM $MgSO_4$, 0.2 % arabinose; NCEx50: 19.7 g/l $KH_2PO_4$, 32.3 g/l $K_2HPO_4$ x $3H_2O$, 17.5 g/l $NaNH_4PO_4$ x $4H_2O$, 2.5 % chloroform |
| $Tet^S$ agar | 5 g/l tryptone, 5 g/l yeast extract, 12 g/l agar, 10 g/l NaCl, 10 g/l $NaH_2PO_4$ x $H_2O$, 0.1 mM $ZnCl_2$, 12 mg/l fusaric acid, 1 mg/l anhydrotetracycline |

**Table 7.8: Supplements used in this thesis.**

| Supplement | Stock concentration | Final concentration |
|---|---|---|
| Antibiotics | | |
| Ampicillin | 20 mg/ml | 0.1 mg/ml |
| Anhydrotetracycline | 0.2 mg/ml in 50 % ethanol | 0.1 µg/ml |
| Chloramphenicol | 2.5 mg/ml | 12.5 µg/ml |
| Gentamycin | 50 mg/ml | 100 µg/ml |
| Kanamycin | 10 mg/ml | 50 µg/ml |

| Supplement | Stock concentration | Final concentration |
|---|---|---|
| Tetracycline | 3 mg/ml in 50 % ethanol | 15 µg/ml |
| Other additives | | |
| L-arabinose | 20 % (w/v) | 0.2 % |
| Ficoll400 | | 10 % (w/v) |
| Fusaric acid | 2.4 mg/ml in DMF | 12 µg/ml |
| D-glucose | 40 % (w/v) | 0.2 % |
| D-mannose | 40 % (w/v) | 0.2 % |

## 7.2 Cultivation and genetic manipulation of biological material

### 7.2.1 Cultivation and storage of bacteria

All bacterial strains were cultivated under aerobic conditions at 37 °C in liquid culture or on solid media. Strains harbouring the temperature-sensitive plasmids pCP20 and pKD46 were grown aerobically at 30 °C. In general, overnight cultures were diluted 1:100 and grown 2-3 h to mid exponential phase, if not stated otherwise. For selection, appropriate antibiotics were added. Induction of $P_{araBAD}$ or $P_{tet}$ promoters was conducted by addition of 0.2 % arabinose and anhydrotetracycline, respectively. To determine bacterial growth, the optical density at a wavelength of 600 nm ($OD_{600}$) was measured by an Ultrospec 2100 pro or Ultrospec 10 spectrophotometer (Amersham Bioscences). An $OD_{600}$ of 0.942 resembles a cell density of $10^9$ cells/ml. Bacterial strains were stored in 10 % DMSO at -80 °C.

### 7.2.2 Cell viability assays

ATP levels were monitored using the BacTiter-Glo$^{TM}$ Reagent (Promega) as described in the user manual. For oxygen level assessment, 1:100 ruthenium tris(2,2'-dipyridyl) dichloride hexahydrate (RTDP) was added to 1 ml samples of bacterial main cultures with an $OD_{600}$ of 0.9. Fluorescent intensities were measured as described in Chapter 7.4.3 at an excitation of 457 nm and emission of 580 nm.

### 7.2.3 Transformation/Electroporation

For preparation of electrocompetent cells, bacterial cultures of 25 ml total volume were harvested at an $OD_{600}$ of 0.6-0.9. The pellet was washed twice and resuspended in 300 µl cold $ddH_2O$. An aliquot of 50 µl electrocompetent cells was mixed with a maximum of 5 µl DNA (200-300 ng) and transferred to a 1 mm gap electroporation cuvette. The cells were pulsed at 1.6 kV, 200 Ω, and 25 µF (Eporator, Eppendorf). For phenotypic expression, 1 ml LB medium was added and

the cells were incubated for 1 h. Selection of transformed cells was enabled by spreading and incubation on selective medium.

### 7.2.4 Homologous recombination with the λ-Red system

Mutations in the *S.* Typhimurium chromosome were introduced using the λ-Red system as described in [Karlinsey, 2007]. Briefly, a *tetRA* element, which confers tetracycline resistance, was PCR amplified with flanking homologous regions of 40 bp to the target location in the chromosome. These fragments were inserted specifically through arabinose-inducible expression of λ-Red phage recombination proteins located on pKD46 [Datsenko and Wanner, 2000]. The desired mutation was then introduced by counter-selection on tetracycline-sensitive medium ($Tet^S$). Recombinant colonies were verified by PCR and sequencing.

### 7.2.5 Site-specific recombination with Flp

Chromosomal resistance cassettes flanked by FRT (Flp recombination target) sites (FKF for $Kan^R$ or FCF for $Cmn^R$) were removed using the Flp enzyme as described before [Cherepanov and Wackernagel, 1995]. The temperature-sensitive plasmid pCP20 was introduced into *S.* Typhimurium strains containing FKF or FCF cassettes. This resulted in expression by the yeast Flp recombinase, which removed the antibiotic resistance cassette through homologous recombination between FRT sites. Through incubation at 42 °C the strains were cured from pCP20 and a single FRT scar remained.

### 7.2.6 DNA transfer via P22 transduction

#### Production of P22 phage lysates

For transfer of chromosomal mutations between *S.* Typhimurium strains, the generalised transducing phage P22 *HT105/1 int-201* was used in all transductional crosses [Sanderson and Roth, 1988]. Phage lysates were produced by addition of 4 ml P22 broth (2 % Ex50, 0.2 % D-glucose, $10^8$ pfu/ml P22 *HT105/1 int-201*) to 1 ml overnight culture. After incubation at 37 °C for 8-16 h, the cell debris was removed and 500 µl chloroform was added. All lysates were stored at 4 °C.

#### Transduction and clean-up

For transduction, a recipient overnight culture was mixed 1:1 with the donor phage lysate and incubated for 1 h at 37 °C. Selection of transduced colonies was enabled by plating the mixture on selective media and incubating overnight. Spreading of the recipient culture and the phage lysate alone served as negative control. Phage-free transductants were isolated on green agar plates and cross-streaked against P22-H5 to avoid phage-resistant bacteria.

## 7.3 Isolation and *in vitro* modification of nucleic acids

### 7.3.1 Isolation of plasmids and genomic DNA

Plasmids were isolated using the QIAprep Spin Miniprep Kit (QIAGEN) as described in the user manual. The extraction of genomic DNA was performed using the DNeasy Blood & Tissue Kit (QIAGEN) using harvested bacteria from an overnight culture instead of tissue or blood samples. Plasmids and genomic DNA was stored at -20 °C.

### 7.3.2 Isolation of RNA

Total RNA from *S.* Typhimurium was isolated using the RNeasy® Mini kit (QIAGEN) according to the manufacturer's instructions. Briefly, one volume RNAprotect® Bacteria Reagent (QIAGEN) was added to logarithmically grown cultures. Bacteria were lysed through addition of lysozyme and total RNA was purified. For transcriptome analyses, total RNA was isolated according to the "hot-phenole" method. Logarithmically grown bacteria were harvested and resuspended in 250 µl resuspension buffer (0.3 M sucrose, 0.01 M sodium acetate pH 4) and lysed in lysis buffer (2 % SDS in 0.01 M sodium acetate pH 4) at 65 °C for 1.5 h. 500 µl pre-heated aqua-phenole was added and the samples were incubated for 3 min at 65 °C. After shock-freezing of samples in liquid nitrogen for 1 min, the samples were centrifuged and the upper phase was transferred into a new tube. Aqua-phenole addition and subsequent steps were repeated twice. To extract the phenol from all samples, 400 µl chloroform was added. The RNA was vortexed for 30 sec and centrifuged. The upper phase was transferred into a new tube and chloroform addition was repeated 3-4 times. 3/10 volumes of 1 M sodium acetate pH 4 and 2.5 volumes of 95 % ethanol were added and the samples were incubated for 1 h. After centrifugation at 4 °C for 30 min, the pellet was washed twice with 70 % RNase-free ethanol, dried and resuspended in 100 µl RNase-free water. Subsequent to RNA purification, the TURBO DNA-free™ kit was used to remove genomic DNA from RNA samples. Samples were tested for purity and integrity by PCR and agarose gel electrophoresis and stored at -20 °C for up to 1 week.

### 7.3.3 Polymerase Chain Reaction

Double stranded DNA fragments were amplified by polymerase chain reaction (PCR). For construction of chromosomal mutations, the proof-reading Phusion DNA polymerase (pfu-sso7d, [Wang et al., 2004b]) with 5x Phusion HF Reaction Buffer (NEB) was used. Test colony PCRs were performed using Taq DNA polymerase with 5x Green GoTaq Reaction Buffer (Promega). Single colonies were lysed by incubation at 95 °C for 10 min and used as template. Standard PCR reactions and cycling conditions are listed in Tabs. 7.9 and 7.10. Annealing temperatures were calculated according to the used oligonucleotides. Elongation times were determined according to DNA polymerase and fragment size. The amplified DNA was checked via agarose

gel electrophoresis (see Chapter 7.3.5) and purified with the NucleoSpin® Gel and PCR Clean-up Kit (Macherey-Nagel).

**Table 7.9: Standard PCR reaction.**

| Component | Final concentration |
|---|---|
| 5x PCR reaction buffer | 1x |
| 25 mM $MgCl_2$ (for Taq polymerase) | 1.5 mM |
| 20 mM dNTP mix (5 mM each; NEB) | 0.8 mM |
| 10 µM oligonucleotide each (see Tab. 7.3) | 0.5 µM each |
| DNA polymerase | 0.5 µl |
| Template (genomic DNA or plasmid) | 1-500 ng |
| $ddH_2O$ | ad 50 µl |

**Table 7.10: PCR cycling conditions.**

| Cycle* | Phusion polymerase | Taq polymerase |
|---|---|---|
| 1. Initial denaturing | 2 min, 98 °C | |
| 2. Denaturing | 15 sec, 98 °C | |
| 3. Annealing | 30 sec, oligonucleotide specific temperature | |
| 4. Elongation | 30 sec/kb fragment size, 72 °C | 1 min/kb fragment size, 72 °C |
| 5. Final elongation | 5 min, 72 °C | |
| 6. Hold at 8 °C | | |

* Steps 2 to 4 were repeated for 35 cycles.

### 7.3.4 Measurement of nucleic acid concentrations

Nucleic acid concentrations (DNA and RNA) were measured by absorbance at 260 nm by a nanospectrophotometer (NanoDrop 1000, Peqlab and NanoPhotometerTM P330, Midsci). Nucleic acid purity was determined according to 260/280 nm and 260/230 nm ratios.

### 7.3.5 Agarose gel electrophoresis

Correct amplification of PCR fragments was checked via agarose gel electrophoresis. For this purpose, the DNA samples were loaded on a 1 % agarose TAE gel (40 mM Tris Base, 20 mM acetic acid, 1 mM EDTA). RNA samples were mixed 1:5 with 6x loading dye (30 % glycerol, 2.5 g/l bromophenol blue) before loading. Fractionation of PCR fragments or total RNA was performed in 1x TAE buffer at 100 V or 50 V, respectively. The exACTGene™ 1 kb Plus DNA Ladder (Fisher BioReagents) was used as a marker. Migrated DNA bands were stained with

ethidium bromide (1 µg/ml in dd$H_2O$), observed via UV transillumination in a Gel Doc$^{TM}$ XR+ documentation system (Bio-Rad), and analysed by the Image Lab$^{TM}$ software (Bio-Rad).

### 7.3.6 Molecular cloning

Sticky-end cloning and construction of plasmids was performed using enzymes from New England Biolabs according to the manufacturer's protocol. Vectors and PCR-amplified inserts were digested with restriction enzymes for 3 h at 37 °C. Inserts were incubated at enzyme-specific inactivation temperatures, whereas vectors were dephosphorylated using the Antarctic Phosphatase for 30 min at 37 °C with subsequent heat-inactivation at 70 °C for 5 min. All samples were gel-purified according to Chapter 7.3.1 and ligation was performed using the T4 DNA ligase with a molar vector-to-insert ratio of 1:3 and 1:5. Ligations were incubated overnight at 4 °C and transformed into the *E. coli* EM902 strain. Cells were plated on selective media and transformants were tested by PCR and sequencing of isolated plasmids.

### 7.3.7 Sequencing

DNA sequencing of chromosomal mutations and plasmids was performed at the in-house facility of the Helmholtz Centre for Infection Research (Department of Genome Analysis, GMAK). Sequencing results were analysed using the 4Peaks V1.7.2 (Mekentosj) and SerialCloner (Franck Perez; Serial Basics) softwares.

## 7.4 Gene expression analyses

### 7.4.1 $\beta$-galactosidase assay

The expression of a gene of interest was analysed according the method of [Zhang and Bremer, 1995] using transcriptional *lacZ* fusions via the Mu*dJ* transposon. The Mu*dJ* transposon comprises a promoterless *lac* operon and a kanamycin resistance cassette. Once the *lac* operon is expressed, the *lacZ* gene encodes the enzyme $\beta$-galactosidase, which converts the colorless substrate o-nitrophenyl-$\beta$-D-galactopyranoside (ONPG) to a yellow product.

Main cultures were grown until $OD_{600}$ of 0.6-0.9 and the $OD_{600}$ was recorded. 20 µl of main culture ($V_{culture}$) was added to 80 µl permeabilisation solution (100 mM $Na_2HPO_4$, 20 mM KCl, 2 mM $MgSO_4$, 0.08 % CTAB, 0.04 % sodium deoxycholate, 5.4 µl/ml $\beta$-mercaptoethanol). The enzymatic reaction is then started by addition of 600 µl substrate solution (60 mM $Na_2HPO_4$, 40 mM $NaH_2PO_4$, 1 mg/ml ONPG, 2.7 µg/ml $\beta$-mercaptoethanol) and stopped after sufficient yellow color has developed with 700 µl 1 M sodium carbonate. Samples without color change were stopped after several hours of incubation. All samples were centrifuged for 10 min at maximal speed and the absorbance of the supernatant at 420 nm ($OD_{420}$) was measured. The activity of

the $\beta$-galactosidase in Miller Units was calculated using the following formula:

$$\text{Miller Units} = \frac{\text{OD}_{420} \text{ x } 1000}{\text{V}_{\text{culture}}[\text{ml}] \text{ x reaction time [min] x OD}_{420}}$$

### 7.4.2 Quantitative real-time PCR

Total bacterial RNA was isolated as described in Chapter 7.3.2 and used as template. Reverse transcription and quantitative real-time PCR (qRT-PCR) were performed using the SensiFAST™ SYBR® No-ROX One Step Kit (Bioline) in a Rotor-Gene Q lightcycler (QIAGEN). A standard reaction and cycling conditions are shown in Tab. 7.11 and 7.12, respectively. Primer efficiencies were determined from serial dilutions of *S.* Typhimurium genomic DNA. Relative changes in mRNA levels were analysed according to [Pfaffl, 2001] and normalised against the transcription levels of multiple reference genes (*gyrB*, *gmk*, and *rpoD*) according to the method described by [Vandesompele et al., 2002].

**Table 7.11: Standard qRT-PCR reaction.**

| Component | Volume (10 µl total) |
|---|---|
| 2x SensiFAST SYBR No-ROX One-Step Mix | 5 µl |
| 10 µM oligonucleotide each (see Tab. 7.3) | 0.4 µl |
| RiboSafe RNase inhibitor | 0.2 µl |
| Reverse transcriptase | 0.1 µl |
| RNase-free water | 1.9 µl |
| RNA template | 2 µl |

**Table 7.12: qRT-PCR cycling conditions.**

| Cycle* | Conditions |
|---|---|
| 1. Reverse transcription | 20 min, 45 °C |
| 2. Polymerase activation | 5 min, 95 °C |
| 3. Denaturing | 10 sec, 95 °C |
| 4. Annealing | 20 sec, 58 °C |
| 5. Extension | 10 sec, 72 °C |
| 6. Final extension | 10 min, 72 °C |
| 7. Melting profile analysis | 58 °C to 99 °C |

* Steps 3 to 5 were repeated for 34 cycles.

### 7.4.3 Measurement of fluorescence intensities

Fluorescence intensities were determined in black 96-well plates in a Varioskan Flash plate reader (Thermo Scientific). Gene expression was analysed by eGFP fused to the gene of interest. Samples were exposed to light with a wavelength of 488 nm and the emission at a wavelength of 509 nm was measured.

### 7.4.4 Transcriptome analysis

Total bacterial RNA was isolated from main cultures grown logarithmically by hot phenol extraction and subsequent DNase treatment (see Chapter 7.3.2). Sequencing and transcriptome analyses were performed at the in-house facility of the Helmholtz Centre for Infection Research (Department of Genome Analysis, GMAK). Briefly, RNA qualities were assessed using Agilent Technologies 2100 Bioanalyzer. Ribosomal RNA was depleted via Ribo-Zero rRNA Removal Kit (Epicenter) and sequencing was performed on HiSeq 2500 (Illumina) using TruSeq SBS Kit v3-HS (Illumina) for 50 cycles. Image analysis and base calling were accomplished using Illumina pipeline v1.8.
Bioinformatic interpretation of data was assessed by Abilash Chakravarthy Durairaj (IBIS, Helmholtz Centre for Infection Research). First, RNA reads were subjected to quality control using Trimmomatic and rRNA reads were removed using sortmeRNA. Remaining RNA reads were mapped against the *Salmonella* Typhimurium LT2 genome. DESeq2 was used to obtain the differential expression value and the corresponding adjusted p values for each gene.

## 7.5 Protein extraction and analysis

### 7.5.1 Analysis of protein levels

Protein concentrations were determined using the Quick Start$^{TM}$ Bradford Protein Assay (Bio-Rad) with the Bovine Serum Albumin Standard set (Bio-Rad). 5 µl of protein samples and the standard set were pipetted into a 96-well plate in duplicates and 250 µl 1x Dye Reagent was added. Samples were incubated for 5 min and measured at 595 nm in a Varioskan spectrophotometer (Thermo Scientific). Protein concentrations were calculated according to the BSA standard curve.

### 7.5.2 Protein secretion assay

For analysis of secreted proteins into the culture supernatant, main cultures were grown logarithmically and the culture supernatant was collected. Spi-1 effector protein secretion was induced by addition of 0.3 mM NaCl and analysed from overnight cultures. Secreted proteins were precipitated by addition of 10 % trichloroacetic acid (TCA) for 30 min and centrifuged at

4 °C for 30 min at maximum speed. The pellet was washed with 800 µl ice-cold acetone and dried. Samples were stored at -20 °C and separated on a SDS-gel as described in Chapter 7.5.3.

### 7.5.3 SDS polyacrylamide gel electrophoresis

Fractionation of proteins was performed under denaturised conditions according to their molecular weight via sodium dodecyl sulfate polyacrilamide gel electrophoresis (SDS-PAGE). Samples were resuspended in 2x SDS sample buffer (100 mM Tris-HCl pH 6.8, 4 % SDS, 20 % glycerol, 25 mM EDTA, 0.04 % bromophenol blue, 2 % $\beta$-mercaptoethanol) and incubated at 95 °C for 10 min. All samples were adjusted to equal amounts of OD-units. Protein fractionation was carried out using Bio-Rad SDS-PAGE systems (Mini-PROTEAN Tetra Cell) and 12 % SDS-gels as described in Tab. 7.13. Electrophoresis was performed at 200 V in 1x SDS running buffer (Rotiphorese, Roth). The Fisher BioReagents EZ-Run Pre-stained Rec Protein Ladder and Roti-Mark Standard (Roth) were used as protein standards.
SDS gels were stained with coomassie-blue R250 staining solution (0.1 % brilliant blue R250, 40 % ethanol, 10 % acetic acid) for 30 min and destained in coomassie-destaining solution (20 % ethanol, 5 % acetic acid).

**Table 7.13: Pipetting scheme for 12 % SDS gels.***

| Components | Resolving gel (12 %) | Stacking gel |
|---|---|---|
| 40 % acrylamide/bis | 6 ml | 1.25 ml |
| 0.5 M Tris pH 6.8 | - | 3.75 ml |
| 1.5 M Tris pH 8.8 | 5 ml | - |
| 10 % SDS | 200 µl | 100 µl |
| 10 % APS | 200 µl | 100 µl |
| TEMED | 15 µl | 10 µl |
| ddH2O | 8.6 ml | 4.3 ml |

* Composition for 4 SDS gels.

### 7.5.4 Western Blot analysis

For protein transfer on nitrocellulose membranes (Bio-Rad), the Bio-Rad wet-blotting tank system (Mini Trans-Blot® Cell) was used. Proteins were transferred for 1 h at 100 V in pre-cooled transfer buffer (25 mM Tris base, 192 mM glycine, 20 % methanol). The membrane was blocked for 1 h in 5 % skim milk powder in TBS (20 mM Tris-HCl pH 7.5, 150 mM NaCl) and the primary antibody was added for 1 h. After 3 washing steps with TBS, the secondary antibody was added for 30 min. Washing of the membrane was repeated. Protein bands were detected

using the Clarity™ Western ECL Blotting substrate (Bio-Rad) and a ChemiDoc™ XRS+ documentation system (Bio-Rad) with the Image Lab™ software (Bio-Rad).

### 7.5.5 Flagella immunostaining

For immunostaining of flagellar filaments, FliC locked strains (Δ*hin*-5717::FRT) were used according to the protocol of [Erhardt et al., 2011]. Logarithmically grown bacterial cells were fixed on poly-lysine coated coverslips by addition of 2 % formaldehyde and 0.2 % gluteraldehyde for 10 min. After washing with 1x PBS (115 mM NaCl, 16 mM $Na_2HPO_4$, 4 mM $KH_2PO_4$), immunostaining was performed. First, samples were blocked by addition of 10 % bovine serum albumin (BSA) for 10 min. The polyclonal α-FliC primary antibody was added and incubated overnight at 4 °C. The microscopy slides were washed with 1x PBS, blocked by 10 % BSA for 10 min, followed by addition of a secondary Alexa488-conjugated α-rabbit antibody (Invitrogen) for 30 min. Bacterial DNA was stained via Fluoreshield™ with DAPI (Sigma) and membranes were stained using 5 µg/ml FM 4-46 Dye (Invitrogen). Images were acquired by an inverted microscope (Axio Observer Z1, Zeiss) with an Axiocam HR CCD camera (Zeiss) and analysed using the ZEN 2012 software (Zeiss).

### 7.5.6 Electron microscopy

Electron microscopy was performed in-house at the Central Facility of Microscopy (Helmholtz Centre for Infection Research) by Prof. Dr. Manfred Rohde. For negative staining, thin carbon support films were prepared by sublimation of a carbon thread onto a freshly cleaved mica surface. Fixed bacteria (2 % gluteraldehyde) were adsorbed onto the carbon film and negatively stained with 0.5 % (w/v) aqueous uranyl acetate, pH 5.0, according to the method of [Valentine et al., 1968]. Images were acquired in a TEM 910 transmission electron microscope (Zeiss) at an acceleration voltage of 80 kV with a Slow-Scan CCD camera (ProScan) and ITEM software (Olympus Soft Imaging Solutions).
For scanning electron microscopy, samples were fixed with 2 % gluteraldehyde and dehydrated with a graded series of acetone. After critical point drying with $CO_2$ and sputter coating with gold-palladium, samples were monitored in a Zeiss Merlin at an acceleration voltage of 5 kV using the Everhart-Thornley SE-detector and the Inlens SE-detector in a 25:75 ratio.

### 7.5.7 Flagella purification and depolymerisation assay

Flagella purification was performed as described in [Erhardt et al., 2011] with minor changes. Briefly, 500 ml logarithmically grown cultures were pelleted and resuspended in ice-cold sucrose solution, pH 8 (0.5 M sucrose, 0.1 M Tris). 3 ml 10 mg/ml lysozyme and 3 ml 0.1 M EDTA were added drop-wise and samples were incubated for 30 min at 4 °C. Afterwards, 3 ml 10 % triton X-100 and 3 ml 0.1 M $MgSO_4$ were added, followed by overnight incubation at 4 °C. After lysis

occurred, 3 ml 0.1 M EDTA, pH 11, was added and samples were centrifuged at 17,000 xg and 4 °C for 20 min. The supernatant was adjusted to pH 11 with 5 M NaOH and centrifuged again. Flagella were collected by ultracentrifugation at 100,000 xg and 4 °C for 1 h in a Sorvall WX Ultra Series centrifuge with a surespin 630 rotor (Thermo Scientific), resuspended in pH 11 buffer (10 % sucrose, 0.1 M KCl, 0.1 % triton X-100) and centrifuged at 17,000 xg and 4 °C for 20 min. Finally, purified flagella were washed in TET buffer (10 mM Tris-HCl, 5 mM EDTA, pH 8, 0.1 % triton X-100), air dried and resuspended in 200 µl TE buffer (10 mM Tris-HCl, 5 mM EDTA, pH 8).
For analysis of filament stability, flagella were treated at various conditions (temperature, SDS addition, and pH) for 10 min. Samples were fractionated on NativePAGE™ 3-12 % Bis-Tris gels (Invitrogen) and proteins were stained using Coomassie as described in Chapter 7.5.3.

### 7.5.8 Adhesion to chitin beads

Magnetic chitin beads (NEB) were washed with 1x PBS before usage. Bacterial cultures that express mCherry constitutively from pFS48 were exponentially grown and incubated on chitin beads for 1 h at 37 °C. Non-adherent bacteria were washed with 1x PBS and fluorescence intensities were measured as described in Chapter 7.4.3 at an absorption/emission peak of 587 nm and 610 nm, respectively.

### 7.5.9 Adhesion to extracellular matrix proteins

For extracellular matrix (ECM) protein adhesion assays, a 96-well plate pre-coated with a variety of ECM proteins was used (EMD Millipore; Collagen I, II, IV, Fibronectin, Laminin, Tenascin, Vitronectin). Wells were rehydrated according to the user's manual and $5x10^7$ cells/ml were added. After incubation for 1 h at 37 °C, wells were washed extensively and 1 % Triton X-100 was added. Colony forming units (CFU)/ml were calculated after plating of serial dilutions and normalised to the inoculum and BSA control.

## 7.6 Analysis of bacterial motility

### 7.6.1 Swimming and swarming motility

Swimming and swarming motility were assessed on semi-solid agar plates containing 0.3 % and 0.5 % agar, respectively. Strains of interest were pre-incubated with appropriate additives. Swimming motility plates were inoculated with single colonies and incubated at 37 °C for 3-6 h. Swarming motility plates were inoculated with 5 µl of overnight cultures, dried and incubated at 37 °C for 7-9 h in a closed box with wet paper to ensure 100 % humidity. Diameters of swimming halos or swarming areas were measured using the ImageJ/Fiji software and normalised to the WT control.

### 7.6.2 Single-cell tracking

Tracking of single bacterial cells and analysis were performed by Erik Zschieschang (Department for Structural Infection Biology, Center for Structural Systems Biology). Briefly, single-cell tracking was observed in ibidi microscopy chambers at 20 °C using a Leica TCS SP8 microscope (20x objective) with 40 frames per second and a scanning speed of 12 kHz. Trajectories were detected using the plugin Spot Tracking [Chenouard et al., 2013].

## 7.7 Cell culture techniques

### 7.7.1 Cultivation of eukaryotic cell lines

Eukaryotic cells were cultivated in DMEM supplemented with 4.5 g/l D-glucose, L-glutamine, 110 mg/l sodium pyruvate, 10 % fetal calve serum (FCS) and 1 % non-essential amino acids (NEAA). To detach adherent cells, trypsin-EDTA (Sigma-Aldrich) was added for several minutes at 37 °C. J774 macrophage cells were scratched. All cell lines were stored in liquid nitrogen in cryo medium (70 % DMEM, 20 % FCS, 10 % DMSO) and tested for mycoplasma contamination using the mycoplasma test kit (AppliChem) at a regular basis.

### 7.7.2 Immunostaining of epithelial cell lines

MUC2 immunostaining was performed by Theresa Truschel (InSCREENeX GmbH). Cells were fixed with 4 % formaldehyde and permeabilised with 0.5 % Triton X-100. MUC2 was stained using primary $\alpha$-MUC2 antibody (1:100 in 3 % BSA/PBS, Thermo Fisher) and secondary Cy3-conjugated $\alpha$-rabbit antibody.

### 7.7.3 Isolation of bone marrow-derived macrophages

Bone marrow-derived macrophages were isolated from 6-week old mice freshly before every experiment. Isolation was executed by Achim Gronow (Junior Research Group Microbial Immune Regulation, Helmholtz Center for Infection Research). Cells were flushed out of isolated murine femurs, washed in 1x PBS supplemented with penicillin and streptomycin, and cultivated in DMEM with L-glutamine, 10 % FCS, 5 % horse serum and 20 % L929 SN.

### 7.7.4 Macrophage cell death

Macrophage cell death was monitored using murine bone marrow-derived macrophages as described in Chapter 7.7.3. The cells were seeded with an amount of $5x10^4$ cells onto black 96-well plates in medium supplemented with 12 µg/ml propidium iodide (PI). Infection with *Salmonella* strains was conducted at a MOI of 50 and centrifugation of the bacterial cells on the eukaryotic cell layer. PI fluorescence (Ex 535 nm/ Em 617 nm) was measured every 5 min in a

Varioskan Flash plate reader (Thermo Scientific). After 1 h, 500 µg/ml gentamycin was added and fluorescence was measured every 10 min for 5 additional hours.

### 7.7.5 Macrophage survival assay

The murine macrophage cell line J774 was used to analyse intracellular survival of bacteria. $5x10^5$ cells/ml were seeded and infected with *Salmonella* strains at a MOI of 10. After centrifugation of bacteria onto the cell surface, bacterial uptake was allowed for 30 min at 37 °C. To compare uptake and intracellular survival, 100 µg/ml gentamycin was added for 1 h and 21 h. Macrophages were lysed by addition of 1 % Triton X-100 and plated in serial dilutions to calculate the colony forming units (CFU)/ml. Values for 21 h post-infection were normalised to the uptake rate after 1 h.

### 7.7.6 Epithelial cell adhesion and invasion

For adhesion and invasion experiments, $2.5x10^5$ cells/ml were seeded and infected with *Salmonella* strains at a MOI of 10 for 1 h with or without centrifugation. Cell adhesion was analysed using strains lacking Spi-1 genes to prevent cell invasion. Non-adherent bacteria were washed with 1x PBS and eukaryotic cells were lysed for CFU assessment. Cell invasion was monitored by addition of 100 µg/ml gentamycin for 1 h at 37 °C to kill adhesive extracellular bacteria prior to cell lysis and CFU assessment. The CFU/ml were normalised to the control strain.

### 7.7.7 Near surface swimming

Swimming on the epithelial cell surface was performed as described in [Misselwitz et al., 2012] with *Salmonella* strains constitutively expressing mCherry from pFS48. $5x10^5$ MODE-K epithelial cells/ml were seeded in 8-well µ-slides (ibidi) and grown confluently. Cells were infected with *Salmonella* at a MOI of 10 and the epithelial cell surface was immediately recorded for 33 sec using an Axiovert 135TV microscope (3 frames/sec). Near surface swimming was divided into landing, near surface swimming, stop, and take off phases and quantified.

## 7.8 Mouse infection experiments

### 7.8.1 Survival assay

For mouse survival experiments, seven weeks old female C57BL/6 mice (Janvier) were pre-treated with 100 mg/ml streptomycin. Mice were infected orally with $10^5$ CFU. The bodyweights were recorded each day post-infection and mice were scored according to Tab. 7.14. Once a mouse lost more than 20 % of the starting bodyweight or the score was 1-2, mice were sacrificed.

**Table 7.14: Score table for characterisation of mice behaviour.**

| Score | Quality | Characteristics |
|---|---|---|
| 6 | Very active | Strong, curious, fast movements |
| 5 | Active | Curious, fast, short activity pauses |
| 4 | Limited active | Reacts to care, frequent activity pauses |
| 3 | Tranquil | No interest in surroundings, hardly activity, somnolent, less food consumption |
| 2 | Lethargic | No activity, persistence, no food consumption |
| 1 | Moribund | No activity, difficulty in breathing, death expected |

### 7.8.2 Competition assay

Streptomycin pre-treated female C57BL/6 mice (Janvier) were infected with $10^7$ CFU of each strain of interest. Mice, which were not pre-treated were infected with a dose of $10^8$ CFU of each strain. For competition experiments, each strain harboured a distinct antibiotic resistance cassette. 6 h, 24 h, and 48 h post-infection, the small intestine, ceacum, colon, and mesentheric lymph nodes (MLN) were isolated. Intestinal organs were washed and the luminal content was collected. All samples were homogenised and plated in serial dilutions on LB plates with appropriate antibiotics. CFU were counted and reported as CFU/g organ. Competitive indices (CI) were calculated by normalising the percentage of each strain within an organ to the inoculum and the challenge strain.

## References

Abby, S. S. and Rocha, E. P. C. (2012). The non-flagellar type III secretion system evolved from the bacterial flagellum and diversified into host-cell adapted systems. *PLoS genetics*, 8(9):e1002983.

Adams, P., Fowler, R., Kinsella, N., Howell, G., Farris, M., Coote, P., and O'Connor, C. D. (2001). Proteomic detection of PhoPQ- and acid-mediated repression of *Salmonella* motility. *Proteomics*, 1(4):597–607.

Akeda, Y. and Galán, J. E. (2005). Chaperone release and unfolding of substrates in type III secretion. *Nature*, 437(7060):911–915.

Akira, S., Uematsu, S., and Takeuchi, O. (2006). Pathogen recognition and innate immunity. *Cell*, 124(4):783–801.

Aldridge, C., Poonchareon, K., Saini, S., Ewen, T., Soloyva, A., Rao, C. V., Imada, K., Minamino, T., and Aldridge, P. D. (2010). The interaction dynamics of a negative feedback loop regulates flagellar number in *Salmonella enterica* serovar Typhimurium. *Molecular microbiology*, 78(6):1416–1430.

Aldridge, P. D., Wu, C., Gnerer, J., Karlinsey, J. E., Hughes, K. T., and Sachs, M. S. (2006). Regulatory protein that inhibits both synthesis and use of the target protein controls flagellar phase variation in *Salmonella enterica*. *Proceedings of the National Academy of Sciences of the United States of America*, 103(30):11340–11345.

Altier, C., Suyemoto, M., and Lawhon, S. D. (2000a). Regulation of *Salmonella enterica* serovar Typhimurium invasion genes by *csrA*. *Infection and immunity*, 68(12):6790–6797.

Altier, C., Suyemoto, M., Ruiz, A. I., Burnham, K. D., and Maurer, R. (2000b). Characterization of two novel regulatory genes affecting *Salmonella* invasion gene expression. *Molecular microbiology*, 35(3):635–646.

Ambler, R. P. and Rees, M. W. (1959). Epsilon-N-Methyl-lysine in bacterial flagellar protein. *Nature*, 184:56–57.

Anderson, J. K., Smith, T. G., and Hoover, T. R. (2010). Sense and sensibility: flagellum-mediated gene regulation. *Trends in microbiology*, 18(1):30–37.

Anwar, N., Rouf, S. F., Römling, U., and Rhen, M. (2014). Modulation of biofilm-formation in *Salmonella enterica* serovar Typhimurium by the periplasmic DsbA/DsbB oxidoreductase system requires the GGDEF-EAL domain protein STM3615. *PloS one*, 9(8):e106095.

Arora, S. K., Neely, A. N., Blair, B., Lory, S., and Ramphal, R. (2005). Role of motility and flagellin glycosylation in the pathogenesis of *Pseudomonas aeruginosa* burn wound infections. *Infection and immunity*, 73(7):4395–4398.

Arora, S. K., Ritchings, B. W., Almira, E. C., Lory, S., and Ramphal, R. (1998). The *Pseudomonas aeruginosa* flagellar cap protein, FliD, is responsible for mucin adhesion. *Infection and immunity*, 66(3):1000–1007.

Bajaj, V., Hwang, C., and Lee, C. A. (1995). HilA is a novel OmpR/ToxR family member that activates the expression of *Salmonella typhimurium* invasion genes. *Molecular microbiology*, 18(4):715–727.

Bajaj, V., Lucas, R. L., Hwang, C., and Lee, C. A. (1996). Co-ordinate regulation of *Salmonella typhimurium* invasion genes by environmental and regulatory factors is mediated by control of *hilA* expression. *Molecular microbiology*, 22(4):703–714.

Bakshi, C. S., Singh, V. P., Wood, M. W., Jones, P. W., Wallis, T. S., and Galyov, E. E. (2000). Identification of SopE2, a *Salmonella* secreted protein which is highly homologous to SopE and involved in bacterial invasion of epithelial cells. *Journal of bacteriology*, 182(8):2341–2344.

Barnhart, M. M. and Chapman, M. R. (2006). Curli biogenesis and function. *Annual review of microbiology*, 60(1):131–147.

Bäumler, A. J., Tsolis, R. M., and Heffron, F. (1996). The *lpf* fimbrial operon mediates adhesion of *Salmonella typhimurium* to murine Peyer's patches. *Proceedings of the National Academy of Sciences of the United States of America*, 93(1):279–283.

Bäumler, A. J., Tsolis, R. M., and Heffron, F. (1997). Fimbrial adhesins of *Salmonella typhimurium*. Role in bacterial interactions with epithelial cells. *Advances in experimental medicine and biology*, 412:149–158.

Baxter, M. A., Fahlen, T. F., Wilson, R. L., and Jones, B. D. (2003). HilE interacts with HilD and negatively regulates *hilA* transcription and expression of the *Salmonella enterica* serovar Typhimurium invasive phenotype. *Infection and immunity*, 71(3):1295–1305.

Bearson, S. M., Benjamin, W. H., Swords, W. E., and Foster, J. W. (1996). Acid shock induction of RpoS is mediated by the mouse virulence gene *mviA* of *Salmonella typhimurium*. *Journal of Bacteriology*.

Beatson, S. A., Minamino, T., and Pallen, M. J. (2006). Variation in bacterial flagellins: from sequence to structure. *Trends in microbiology*, 14(4):151–155.

Behlau, I. and Miller, S. I. (1993). A PhoP-repressed gene promotes *Salmonella typhimurium* invasion of epithelial cells. *Journal of bacteriology*, 175(14):4475–4484.

Belas, R. (1994). Expression of multiple flagellin-encoding genes of *Proteus mirabilis*. *Journal of bacteriology*, 176(23):7169–7181.

Belden, W. J. and Miller, S. I. (1994). Further characterization of the PhoP regulon: identification of new PhoP-activated virulence loci. *Infection and immunity*, 62(11):5095–5101.

Berke, A. P., Turner, L., Berg, H. C., and Lauga, E. (2008). Hydrodynamic attraction of swimming microorganisms by surfaces. *Physical review letters*, 101(3):038102.

Bertani, G. (2004). Lysogeny at mid-twentieth century: P1, P2, and other experimental systems. *Journal of bacteriology*, 186(3):595–600.

Bijlsma, J. J. E. and Groisman, E. A. (2005). The PhoP/PhoQ system controls the intramacrophage type three secretion system of *Salmonella enterica*. *Molecular microbiology*, 57(1):85–96.

Blocker, A., Komoriya, K., and Aizawa, S.-I. (2003). Type III secretion systems and bacterial flagella: insights into their function from structural similarities. *Proceedings of the National Academy of Sciences of the United States of America*, 100(6):3027–3030.

Boddicker, J. D., Knosp, B. M., and Jones, B. D. (2003). Transcription of the *Salmonella* invasion gene activator, *hilA*, requires HilD activation in the absence of negative regulators. *Journal of bacteriology*, 185(2):525–533.

Boehm, A., Kaiser, M., Li, H., Spangler, C., Kasper, C. A., Ackermann, M., Kaever, V., Sourjik, V., Roth, V., and Jenal, U. (2010). Second messenger-mediated adjustment of bacterial swimming velocity. *Cell*, 141(1):107–116.

Bogomolnaya, L. M., Aldrich, L., Ragoza, Y., Talamantes, M., Andrews, K. D., McClelland, M., and Andrews-Polymenis, H. L. (2014). Identification of novel factors involved in modulating motility of *Salmonella enterica* serotype Typhimurium. *PloS one*, 9(11):e111513.

Bonifield, H. R. and Hughes, K. T. (2003). Flagellar phase variation in *Salmonella enterica* is mediated by a posttranscriptional control mechanism. *Journal of bacteriology*, 185(12):3567–3574.

Boyd, A. and Simon, M. (1982). Bacterial chemotaxis. *Annual review of physiology*, 44(1):501–517.

Boyen, F., Haesebrouck, F., Vanparys, A., Volf, J., Mahu, M., Van Immerseel, F., Rychlik, I., Dewulf, J., Ducatelle, R., and Pasmans, F. (2008). Coated fatty acids alter virulence properties of *Salmonella* Typhimurium and decrease intestinal colonization of pigs. *Veterinary microbiology*, 132(3-4):319–327.

Briegel, A., Li, X., Bilwes, A. M., Hughes, K. T., Jensen, G. J., and Crane, B. R. (2012). Bacterial chemoreceptor arrays are hexagonally packed trimers of receptor dimers networked by rings of kinase and coupling proteins. *Proceedings of the National Academy of Sciences of the United States of America*, 109(10):3766–3771.

Brimer, C. D. and Montie, T. C. (1998). Cloning and comparison of *fliC* genes and identification of glycosylation in the flagellin of *Pseudomonas aeruginosa* a-type strains. *Journal of bacteriology*, 180(12):3209–3217.

Brosnahan, A. J. and Brown, D. R. (2012). Porcine IPEC-J2 intestinal epithelial cells in microbiological investigations. *Veterinary microbiology*, 156(3-4):229–237.

Bruno, J. C. and Freitag, N. E. (2010). Constitutive activation of PrfA tilts the balance of *Listeria monocytogenes* fitness towards life within the host versus environmental survival. *PLoS ONE*, 5(12):e15138.

Bustamante, V. H., Martínez, L. C., Santana, F. J., Knodler, L. A., Steele-Mortimer, O., and Puente, J. L. (2008). HilD-mediated transcriptional cross-talk between SPI-1 and SPI-2. *Proceedings of the National Academy of Sciences of the United States of America*, 105(38):14591–14596.

Cano, D. A., Domínguez-Bernal, G., Tierrez, A., Garcia-Del Portillo, F., and Casadesús, J. (2002). Regulation of capsule synthesis and cell motility in *Salmonella enterica* by the essential gene *igaA*. *Genetics*, 162(4):1513–1523.

Chaban, B., Hughes, H. V., and Beeby, M. (2015). The flagellum in bacterial pathogens: For motility and a whole lot more. *Seminars in cell & developmental biology*, 46:91–103.

Chadsey, M. S., Karlinsey, J. E., and Hughes, K. T. (1998). The flagellar anti-sigma factor FlgM actively dissociates *Salmonella typhimurium* sigma28 RNA polymerase holoenzyme. *Genes & development*, 12(19):3123–3136.

Chenouard, N., Bloch, I., and Olivo-Marin, J.-C. (2013). Multiple hypothesis tracking for cluttered biological image sequences. *IEEE transactions on pattern analysis and machine intelligence*, 35(11):2736–3750.

Cherepanov, P. P. and Wackernagel, W. (1995). Gene disruption in *Escherichia coli*: $Tc^R$ and $Km^R$ cassettes with the option of Flp-catalyzed excision of the antibiotic-resistance determinant. *Gene*, 158(1):9–14.

Chessa, D., Dorsey, C. W., Winter, M., and Bäumler, A. J. (2008a). Binding specificity of *Salmonella* plasmid-encoded fimbriae assessed by glycomics. *The Journal of biological chemistry*, 283(13):8118–8124.

Chessa, D., Winter, M. G., Jakomin, M., and Bäumler, A. J. (2009). *Salmonella enterica* serotype Typhimurium Std fimbriae bind terminal alpha(1,2)fucose residues in the cecal mucosa. *Molecular microbiology*, 71(4):864–875.

Chessa, D., Winter, M. G., Nuccio, S.-P., Tükel, C., and Bäumler, A. J. (2008b). RosE represses Std fimbrial expression in *Salmonella enterica* serotype Typhimurium. *Molecular microbiology*, 68(3):573–587.

Chevance, F. F. V. and Hughes, K. T. (2008). Coordinating assembly of a bacterial macromolecular machine. *Nature reviews. Microbiology*, 6(6):455–465.

Chilcott, G. S. and Hughes, K. T. (2000). Coupling of flagellar gene expression to flagellar assembly in *Salmonella enterica* serovar Typhimurium and *Escherichia coli*. *Microbiology and molecular biology reviews : MMBR*, 64(4):694–708.

Cirillo, D. M., Valdivia, R. H., Monack, D. M., and Falkow, S. (1998). Macrophage-dependent induction of the *Salmonella* pathogenicity island 2 type III secretion system and its role in intracellular survival. *Molecular microbiology*, 30(1):175–188.

Coburn, B., Grassl, G. A., and Finlay, B. B. (2007). *Salmonella*, the host and disease: a brief review. *Immunology and cell biology*, 85(2):112–118.

Colgan, A. M., Kröger, C., Diard, M., Hardt, W.-D., Puente, J. L., Sivasankaran, S. K., Hokamp, K., and Hinton, J. C. D. (2016). The impact of 18 ancestral and horizontally-acquired regulatory proteins upon the transcriptome and sRNA landscape of *Salmonella enterica* serovar Typhimurium. *PLoS genetics*, 12(8):e1006258.

Collinson, S. K., Doig, P. C., Doran, J. L., Clouthier, S., Trust, T. J., and Kay, W. W. (1993). Thin, aggregative fimbriae mediate binding of *Salmonella enteritidis* to fibronectin. *Journal of bacteriology*, 175(1):12–18.

Collinson, S. K., Emödy, L., Müller, K. H., Trust, T. J., and Kay, W. W. (1991). Purification and characterization of thin, aggregative fimbriae from *Salmonella enteritidis*. *Journal of bacteriology*, 173(15):4773–4781.

Crawford, R. W., Reeve, K. E., and Gunn, J. S. (2010). Flagellated but not hyperfimbriated *Salmonella enterica* serovar Typhimurium attaches to and forms biofilms on cholesterol-coated surfaces. *Journal of bacteriology*, 192(12):2981–2990.

Cummings, L. A., Barrett, S. L. R., Wilkerson, W. D., Fellnerova, I., and Cookson, B. T. (2005). FliC-specific $CD4^+$ T cell responses are restricted by bacterial regulation of antigen expression. *Journal of immunology (Baltimore, Md. : 1950)*, 174(12):7929–7938.

Cummings, L. A., Wilkerson, W. D., Bergsbaken, T., and Cookson, B. T. (2006). *In vivo*, *fliC* expression by *Salmonella enterica* serovar Typhimurium is heterogeneous, regulated by ClpX, and anatomically restricted. *Molecular microbiology*, 61(3):795–809.

Danese, P. N., Pratt, L. A., Dove, S. L., and Kolter, R. (2000a). The outer membrane protein, antigen 43, mediates cell-to-cell interactions within *Escherichia coli* biofilms. *Molecular microbiology*, 37(2):424–432.

Danese, P. N., Pratt, L. A., and Kolter, R. (2000b). Exopolysaccharide production is required for development of *Escherichia coli* K-12 biofilm architecture. *Journal of bacteriology*, 182(12):3593–3596.

Darwin, K. H. and Miller, V. L. (1999). InvF is required for expression of genes encoding proteins secreted by the SPI1 type III secretion apparatus in *Salmonella typhimurium*. *Journal of bacteriology*, 181(16):4949–4954.

Datsenko, K. A. and Wanner, B. L. (2000). One-step inactivation of chromosomal genes in *Escherichia coli* K-12 using PCR products. *Proceedings of the National Academy of Sciences of the United States of America*, 97(12):6640–6645.

de Jong, H. K., Parry, C. M., van der Poll, T., and Wiersinga, W. J. (2012). Host-pathogen interaction in invasive Salmonellosis. *PLoS pathogens*, 8(10):e1002933.

De Maayer, P. and Cowan, D. A. (2016). Flashy flagella: flagellin modification is relatively common and highly versatile among the *Enterobacteriaceae*. *BMC genomics*, 17(1):377.

Deditius, J. A. (2013). Effect of the *Salmonella* virulence master regulator HilD on flagellar gene expression and motility. Master's thesis.

Deditius, J. A., Felgner, S., Spöring, I., Kühne, C., Frahm, M., Rohde, M., Weiß, S., and Erhardt, M. (2015). Characterization of novel factors involved in swimming and swarming motility in *Salmonella enterica* serovar Typhimurium. *PloS one*, 10(8):e0135351.

Dibb-Fuller, M. P., Allen-Vercoe, E., Thorns, C. J., and Woodward, M. J. (1999). Fimbriae- and flagella-mediated association with and invasion of cultured epithelial cells by *Salmonella enteritidis*. *Microbiology (Reading, England)*, 145 ( Pt 5)(5):1023–1031.

Diepold, A. and Wagner, S. (2014). Assembly of the bacterial type III secretion machinery. *FEMS Microbiol. Rev.*, 38(4):802–822.

Ding, L., Wang, Y., Hu, Y., Atkinson, S., Williams, P., and Chen, S. (2009). Functional characterization of FlgM in the regulation of flagellar synthesis and motility in *Yersinia pseudotuberculosis*. *Microbiology (Reading, England)*, 155(Pt 6):1890–1900.

Dons, L., Eriksson, E., Jin, Y., Rottenberg, M. E., Kristensson, K., Larsen, C. N., Bresciani, J., and Olsen, J. E. (2004). Role of flagellin and the two-component CheA/CheY system of *Listeria monocytogenes* in host cell invasion and virulence. *Infection and Immunity*, 72(6):3237–3244.

Eisenbach, M. and Caplan, S. R. (1998). Bacterial chemotaxis: unsolved mystery of the flagellar switch. *Current biology : CB*, 8(13):R444–6.

Elhadad, D., Desai, P., Rahav, G., McClelland, M., and Gal-Mor, O. (2015). Flagellin is required for host cell invasion and normal SPI-1 expression by *Salmonella* Paratyphi A. *Infection and immunity*, pages IAI.00468–15.

Ellermeier, C. D., Ellermeier, J. R., and Slauch, J. M. (2005). HilD, HilC and RtsA constitute a feed forward loop that controls expression of the SPI1 type three secretion system regulator *hilA* in *Salmonella enterica* serovar Typhimurium. *Molecular microbiology*, 57(3):691–705.

Ellermeier, C. D. and Slauch, J. M. (2003). RtsA and RtsB coordinately regulate expression of the invasion and flagellar genes in *Salmonella enterica* serovar Typhimurium. *Journal of bacteriology*, 185(17):5096–5108.

Ellermeier, J. R. and Slauch, J. M. (2007). Adaptation to the host environment: regulation of the SPI1 type III secretion system in *Salmonella enterica* serovar Typhimurium. *Current opinion in microbiology*, 10(1):24–29.

Erdem, A. L., Avelino, F., Xicohtencatl-Cortes, J., and Girón, J. A. (2007). Host protein binding and adhesive properties of H6 and H7 flagella of attaching and effacing *Escherichia coli*. *Journal of bacteriology*, 189(20):7426–7435.

Erhardt, M. and Dersch, P. (2015). Regulatory principles governing *Salmonella* and *Yersinia* virulence. *Frontiers in Microbiology*, 6:949.

Erhardt, M., Hirano, T., Su, Y., Paul, K., Wee, D. H., Mizuno, S., Aizawa, S.-I., and Hughes, K. T. (2010). The role of the FliK molecular ruler in hook-length control in *Salmonella enterica*. *Molecular microbiology*, 75(5):1272–1284.

Erhardt, M., Singer, H. M., Wee, D. H., Keener, J. P., and Hughes, K. T. (2011). An infrequent molecular ruler controls flagellar hook length in *Salmonella enterica*. *The EMBO journal*, 30(14):2948–2961.

Eriksson, S., Lucchini, S., Thompson, A., Rhen, M., and Hinton, J. C. D. (2003). Unravelling the biology of macrophage infection by gene expression profiling of intracellular *Salmonella enterica*. *Molecular microbiology*, 47(1):103–118.

Ewing, C. P., Andreishcheva, E., and Guerry, P. (2009). Functional characterization of flagellin glycosylation in *Campylobacter jejuni* 81-176. *Journal of bacteriology*, 191(22):7086–7093.

Fang, X. and Gomelsky, M. (2010). A post-translational, c-di-GMP-dependent mechanism regulating flagellar motility. *Molecular microbiology*, 76(5):1295–1305.

Feng, X., Oropeza, R., and Kenney, L. J. (2003). Dual regulation by phospho-OmpR of *ssrA/B* gene expression in *Salmonella* pathogenicity island 2. *Molecular microbiology*, 48(4):1131–1143.

Feng, X., Walthers, D., Oropeza, R., and Kenney, L. J. (2004). The response regulator SsrB activates transcription and binds to a region overlapping OmpR binding sites at *Salmonella* pathogenicity island 2. *Molecular microbiology*, 54(3):823–835.

Fierer, J. and Guiney, D. G. (2001). Diverse virulence traits underlying different clinical outcomes of *Salmonella* infection. *The Journal of clinical investigation*, 107(7):775–780.

Finlay, B. B. (1994). Molecular and cellular mechanisms of *Salmonella* pathogenesis. *Current topics in microbiology and immunology*, 192:163–185.

Finlay, B. B. and Falkow, S. (1988). Comparison of the invasion strategies used by *Salmonella choleraesuis*, *Shigella flexneri* and *Yersinia enterocolitica* to enter cultured animal cells: endosome acidification is not required for bacterial invasion or intracellular replication. *Biochimie*, 70(8):1089–1099.

Finlay, B. B. and McFadden, G. (2006). Anti-immunology: evasion of the host immune system by bacterial and viral pathogens. *Cell*, 124(4):767–782.

Finlay, B. B., Ruschkowski, S., and Dedhar, S. (1991). Cytoskeletal rearrangements accompanying *Salmonella* entry into epithelial cells. *Journal of cell science*, 99 ( Pt 2):283–296.

Fortune, D. R., Suyemoto, M., and Altier, C. (2006). Identification of CsrC and characterization of its role in epithelial cell invasion in *Salmonella enterica* serovar Typhimurium. *Infection and immunity*, 74(1):331–339.

Foster, J. W. and Hall, H. K. (1990). Adaptive acidification tolerance response of *Salmonella typhimurium*. *Journal of bacteriology*, 172(2):771–778.

Foster, J. W. and Hall, H. K. (1991). Inducible pH homeostasis and the acid tolerance response of *Salmonella typhimurium*. *Journal of bacteriology*, 173(16):5129–5135.

Francis, C. L., Ryan, T. A., Jones, B. D., Smith, S. J., and Falkow, S. (1993). Ruffles induced by *Salmonella* and other stimuli direct macropinocytosis of bacteria. *Nature*, 364(6438):639–642.

Francis, C. L., Starnbach, M. N., and Falkow, S. (1992). Morphological and cytoskeletal changes in epithelial cells occur immediately upon interaction with *Salmonella typhimurium* grown under low-oxygen conditions. *Molecular microbiology*, 6(21):3077–3087.

Friedrich, M. J., Kinsey, N. E., Vila, J., and Kadner, R. J. (1993). Nucleotide sequence of a 13.9 kb segment of the 90 kb virulence plasmid of *Salmonella typhimurium*: the presence of fimbrial biosynthetic genes. *Molecular microbiology*, 8(3):543–558.

Frye, J., Karlinsey, J. E., Felise, H. R., Marzolf, B., Dowidar, N., McClelland, M., and Hughes, K. T. (2006). Identification of new flagellar genes of *Salmonella enterica* serovar Typhimurium. *Journal of bacteriology*, 188(6):2233–2243.

Frymier, P. D., Ford, R. M., Berg, H. C., and Cummings, P. T. (1995). Three-dimensional tracking of motile bacteria near a solid planar surface. *Proceedings of the National Academy of Sciences of the United States of America*, 92(13):6195–6199.

Gal-Mor, O., Gibson, D. L., Baluta, D., Vallance, B. A., and Finlay, B. B. (2008). A novel secretion pathway of *Salmonella enterica* acts as an antivirulence modulator during salmonellosis. *PLoS pathogens*, 4(4):e1000036.

García-Calderón, C. B., Casadesús, J., and Ramos-Morales, F. (2007). Rcs and PhoPQ regulatory overlap in the control of *Salmonella enterica* virulence. *Journal of bacteriology*, 189(18):6635–6644.

García-Calderón, C. B., García-Quintanilla, M., Casadesús, J., and Ramos-Morales, F. (2005). Virulence attenuation in *Salmonella enterica rcsC* mutants with constitutive activation of the Rcs system. *Microbiology (Reading, England)*, 151(Pt 2):579–588.

Garcia-del Portillo, F. and Finlay, B. B. (1994). *Salmonella* invasion of nonphagocytic cells induces formation of macropinosomes in the host cell. *Infection and immunity*, 62(10):4641–4645.

García Véscovi, E., Soncini, F. C., and Groisman, E. A. (1996). $Mg^{2+}$ as an extracellular signal: environmental regulation of *Salmonella* virulence. *Cell*, 84(1):165–174.

Garmendia, J., Beuzón, C. R., Ruiz-Albert, J., and Holden, D. W. (2003). The roles of SsrA-SsrB and OmpR-EnvZ in the regulation of genes encoding the *Salmonella typhimurium* SPI-2 type III secretion system. *Microbiology (Reading, England)*, 149(Pt 9):2385–2396.

Gerlach, R. G., Jäckel, D., Geymeier, N., and Hensel, M. (2007a). *Salmonella* pathogenicity island 4-mediated adhesion is coregulated with invasion genes in *Salmonella enterica*. *Infection and immunity*, 75(10):4697–4709.

Gerlach, R. G., Jäckel, D., Stecher, B., Wagner, C., Lupas, A., Hardt, W.-D., and Hensel, M. (2007b). *Salmonella* Pathogenicity Island 4 encodes a giant non-fimbrial adhesin and the cognate type 1 secretion system. *Cellular microbiology*, 9(7):1834–1850.

Gillen, K. L. and Hughes, K. T. (1991). Negative regulatory loci coupling flagellin synthesis to flagellar assembly in *Salmonella typhimurium*. *Journal of bacteriology*, 173(7):2301–2310.

Girón, J. A., Torres, A. G., Freer, E., and Kaper, J. B. (2002). The flagella of enteropathogenic *Escherichia coli* mediate adherence to epithelial cells. *Molecular microbiology*, 44(2):361–379.

Goodier, R. I. and Ahmer, B. M. (2001). SirA orthologs affect both motility and virulence. *Journal of bacteriology*, 183(7):2249–2258.

Grimont, P. and Weill, F. X. (2007). Antigenic formulae of the *Salmonella* serovars. *World Health Organization Collaborating Center for Reference and Research on* Salmonella*, Pasteur Institute, Paris, France*, 9th revision.

Guerry, P., Alm, R. A., Power, M. E., Logan, S. M., and Trust, T. J. (1991). Role of two flagellin genes in *Campylobacter* motility. *Journal of bacteriology*, 173(15):4757–4764.

Gygi, D., Rahman, M. M., Lai, H. C., Carlson, R., Guard-Petter, J., and Hughes, C. (1995). A cell-surface polysaccharide that facilitates rapid population migration by differentiated swarm cells of *Proteus mirabilis*. *Molecular microbiology*, 17(6):1167–1175.

Haiko, J. and Westerlund-Wikström, B. (2013). The role of the bacterial flagellum in adhesion and virulence. *Biology*, 2(4):1242–1267.

Hänisch, J., Ehinger, J., Ladwein, M., Rohde, M., Derivery, E., Bosse, T., Steffen, A., Bumann, D., Misselwitz, B., Hardt, W.-D., Gautreau, A., Stradal, T. E. B., and Rottner, K. (2010). Molecular dissection of *Salmonella*-induced membrane ruffling versus invasion. *Cellular microbiology*, 12(1):84–98.

Hardt, W. D., Chen, L. M., Schuebel, K. E., Bustelo, X. R., and Galán, J. E. (1998). *S. typhimurium* encodes an activator of Rho GTPases that induces membrane ruffling and nuclear responses in host cells. *Cell*, 93(5):815–826.

Harshey, R. M. (2003). Bacterial motility on a surface: many ways to a common goal. *Annual review of microbiology*, 57(1):249–273.

Hartley, R. W. and Smeaton, J. R. (1973). On the reaction between the extracellular ribonuclease of *Bacillus amyloliquefaciens* (barnase) and its intracellular inhibitor (barstar). *The Journal of biological chemistry*, 248(16):5624–5626.

Hautefort, I., Thompson, A., Eriksson-Ygberg, S., Parker, M. L., Lucchini, S., Danino, V., Bongaerts, R. J. M., Ahmad, N., Rhen, M., and Hinton, J. C. D. (2008). During infection of epithelial cells *Salmonella enterica* serovar Typhimurium undergoes a time-dependent transcriptional adaptation that results in simultaneous expression of three type 3 secretion systems. *Cellular microbiology*, 10(4):958–984.

Hayashi, F., Smith, K. D., Ozinsky, A., Hawn, T. R., Yi, E. C., Goodlett, D. R., Eng, J. K., Akira, S., Underhill, D. M., and Aderem, A. (2001). The innate immune response to bacterial flagellin is mediated by Toll-like receptor 5. *Nature*, 410(6832):1099–1103.

Hensel, M., Shea, J. E., Gleeson, C., Jones, M. D., Dalton, E., and Holden, D. W. (1995). Simultaneous identification of bacterial virulence genes by negative selection. *Science (New York, N.Y.)*, 269(5222):400–403.

Herikstad, H., Motarjemi, Y., and Tauxe, R. V. (2002). *Salmonella* surveillance: a global survey of public health serotyping. *Epidemiology and infection*, 129(1):1–8.

Hirai, H., Takai, R., Iwano, M., Nakai, M., Kondo, M., Takayama, S., Isogai, A., and Che, F.-S. (2011). Glycosylation regulates specific induction of rice immune responses by *Acidovorax avenae* flagellin. *The Journal of biological chemistry*, 286(29):25519–25530.

Hirano, T., Yamaguchi, S., Oosawa, K., and Aizawa, S. (1994). Roles of FliK and FlhB in determination of flagellar hook length in *Salmonella typhimurium*. *Journal of bacteriology*, 176(17):5439–5449.

Hobbie, S., Chen, L. M., Davis, R. J., and Galán, J. E. (1997). Involvement of mitogen-activated protein kinase pathways in the nuclear responses and cytokine production induced by *Salmonella typhimurium* in cultured intestinal epithelial cells. *Journal of immunology (Baltimore, Md. : 1950)*, 159(11):5550–5559.

Horstmann, J. A., Zschieschang, E., Truschel, T., de Diego, J., Lunelli, M., Rohde, M., May, T., Strowig, T., Stradal, T., Kolbe, M., and Erhardt, M. (2017). Flagellin phase-dependent swimming on epithelial cell surfaces contributes to productive *Salmonella* gut colonization. *Cellular microbiology*.

Hughes, K. T., Gillen, K. L., Semon, M. J., and Karlinsey, J. E. (1993). Sensing structural intermediates in bacterial flagellar assembly by export of a negative regulator. *Science (New York, N.Y.)*, 262(5137):1277–1280.

Humphries, A., Deridder, S., and Bäumler, A. J. (2005). *Salmonella enterica* serotype Typhimurium fimbrial proteins serve as antigens during infection of mice. *Infection and immunity*, 73(9):5329–5338.

Humphries, A. D., Raffatellu, M., Winter, S., Weening, E. H., Kingsley, R. A., Droleskey, R., Zhang, S., Figueiredo, J., Khare, S., Nunes, J., Adams, L. G., Tsolis, R. M., and Bäumler, A. J. (2003). The use of flow cytometry to detect expression of subunits encoded by 11 *Salmonella enterica* serotype Typhimurium fimbrial operons. *Molecular microbiology*, 48(5):1357–1376.

Ichinose, Y., Taguchi, F., Yamamoto, M., Ohnishi-Kameyama, M., Atsumi, T., Iwaki, M., Manabe, H., Kumagai, M., Nguyen, Q. T., Nguyen, C. L., Inagaki, Y., Ono, H., Chiku, K., Ishii, T., and Yoshida, M. (2013). Flagellin glycosylation is ubiquitous in a broad range of phytopathogenic bacteria. *Journal of General Plant Pathology*, 79(5):359–365.

Ikeda, J. S., Schmitt, C. K., Darnell, S. C., Watson, P. R., Bispham, J., Wallis, T. S., Weinstein, D. L., Metcalf, E. S., Adams, P., O'Connor, C. D., and O'Brien, A. D. (2001). Flagellar phase variation of *Salmonella enterica* serovar Typhimurium contributes to virulence in the murine typhoid infection model but does not influence *Salmonella*-induced enteropathogenesis. *Infection and immunity*, 69(5):3021–3030.

Inoue, T., Shingaki, R., Hirose, S., Waki, K., Mori, H., and Fukui, K. (2007). Genome-wide screening of genes required for swarming motility in *Escherichia coli* K-12. *Journal of bacteriology*, 189(3):950–957.

Iriarte, M., Stainier, I., Mikulskis, A. V., and Cornelis, G. R. (1995). The *fliA* gene encoding sigma 28 in *Yersinia enterocolitica*. *Journal of bacteriology*, 177(9):2299–2304.

Johnson, R. C. and Simon, M. I. (1985). Hin-mediated site-specific recombination requires two 26 bp recombination sites and a 60 bp recombinational enhancer. *Cell*, 41(3):781–791.

Johnston, C., Pegues, D. A., Hueck, C. J., Lee, A., and Miller, S. I. (1996). Transcriptional activation of *Salmonella typhimurium* invasion genes by a member of the phosphorylated response-regulator superfamily. *Molecular microbiology*, 22(4):715–727.

Jones, B. D., Ghori, N., and Falkow, S. (1994). *Salmonella typhimurium* initiates murine infection by penetrating and destroying the specialized epithelial M cells of the Peyer's patches. *The Journal of experimental medicine*, 180(1):15–23.

Jones, G. W., Richardson, L. A., and Uhlman, D. (1981). The invasion of HeLa cells by *Salmonella typhimurium*: reversible and irreversible bacterial attachment and the role of bacterial motility. *Journal of general microbiology*, 127(2):351–360.

Josenhans, C. and Suerbaum, S. (2002). The role of motility as a virulence factor in bacteria. *International journal of medical microbiology : IJMM*, 291(8):605–614.

Kadner, R. J. (2005). Regulation by iron: RNA rules the rust. *Journal of bacteriology*, 187(20):6870–6873.

Kaniga, K., Bossio, J. C., and Galán, J. E. (1994). The *Salmonella typhimurium* invasion genes *invF* and *invG* encode homologues of the AraC and PulD family of proteins. *Molecular microbiology*, 13(4):555–568.

Kaniga, K., Trollinger, D., and Galán, J. E. (1995). Identification of two targets of the type III protein secretion system encoded by the *inv* and *spa* loci of *Salmonella typhimurium* that have homology to the *Shigella* IpaD and IpaA proteins. *Journal of bacteriology*, 177(24):7078–7085.

Karlinsey, J. E. (2007). $\lambda$-Red genetic engineering in *Salmonella enterica* serovar Typhimurium. *Methods in enzymology*, 421:199–209.

Karlinsey, J. E., Tanaka, S., Bettenworth, V., Yamaguchi, S., Boos, W., Aizawa, S. I., and Hughes, K. T. (2000). Completion of the hook-basal body complex of the *Salmonella typhimurium* flagellum is coupled to FlgM secretion and *fliC* transcription. *Molecular microbiology*, 37(5):1220–1231.

Kerridge, D. (1966). Flagellar synthesis in *Salmonella typhimurium*: factors affecting the formation of the flagellar epsilon-N-methyl-lysine. *Journal of general microbiology*, 42(1):71–82.

Kisiela, D. I., Kramer, J. J., Tchesnokova, V., Aprikian, P., Yarov-Yarovoy, V., Clegg, S., and Sokurenko, E. V. (2011). Allosteric catch bond properties of the FimH adhesin from *Salmonella enterica* serovar Typhimurium. *The Journal of biological chemistry*, 286(44):38136–38147.

Knodler, L. A., Celli, J., Hardt, W.-D., Vallance, B. A., Yip, C., and Finlay, B. B. (2002). *Salmonella* effectors within a single pathogenicity island are differentially expressed and translocated by separate type III secretion systems. *Molecular microbiology*, 43(5):1089–1103.

Ko, M. and Park, C. (2000). H-NS-Dependent regulation of flagellar synthesis is mediated by a LysR family protein. *Journal of bacteriology*, 182(16):4670–4672.

Koskiniemi, S., Gibbons, H. S., Sandegren, L., Anwar, N., Ouellette, G., Broomall, S., Karavis, M., McGregor, P., Liem, A., Fochler, E., McNew, L., Rosenzweig, C. N., Rhen, M., Skowronski, E. W., and Andersson, D. I. (2013). Pathoadaptive mutations in *Salmonella enterica* isolated after serial passage in mice. *PloS one*, 8(7):e70147.

Kröger, C., Colgan, A., Srikumar, S., Händler, K., Sivasankaran, S. K., Hammarlöf, D. L., Canals, R., Grissom, J. E., Conway, T., Hokamp, K., and Hinton, J. C. D. (2013). An infection-relevant transcriptomic compendium for *Salmonella enterica* Serovar Typhimurium. *Cell host & microbe*, 14(6):683–695.

Kröger, C., Dillon, S. C., Cameron, A. D. S., Papenfort, K., Sivasankaran, S. K., Hokamp, K., Chao, Y., Sittka, A., Hébrard, M., Händler, K., Colgan, A., Leekitcharoenphon, P., Langridge, G. C., Lohan, A. J., Loftus, B., Lucchini, S., Ussery, D. W., Dorman, C. J., Thomson, N. R., Vogel, J., and Hinton, J. C. D. (2012). The transcriptional landscape and small RNAs of *Salmonella enterica* serovar Typhimurium. *Proceedings of the National Academy of Sciences of the United States of America*, 109(20):E1277–86.

Kuhle, V. and Hensel, M. (2004). Cellular microbiology of intracellular *Salmonella enterica*: functions of the type III secretion system encoded by *Salmonella* pathogenicity island 2. *Cellular and molecular life sciences : CMLS*, 61(22):2812–2826.

Kühne, C., Singer, H. M., Grabisch, E., Codutti, L., Carlomagno, T., Scrima, A., and Erhardt, M. (2016). RflM mediates target specificity of the RcsCDB phosphorelay system for transcriptional repression of flagellar synthesis in *Salmonella enterica*. *Molecular microbiology*, 101(5):841–855.

Kukkonen, M., Raunio, T., Virkola, R., Lähteenmäki, K., Mäkelä, P. H., Klemm, P., Clegg, S., and Korhonen, T. K. (1993). Basement membrane carbohydrate as a target for bacterial adhesion: binding of type I fimbriae of *Salmonella enterica* and *Escherichia coli* to laminin. *Molecular microbiology*, 7(2):229–237.

Kutsukake, K. (1994). Excretion of the anti-sigma factor through a flagellar substructure couples flagellar gene expression with flagellar assembly in *Salmonella typhimurium*. *Molecular & general genetics : MGG*, 243(6):605–612.

Kutsukake, K. and Iino, T. (1980). A trans-acting factor mediates inversion of a specific DNA segment in flagellar phase variation of *Salmonella*. *Nature*, 284(5755):479–481.

Kutsukake, K., Ikebe, T., and Yamamoto, S. (1999). Two novel regulatory genes, *fliT* and *fliZ*, in the flagellar regulon of *Salmonella*. *Genes & genetic systems*, 74(6):287–292.

Lai, M. A., Quarles, E. K., López-Yglesias, A. H., Zhao, X., Hajjar, A. M., and Smith, K. D. (2013). Innate immune detection of flagellin positively and negatively regulates *Salmonella* infection. *PLoS ONE*, 8(8):e72047.

Lamprokostopoulou, A., Monteiro, C., Rhen, M., and Römling, U. (2010). Cyclic di-GMP signalling controls virulence properties of *Salmonella enterica* serovar Typhimurium at the mucosal lining. *Environmental microbiology*, 12(1):40–53.

Lan, R., Reeves, P. R., and Octavia, S. (2009). Population structure, origins and evolution of major *Salmonella enterica* clones. *Infection, genetics and evolution : journal of molecular epidemiology and evolutionary genetics in infectious diseases*, 9(5):996–1005.

Lauga, E., DiLuzio, W. R., Whitesides, G. M., and Stone, H. A. (2006). Swimming in circles: motion of bacteria near solid boundaries. *Biophysical journal*, 90(2):400–412.

Ledeboer, N. A., Frye, J. G., McClelland, M., and Jones, B. D. (2006). *Salmonella enterica* serovar Typhimurium requires the Lpf, Pef, and Tafi fimbriae for biofilm formation on HEp-2 tissue culture cells and chicken intestinal epithelium. *Infection and immunity*, 74(6):3156–3169.

Lee, C. A., Jones, B. D., and Falkow, S. (1992). Identification of a *Salmonella typhimurium* invasion locus by selection for hyperinvasive mutants. *Proceedings of the National Academy of Sciences of the United States of America*, 89(5):1847–1851.

Lee, J., Page, R., García-Contreras, R., Palermino, J.-M., Zhang, X.-S., Doshi, O., Wood, T. K., and Peti, W. (2007). Structure and function of the *Escherichia coli* protein YmgB: a protein critical for biofilm formation and acid-resistance. 373(1):11–26.

Lertsethtakarn, P., Ottemann, K. M., and Hendrixson, D. R. (2011). Motility and chemotaxis in *Campylobacter* and *Helicobacter*. *Annual review of microbiology*, 65(1):389–410.

Li, G., Bensson, J., Nisimova, L., Munger, D., Mahautmr, P., Tang, J. X., Maxey, M. R., and Brun, Y. V. (2011). Accumulation of swimming bacteria near a solid surface. *Physical review. E, Statistical, nonlinear, and soft matter physics*, 84(4 Pt 1):041932.

Lillehoj, E. P., Kim, B. T., and Kim, K. C. (2002). Identification of *Pseudomonas aeruginosa* flagellin as an adhesin for Muc1 mucin. *American journal of physiology. Lung cellular and molecular physiology*, 282(4):L751–6.

Liu, X. and Matsumura, P. (1994). The FlhD/FlhC complex, a transcriptional activator of the *Escherichia coli* flagellar class II operons. *Journal of bacteriology*, 176(23):7345–7351.

Liu, X. and Matsumura, P. (1995). An alternative sigma factor controls transcription of flagellar class-III operons in *Escherichia coli*: gene sequence, overproduction, purification and characterization. *Gene*, 164(1):81–84.

Lockman, H. A. and Curtiss, R. (1990). *Salmonella typhimurium* mutants lacking flagella or motility remain virulent in BALB/c mice. *Infection and Immunity*, 58(1):137–143.

Logan, S. M. (2006). Flagellar glycosylation - a new component of the motility repertoire? *Microbiology (Reading, England)*, 152(Pt 5):1249–1262.

Logan, S. M., Trust, T. J., and Guerry, P. (1989). Evidence for posttranslational modification and gene duplication of *Campylobacter* flagellin. *Journal of bacteriology*, 171(6):3031–3038.

Lucas, R. L., Lostroh, C. P., DiRusso, C. C., Spector, M. P., Wanner, B. L., and Lee, C. A. (2000). Multiple factors independently regulate *hilA* and invasion gene expression in *Salmonella enterica* serovar Typhimurium. *Journal of bacteriology*, 182(7):1872–1882.

Macnab, R. M. (1992). Genetics and biogenesis of bacterial flagella. *Annual review of genetics*, 26(1):131–158.

Mahajan, A., Currie, C. G., Mackie, S., Tree, J., McAteer, S., McKendrick, I., McNeilly, T. N., Roe, A., La Ragione, R. M., Woodward, M. J., Gally, D. L., and Smith, D. G. E. (2009). An investigation of the expression and adhesin function of H7 flagella in the interaction of *Escherichia coli* O157 : H7 with bovine intestinal epithelium. *Cellular microbiology*, 11(1):121–137.

Main-Hester, K. L., Colpitts, K. M., Thomas, G. A., Fang, F. C., and Libby, S. J. (2008). Coordinate regulation of *Salmonella* pathogenicity island 1 (SPI1) and SPI4 in *Salmonella enterica* serovar Typhimurium. *Infection and immunity*, 76(3):1024–1035.

Martínez, L. C., Banda, M. M., Fernández-Mora, M., Santana, F. J., and Bustamante, V. H. (2014). HilD induces expression of *Salmonella* pathogenicity island 2 genes by displacing the global negative regulator H-NS from *ssrAB*. *Journal of bacteriology*, 196(21):3746–3755.

McClelland, M., Sanderson, K. E., Spieth, J., Clifton, S. W., Latreille, P., Courtney, L., Porwollik, S., Ali, J., Dante, M., Du, F., Hou, S., Layman, D., Leonard, S., Nguyen, C., Scott, K., Holmes, A., Grewal, N., Mulvaney, E., Ryan, E., Sun, H., Florea, L., Miller, W., Stoneking, T., Nhan, M., Waterston, R., and Wilson, R. K. (2001). Complete genome sequence of *Salmonella enterica* serovar Typhimurium LT2. *Nature*, 413(6858):852–856.

McQuiston, J. R., Fields, P. I., Tauxe, R. V., and Logsdon, J. M. (2008). Do *Salmonella* carry spare tyres? *Trends in microbiology*, 16(4):142–148.

Méresse, S., Unsworth, K. E., Habermann, A., Griffiths, G., Fang, F., Martínez-Lorenzo, M. J., Waterman, S. R., Gorvel, J. P., and Holden, D. W. (2001). Remodelling of the actin cytoskeleton is essential for replication of intravacuolar *Salmonella*. *Cellular microbiology*, 3(8):567–577.

Merino, S. and Tomás, J. M. (2014). Gram-negative flagella glycosylation. *International journal of molecular sciences*, 15(2):2840–2857.

Miao, E. A., Alpuche-Aranda, C. M., Dors, M., Clark, A. E., Bader, M. W., Miller, S. I., and Aderem, A. (2006). Cytoplasmic flagellin activates caspase-1 and secretion of interleukin 1beta via Ipaf. *Nature immunology*, 7(6):569–575.

Miao, E. A., Andersen-Nissen, E., Warren, S. E., and Aderem, A. (2007). TLR5 and Ipaf: dual sensors of bacterial flagellin in the innate immune system. *Seminars in immunopathology*, 29(3):275–288.

Miao, E. A., Leaf, I. A., Treuting, P. M., Mao, D. P., Dors, M., Sarkar, A., Warren, S. E., Wewers, M. D., and Aderem, A. (2010). Caspase-1-induced pyroptosis is an innate immune effector mechanism against intracellular bacteria. *Nature immunology*, 11(12):1136–1142.

Miller, S. I., Kukral, A. M., and Mekalanos, J. J. (1989). A two-component regulatory system (*phoP phoQ*) controls *Salmonella typhimurium* virulence. *Proceedings of the National Academy of Sciences of the United States of America*, 86(13):5054–5058.

Miller, W. L., Matewish, M. J., McNally, D. J., Ishiyama, N., Anderson, E. M., Brewer, D., Brisson, J.-R., Berghuis, A. M., and Lam, J. S. (2008). Flagellin glycosylation in *Pseudomonas aeruginosa* PAK requires the O-antigen biosynthesis enzyme WbpO. *The Journal of biological chemistry*, 283(6):3507–3518.

Minamino, T., González-Pedrajo, B., Kihara, M., Namba, K., and Macnab, R. M. (2003). The ATPase FliI can interact with the type III flagellar protein export apparatus in the absence of its regulator, FliH. *Journal of bacteriology*, 185(13):3983–3988.

Minamino, T. and Namba, K. (2008). Distinct roles of the FliI ATPase and proton motive force in bacterial flagellar protein export. *Nature*, 451(7177):485–488.

Mireles, J. R., Toguchi, A., and Harshey, R. M. (2001). *Salmonella enterica* serovar Typhimurium swarming mutants with altered biofilm-forming abilities: surfactin inhibits biofilm formation. *Journal of bacteriology*, 183(20):5848–5854.

Mirold, S., Rabsch, W., Rohde, M., Stender, S., Tschape, H., Rüssmann, H., Igwe, E., and Hardt, W. D. (1999). Isolation of a temperate bacteriophage encoding the type III effector protein SopE from an epidemic *Salmonella typhimurium* strain. *Proceedings of the National Academy of Sciences of the United States of America*, 96(17):9845–9850.

Misselwitz, B., Barrett, N., Kreibich, S., Vonaesch, P., Andritschke, D., Rout, S., Weidner, K., Sormaz, M., Songhet, P., Horvath, P., Chabria, M., Vogel, V., Spori, D. M., Jenny, P., and Hardt, W.-D. (2012). Near surface swimming of *Salmonella* Typhimurium explains target-site selection and cooperative invasion. *PLoS pathogens*, 8(7):e1002810.

Morgan, E., Campbell, J. D., Rowe, S. C., Bispham, J., Stevens, M. P., Bowen, A. J., Barrow, P. A., Maskell, D. J., and Wallis, T. S. (2004). Identification of host-specific colonization factors of *Salmonella enterica* serovar Typhimurium. *Molecular microbiology*, 54(4):994–1010.

Morimoto, Y. V. and Minamino, T. (2014). Structure and function of the bi-directional bacterial flagellar motor. *Biomolecules*, 4(1):217–234.

Mouslim, C. and Hughes, K. T. (2014). The effect of cell growth phase on the regulatory cross-talk between flagellar and Spi1 virulence gene expression. *PLoS pathogens*, 10(3):e1003987.

Murray, P. R., Baron, E. J., Pfaller, M. A., Tenover, F. C., and Yolken, R. H. (1999). Manual of clinical microbiology. *ASM Press, Washington, DC*, 7th edition.

Navabi, N., McGuckin, M. A., and Lindén, S. K. (2013). Gastrointestinal cell lines form polarized epithelia with an adherent mucus layer when cultured in semi-wet interfaces with mechanical stimulation. *PloS one*, 8(7):e68761.

Nicholson, B. and Low, D. (2000). DNA methylation-dependent regulation of *pef* expression in *Salmonella typhimurium*. *Molecular microbiology*, 35(4):728–742.

Norris, F. A., Wilson, M. P., Wallis, T. S., Galyov, E. E., and Majerus, P. W. (1998). SopB, a protein required for virulence of *Salmonella dublin*, is an inositol phosphate phosphatase. *Proceedings of the National Academy of Sciences of the United States of America*, 95(24):14057–14059.

O'Byrne, C. P. and Dorman, C. J. (1994). Transcription of the *Salmonella typhimurium spv* virulence locus is regulated negatively by the nucleoid-associated protein H-NS. *FEMS microbiology letters*, 121(1):99–105.

Ochman, H., Soncini, F. C., Solomon, F., and Groisman, E. A. (1996). Identification of a pathogenicity island required for *Salmonella* survival in host cells. *Proceedings of the National Academy of Sciences of the United States of America*, 93(15):7800–7804.

Ohnishi, K., Kutsukake, K., Suzuki, H., and Lino, T. (1992). A novel transcriptional regulation mechanism in the flagellar regulon of *Salmonella typhimurium*: an antisigma factor inhibits the activity of the flagellum-specific sigma factor, sigma F. *Molecular microbiology*, 6(21):3149–3157.

Okada, N., Oi, Y., Takeda-Shitaka, M., Kanou, K., Umeyama, H., Haneda, T., Miki, T., Hosoya, S., and Danbara, H. (2007). Identification of amino acid residues of *Salmonella* SlyA that are critical for transcriptional regulation. *Microbiology (Reading, England)*, 153(Pt 2):548–560.

Olekhnovich, I. N. and Kadner, R. J. (2006). Crucial roles of both flanking sequences in silencing of the *hilA* promoter in *Salmonella enterica*. 357(2):373–386.

Olekhnovich, I. N. and Kadner, R. J. (2007). Role of nucleoid-associated proteins Hha and H-NS in expression of *Salmonella enterica* activators HilD, HilC, and RtsA required for cell invasion. *Journal of bacteriology*, 189(19):6882–6890.

Olsen, J. E., Hoegh-Andersen, K. H., Casadesús, J., Rosenkranzt, J., Chadfield, M. S., and Thomsen, L. E. (2013). The role of flagella and chemotaxis genes in host pathogen interaction of the host adapted *Salmonella enterica* serovar Dublin compared to the broad host range serovar *S.* Typhimurium. *BMC microbiology*, 13:67.

Patel, J. C. and Galán, J. E. (2006). Differential activation and function of Rho GTPases during *Salmonella*-host cell interactions. *The Journal of cell biology*, 175(3):453–463.

Paul, K., Erhardt, M., Hirano, T., Blair, D. F., and Hughes, K. T. (2008). Energy source of flagellar type III secretion. *Nature*, 451(7177):489–492.

Paul, K., Nieto, V., Carlquist, W. C., Blair, D. F., and Harshey, R. M. (2010). The c-di-GMP binding protein YcgR controls flagellar motor direction and speed to affect chemotaxis by a "backstop brake" mechanism. *Molecular cell*, 38(1):128–139.

Pegues, D. A., Hantman, M. J., Behlau, I., and Miller, S. I. (1995). PhoP/PhoQ transcriptional repression of *Salmonella typhimurium* invasion genes: evidence for a role in protein secretion. *Molecular microbiology*, 17(1):169–181.

Petrone, B. L., Stringer, A. M., and Wade, J. T. (2014). Identification of HilD-regulated genes in *Salmonella enterica* serovar Typhimurium. *Journal of bacteriology*, 196(5):1094–1101.

Pfaffl, M. W. (2001). A new mathematical model for relative quantification in real-time RT-PCR. *Nucleic acids research*, 29(9):e45.

Porwollik, S., Wong, R. M.-Y., and McClelland, M. (2002). Evolutionary genomics of *Salmonella*: gene acquisitions revealed by microarray analysis. *Proceedings of the National Academy of Sciences of the United States of America*, 99(13):8956–8961.

Power, P. M. and Jennings, M. P. (2003). The genetics of glycosylation in Gram-negative bacteria. *FEMS microbiology letters*, 218(2):211–222.

Pratt, L. A. and Kolter, R. (1998a). Genetic analysis of *Escherichia coli* biofilm formation: roles of flagella, motility, chemotaxis and type I pili. *Molecular microbiology*, 30(2):285–293.

Pratt, L. A. and Kolter, R. (1998b). Genetic analysis of *Escherichia coli* biofilm formation: roles of flagella, motility, chemotaxis and type I pili. *Molecular Microbiology*, 30(2):285–293.

Prehna, G., Li, Y., Stoynov, N., Okon, M., Vuckovic, M., McIntosh, L. P., Foster, L. J., Finlay, B. B., and Strynadka, N. C. J. (2012). The zinc regulated antivirulence pathway of *Salmonella* is a multiprotein immunoglobulin adhesion system. *The Journal of biological chemistry*, 287(39):32324–32337.

Prigent-Combaret, C., Brombacher, E., Vidal, O., Ambert, A., Lejeune, P., Landini, P., and Dorel, C. (2001). Complex regulatory network controls initial adhesion and biofilm formation in *Escherichia coli* via regulation of the *csgD* gene. *Journal of bacteriology*, 183(24):7213–7223.

Raetz, C. R. H. and Whitfield, C. (2002). Lipopolysaccharide endotoxins. *Annual review of biochemistry*, 71(1):635–700.

Rajashekar, R., Liebl, D., Seitz, A., and Hensel, M. (2008). Dynamic remodeling of the endosomal system during formation of *Salmonella*-induced filaments by intracellular *Salmonella enterica*. *Traffic (Copenhagen, Denmark)*, 9(12):2100–2116.

Reid, S. D., Selander, R. K., and Whittam, T. S. (1999). Sequence diversity of flagellin (*fliC*) alleles in pathogenic *Escherichia coli*. *Journal of bacteriology*, 181(1):153–160.

Ren, C.-P., Beatson, S. A., Parkhill, J., and Pallen, M. J. (2005). The Flag-2 locus, an ancestral gene cluster, is potentially associated with a novel flagellar system from *Escherichia coli*. *Journal of bacteriology*, 187(4):1430–1440.

Renault, T. T., Abraham, A. O., Bergmiller, T., Paradis, G., Rainville, S., Charpentier, E., Guet, C. C., Tu, Y., Namba, K., Keener, J. P., Minamino, T., and Erhardt, M. (2017). Bacterial flagella grow through an injection-diffusion mechanism. *eLife*.

Rivera-Chávez, F., Lopez, C. A., Zhang, L. F., García-Pastor, L., Chávez-Arroyo, A., Lokken, K. L., Tsolis, R. M., Winter, S. E., and Bäumler, A. J. (2016). Energy taxis toward host-derived nitrate supports a *Salmonella* pathogenicity island 1-independent mechanism of invasion. *mBio*, 7(4):e00960–16.

Robert-Koch Institut (2015). Infektionsepidemiologisches Jahrbuch 2015.

Romeo, T., Gong, M., Liu, M. Y., and Brun-Zinkernagel, A. M. (1993). Identification and molecular characterization of *csrA*, a pleiotropic gene from *Escherichia coli* that affects glycogen biosynthesis, gluconeogenesis, cell size, and surface properties. *Journal of bacteriology*, 175(15):4744–4755.

Römling, U., Bian, Z., Hammar, M., Sierralta, W. D., and Normark, S. (1998). Curli fibers are highly conserved between *Salmonella typhimurium* and *Escherichia coli* with respect to operon structure and regulation. *Journal of bacteriology*, 180(3):722–731.

Rossez, Y., Wolfson, E. B., Holmes, A., Gally, D. L., and Holden, N. J. (2015). Bacterial flagella: twist and stick, or dodge across the kingdoms. *PLoS pathogens*, 11(1):e1004483.

Roy, K., Hilliard, G. M., Hamilton, D. J., Luo, J., Ostmann, M. M., and Fleckenstein, J. M. (2009). Enterotoxigenic *Escherichia coli* EtpA mediates adhesion between flagella and host cells. *Nature*, 457(7229):594–598.

Saini, S. and Rao, C. V. (2010). SprB is the molecular link between *Salmonella* pathogenicity island 1 (SPI1) and SPI4. *Journal of bacteriology*, 192(9):2459–2462.

Saini, S., Slauch, J. M., Aldridge, P. D., and Rao, C. V. (2010). Role of cross talk in regulating the dynamic expression of the flagellar *Salmonella* pathogenicity island 1 and type 1 fimbrial genes. *Journal of bacteriology*, 192(21):5767–5777.

Sanderson, K. E. and Roth, J. R. (1988). Linkage map of *Salmonella typhimurium*, edition VII. *Microbiological reviews*, 52(4):485–532.

Sano, G.-i., Takada, Y., Goto, S., Maruyama, K., Shindo, Y., Oka, K., Matsui, H., and Matsuo, K. (2007). Flagella facilitate escape of *Salmonella* from oncotic macrophages. *Journal of bacteriology*, 189(22):8224–8232.

Sansonetti, P. (2002). Host-pathogen interactions: the seduction of molecular cross talk. *Gut*, 50 Suppl 3:III2–8.

Santiviago, C. A., Reynolds, M. M., Porwollik, S., Choi, S.-H., Long, F., Andrews-Polymenis, H. L., and McClelland, M. (2009). Analysis of pools of targeted *Salmonella* deletion mutants identifies novel genes affecting fitness during competitive infection in mice. *PLoS pathogens*, 5(7):e1000477.

Sato, Y., Takaya, A., Mouslim, C., Hughes, K. T., and Yamamoto, T. (2014). FliT selectively enhances proteolysis of FlhC subunit in FlhD4C2 complex by an ATP-dependent protease, ClpXP. *The Journal of biological chemistry*, 289(47):33001–33011.

Schechter, L. M., Damrauer, S. M., and Lee, C. A. (1999). Two AraC/XylS family members can independently counteract the effect of repressing sequences upstream of the *hilA* promoter. *Molecular microbiology*, 32(3):629–642.

Schreiber, F., Kay, S., Frankel, G., Clare, S., Goulding, D., van de Vosse, E., van Dissel, J. T., Strugnell, R., Thwaites, G., Kingsley, R. A., Dougan, G., and Baker, S. (2015). The Hd, Hj, and Hz66 flagella variants of *Salmonella enterica* serovar Typhi modify host responses and cellular interactions. *Scientific reports*, 5:7947.

Schultz, M. (2010). Theobald Smith. *Emerg Infect Dis*, 14:1940–1942.

Silverman, M. and Simon, M. (1980). Phase variation: genetic analysis of switching mutants. *Cell*, 19(4):845–854.

Silverman, M., Zieg, J., and Simon, M. (1979). Flagellar-phase variation: isolation of the *rh1* gene. *Journal of bacteriology*, 137(1):517–523.

Simm, R., Lusch, A., Kader, A., Andersson, M., and Römling, U. (2007). Role of EAL-containing proteins in multicellular behavior of *Salmonella enterica* serovar Typhimurium. *Journal of bacteriology*, 189(9):3613–3623.

Simm, R., Morr, M., Kader, A., Nimtz, M., and Römling, U. (2004). GGDEF and EAL domains inversely regulate cyclic di-GMP levels and transition from sessility to motility. *Molecular microbiology*, 53(4):1123–1134.

Singer, H. M., Erhardt, M., and Hughes, K. T. (2013). RflM functions as a transcriptional repressor in the autogenous control of the *Salmonella* flagellar master operon *flhDC*. *Journal of bacteriology*, 195(18):4274–4282.

Singer, H. M., Kühne, C., Deditius, J. A., Hughes, K. T., and Erhardt, M. (2014). The *Salmonella* Spi1 virulence regulatory protein HilD directly activates transcription of the flagellar master operon *flhDC*. *Journal of bacteriology*, 196(7):1448–1457.

Smith, C., Stringer, A. M., Mao, C., Palumbo, M. J., and Wade, J. T. (2016). Mapping the Regulatory Network for *Salmonella enterica* Serovar Typhimurium Invasion. *mBio*, 7(5):e01024–16.

Smith, K. D., Andersen-Nissen, E., Hayashi, F., Strobe, K., Bergman, M. A., Barrett, S. L. R., Cookson, B. T., and Aderem, A. (2003). Toll-like receptor 5 recognizes a conserved site on flagellin required for protofilament formation and bacterial motility. *Nature immunology*, 4(12):1247–1253.

Soto, G. E. and Hultgren, S. J. (1999). Bacterial adhesins: common themes and variations in architecture and assembly. *Journal of bacteriology*, 181(4):1059–1071.

Sourjik, V. and Wingreen, N. S. (2011). Responding to chemical gradients: bacterial chemotaxis. *Current Opinion in Cell Biology*, 24(2):262–268.

Spurbeck, R. R., Alteri, C. J., Himpsl, S. D., and Mobley, H. L. T. (2013). The multifunctional protein YdiV represses P fimbria-mediated adherence in uropathogenic *Escherichia coli*. *Journal of bacteriology*, 195(14):3156–3164.

Stecher, B., Barthel, M., Schlumberger, M. C., Haberli, L., Rabsch, W., Kremer, M., and Hardt, W.-D. (2008). Motility allows *S.* Typhimurium to benefit from the mucosal defence. *Cellular microbiology*, 10(5):1166–1180.

Stecher, B., Hapfelmeier, S., Müller, C., Kremer, M., Stallmach, T., and Hardt, W.-D. (2004). Flagella and chemotaxis are required for efficient induction of *Salmonella enterica* serovar

Typhimurium colitis in streptomycin-pretreated mice. *Infection and immunity*, 72(7):4138–4150.

Stender, S., Friebel, A., Linder, S., Rohde, M., Mirold, S., and Hardt, W. D. (2000). Identification of SopE2 from *Salmonella typhimurium*, a conserved guanine nucleotide exchange factor for Cdc42 of the host cell. *Molecular microbiology*, 36(6):1206–1221.

Stocker, B. A. D., McDonough, M. W., and Ambler, R. P. (1961). A gene determining presence or absence of -N-methyl-lysine in *Salmonella* flagellar protein. *Nature*, 189(4764):556–558.

Sturm, A., Heinemann, M., Arnoldini, M., Benecke, A., Ackermann, M., Benz, M., Dormann, J., and Hardt, W.-D. (2011). The cost of virulence: retarded growth of *Salmonella* Typhimurium cells expressing type III secretion system 1. *PLoS pathogens*, 7(7):e1002143.

Sun, L., Jin, M., Ding, W., Yuan, J., Kelly, J., and Gao, H. (2013). Posttranslational modification of flagellin FlaB in *Shewanella oneidensis*. *Journal of bacteriology*, 195(11):2550–2561.

Swords, W. E., Cannon, B. M., and Benjamin, W. H. (1997). Avirulence of LT2 strains of *Salmonella typhimurium* results from a defective *rpoS* gene. *Infection and Immunity*.

Szymanski, C. M., Logan, S. M., Linton, D., and Wren, B. W. (2003). *Campylobacter*-a tale of two protein glycosylation systems. *Trends in microbiology*, 11(5):233–238.

Takaya, A., Erhardt, M., Karata, K., Winterberg, K., Yamamoto, T., and Hughes, K. T. (2012). YdiV: a dual function protein that targets FlhDC for ClpXP-dependent degradation by promoting release of DNA-bound FlhDC complex. *Molecular microbiology*, 83(6):1268–1284.

Takeuchi, A. (1967). Electron microscope studies of experimental *Salmonella* infection. I. Penetration into the intestinal epithelium by *Salmonella typhimurium*. *The American journal of pathology*, 50(1):109–136.

Teplitski, M., Al-Agely, A., and Ahmer, B. M. M. (2006). Contribution of the SirA regulon to biofilm formation in *Salmonella enterica* serovar Typhimurium. *Microbiology (Reading, England)*, 152(Pt 11):3411–3424.

Teplitski, M., Goodier, R. I., and Ahmer, B. M. M. (2003). Pathways leading from BarA/SirA to motility and virulence gene expression in *Salmonella*. *Journal of bacteriology*, 185(24):7257–7265.

Thijs, I. M. V., De Keersmaecker, S. C. J., Fadda, A., Engelen, K., Zhao, H., McClelland, M., Marchal, K., and Vanderleyden, J. (2007). Delineation of the *Salmonella enterica* serovar Typhimurium HilA regulon through genome-wide location and transcript analysis. *Journal of bacteriology*, 189(13):4587–4596.

Tinker, J. K. and Clegg, S. (2000). Characterization of FimY as a coactivator of type 1 fimbrial expression in *Salmonella enterica* serovar Typhimurium. *Infection and immunity*, 68(6):3305–3313.

Tinker, J. K., Hancox, L. S., and Clegg, S. (2001). FimW is a negative regulator affecting type 1 fimbrial expression in *Salmonella enterica* serovar Typhimurium. *Journal of bacteriology*, 183(2):435–442.

Toguchi, A., Siano, M., Burkart, M., and Harshey, R. M. (2000). Genetics of swarming motility in *Salmonella enterica* serovar typhimurium: critical role for lipopolysaccharide. *Journal of bacteriology*, 182(22):6308–6321.

Tronick, S. R. and Martinez, R. J. (1971). Methylation of the flagellin of *Salmonella typhimurium*. *Journal of bacteriology*, 105(1):211–219.

Troxell, B., Sikes, M. L., Fink, R. C., Vazquez-Torres, A., Jones-Carson, J., and Hassan, H. M. (2011). Fur negatively regulates *hns* and is required for the expression of HilA and virulence in *Salmonella enterica* serovar Typhimurium. *Journal of bacteriology*, 193(2):497–505.

Uchiya, K., Barbieri, M. A., Funato, K., Shah, A. H., Stahl, P. D., and Groisman, E. A. (1999). A *Salmonella* virulence protein that inhibits cellular trafficking. *The EMBO journal*, 18(14):3924–3933.

Valentine, R. C., Shapiro, B. M., and Stadtman, E. R. (1968). Regulation of glutamine synthetase. XII. Electron microscopy of the enzyme from *Escherichia coli*. *Biochemistry*, 7(6):2143–2152.

Vandesompele, J., De Preter, K., Pattyn, F., Poppe, B., Van Roy, N., De Paepe, A., and Speleman, F. (2002). Accurate normalization of real-time quantitative RT-PCR data by geometric averaging of multiple internal control genes. *Genome biology*, 3(7).

Vidal, K., Grosjean, I., evillard, J. P., Gespach, C., and Kaiserlian, D. (1993). Immortalization of mouse intestinal epithelial cells by the SV40-large T gene. Phenotypic and immune characterization of the MODE-K cell line. *Journal of immunological methods*, 166(1):63–73.

Vigeant, M. A.-S., Ford, R. M., Wagner, M., and Tamm, L. K. (2002). Reversible and irreversible adhesion of motile *Escherichia coli* cells analyzed by total internal reflection aqueous fluorescence microscopy. *Applied and environmental microbiology*, 68(6):2794–2801.

Wada, T., Morizane, T., Abo, T., Tominaga, A., Inoue-Tanaka, K., and Kutsukake, K. (2011a). EAL domain protein YdiV acts as an anti-FlhD4C2 factor responsible for nutritional control of the flagellar regulon in *Salmonella enterica* Serovar Typhimurium. *Journal of bacteriology*, 193(7):1600–1611.

Wada, T., Tanabe, Y., and Kutsukake, K. (2011b). FliZ acts as a repressor of the *ydiV* gene, which encodes an anti-FlhD4C2 factor of the flagellar regulon in *Salmonella enterica* serovar Typhimurium. *Journal of bacteriology*, 193(19):5191–5198.

Wadhams, G. H. and Armitage, J. P. (2004). Making sense of it all: bacterial chemotaxis. *Nature reviews. Molecular cell biology*, 5(12):1024–1037.

Wall, D. and Kaiser, D. (1999). Type IV pili and cell motility. *Molecular microbiology*, 32(1):1–10.

Walthers, D., Carroll, R. K., Navarre, W. W., Libby, S. J., Fang, F. C., and Kenney, L. J. (2007). The response regulator SsrB activates expression of diverse *Salmonella* pathogenicity island 2 promoters and counters silencing by the nucleoid-associated protein H-NS. *Molecular microbiology*, 65(2):477–493.

Wang, Q., Frye, J. G., McClelland, M., and Harshey, R. M. (2004a). Gene expression patterns during swarming in *Salmonella typhimurium*: genes specific to surface growth and putative new motility and pathogenicity genes. *Molecular microbiology*, 52(1):169–187.

Wang, Q., Zhao, Y., McClelland, M., and Harshey, R. M. (2007). The RcsCDB signaling system and swarming motility in *Salmonella enterica* serovar Typhimurium: dual regulation of flagellar and SPI-2 virulence genes. *Journal of bacteriology*, 189(23):8447–8457.

Wang, S., Fleming, R. T., Westbrook, E. M., Matsumura, P., and McKay, D. B. (2006). Structure of the *Escherichia coli* FlhDC complex, a prokaryotic heteromeric regulator of transcription. 355(4):798–808.

Wang, Y., Prosen, D. E., Mei, L., Sullivan, J. C., Finney, M., and Vander Horn, P. B. (2004b). A novel strategy to engineer DNA polymerases for enhanced processivity and improved performance *in vitro*. *Nucleic Acids Research*, 32(3):1197–1207.

Weening, E. H., Barker, J. D., Laarakker, M. C., Humphries, A. D., Tsolis, R. M., and Bäumler, A. J. (2005). The *Salmonella enterica* serotype Typhimurium *lpf*, *bcf*, *stb*, *stc*, *std*, and *sth* fimbrial operons are required for intestinal persistence in mice. *Infection and immunity*, 73(6):3358–3366.

Wiedemann, A., Virlogeux-Payant, I., Chaussé, A.-M., Schikora, A., and Velge, P. (2014). Interactions of *Salmonella* with animals and plants. *Frontiers in microbiology*, 5:791.

World Health Organization (2016). Fact sheet No. 139.

Wozniak, C. E., Lee, C., and Hughes, K. T. (2009). T-POP array identifies EcnR and PefI-SrgD as novel regulators of flagellar gene expression. *Journal of bacteriology*, 191(5):1498–1508.

Yamamoto, S. and Kutsukake, K. (2006). FliT acts as an anti-FlhD2C2 factor in the transcriptional control of the flagellar regulon in *Salmonella enterica* serovar Typhimurium. *Journal of bacteriology*, 188(18):6703–6708.

Yanagihara, S., Iyoda, S., Ohnishi, K., Iino, T., and Kutsukake, K. (1999). Structure and transcriptional control of the flagellar master operon of *Salmonella typhimurium*. *Genes & genetic systems*, 74(3):105–111.

Yang, X., Thornburg, T., Suo, Z., Jun, S., Robison, A., Li, J., Lim, T., Cao, L., Hoyt, T., Avci, R., and Pascual, D. W. (2012). Flagella overexpression attenuates *Salmonella* pathogenesis. *PloS one*, 7(10):e46828.

Yeh, K. S., Hancox, L. S., and Clegg, S. (1995). Construction and characterization of a *fimZ* mutant of *Salmonella typhimurium*. *Journal of bacteriology*, 177(23):6861–6865.

Yonekura, K., Maki-Yonekura, S., and Namba, K. (2003). Complete atomic model of the bacterial flagellar filament by electron cryomicroscopy. *Nature*, 424(6949):643–650.

Zenk, S. F., Jantsch, J., and Hensel, M. (2009). Role of *Salmonella enterica* lipopolysaccharide in activation of dendritic cell functions and bacterial containment. *Journal of immunology (Baltimore, Md. : 1950)*, 183(4):2697–2707.

Zgair, A. K. and Chhibber, S. (2011). Adhesion of *Stenotrophomonas maltophilia* to mouse tracheal mucus is mediated through flagella. *Journal of medical microbiology*, 60(Pt 7):1032–1037.

Zhang, X. and Bremer, H. (1995). Control of the *Escherichia coli rrnB* P1 promoter strength by ppGpp. *The Journal of biological chemistry*, 270(19):11181–11189.

Zhou, D., Mooseker, M. S., and Galán, J. E. (1999a). Role of the *S. typhimurium* actin-binding protein SipA in bacterial internalization. *Science (New York, N.Y.)*, 283(5410):2092–2095.

Zhou, D., Mooseker, M. S., and Galán, J. E. (1999b). Role of the *S. typhimurium* actin-binding protein SipA in bacterial internalization. *Science (New York, N.Y.)*, 283(5410):2092–2095.

Zieg, J., Silverman, M., Hilmen, M., and Simon, M. (1977). Recombinational switch for gene expression. *Science (New York, N.Y.)*, 196(4286):170–172.

Zieg, J. and Simon, M. (1980). Analysis of the nucleotide sequence of an invertible controlling element. *Proceedings of the National Academy of Sciences of the United States of America*, 77(7):4196–4200.

Zierler, M. K. and Galán, J. E. (1995). Contact with cultured epithelial cells stimulates secretion of *Salmonella typhimurium* invasion protein InvJ. *Infection and immunity*, 63(10):4024–4028.

# Author Contributions

## Chapter 2 - Characterisation of Novel Factors Involved in Swimming and Swarming Motility in *Salmonella* Typhimurium

I designed and performed all experiments shown in this chapter. I analysed the data, made all figures, and wrote the manuscript except for the following:
SF performed the $\beta$-galactosidase assay in Fig. 2.6B. IS and CK contributed to swimming and swarming motility in Fig. 2.2. MR conducted the transmission electron microscopy of prepared samples in Fig. 2.6A.

## Chapter 4 - Flagellin Phase-dependent Swimming on Cell Surfaces Contributes to Host Cell Invasion in *Salmonella* Typhimurium

I designed and performed all experiments shown in this chapter. I analysed the data, made all figures, and wrote the manuscript except for the following:
EZ performed single cell tracking experiments in Fig. 4.15C. TT generated the Cl10 cell line used in this thesis and performed the immunostaining experiments in Fig. 4.9. MR performed field emission scanning electron microscopy and transmission electron microscopy (Figs. 4.10 and 4.14A).